

Analysis of Center of Pressure and Center of Mass to Determine Patterns of Postural Stability in
Neurotypical Subjects

Natalie Tipton

A Thesis Submitted to the Graduate Faculty of

GRAND VALLEY STATE UNIVERSITY

In

Partial Fulfillment of the Requirements

For the Degree of

Master of Science in Engineering, Biomedical Engineering

Padnos College of Engineering and Computing

August 2020

Acknowledgements

I would like to thank my thesis advisor, Dr. Rhodes, for her guidance throughout the thesis process as well as the past few years during my undergraduate and graduate experience at Grand Valley State University. Her knowledge and ability to always keep things interesting has continued to spark my interest in new topics and has made me a more capable and passionate engineer. She has been an invaluable resource in the completion of my degree requirements.

I would like to thank my committee members, Dr. Alderink and Dr. Ashby, for being available whenever I needed to fill a gap in my knowledge or needed additional guidance throughout the thesis process. Their assistance was invaluable to my completion of this research.

I would like to thank all participants of this study who gave up their time to data collection. Additionally, I would like to thank Diana McCrumb, who collected the data in the process of completing her own thesis.

I would like to thank Jarred Parr who provided expertise on the software side of my research whenever I was unsure how to proceed.

Finally, I would like to thank my friends and family who have supported and encouraged me endlessly throughout my education. Without them, I would not have accomplished all that I have.

Abstract

The body's postural control mechanism is responsible for responding to perturbations of balance and keeping the body upright. One of the main ways that this is completed during quiet standing, where both feet are planted on the ground, is through center of pressure oscillations. In these oscillations, the center of pressure circles around the center of mass, constantly counteracting any lean that exists in the body. These oscillations can be recorded with floor-embedded force plates and center of mass can be recorded with a motion capture system. In this research, these signals were recorded for stances with feet together and feet tandem with eyes opened and eyes closed with neurotypical subjects. Center of pressure and center of mass were compared to determine if they provide the same information as one another. Through different correlation measures, it was shown that they generally have a very strong relationship to one another, and that COP provides as much information as COM.

From there, center of pressure was further analyzed using approximate entropy, velocity measures, and regression. This analysis showed evidence of increased irregularity, increased velocity, and increased frequency content in center of pressure oscillations during standing conditions with lower stability. ApEn indicated significant differences between the most stable eyes open, feet together condition and all of the less stable feet tandem trials for eyes open and eyes closed in nearly every subject. Velocity, however, only indicated significant differences between the most stable condition and the least stable eyes closed, feet tandem trials. Regression analysis showed a decrease in the content that could be explained by the model as stability decreased. Regression also provided a general illustration of what each stability condition may be expected to look like, which can be used to compare future data against. The results of this study will be useful to compare non-neurotypical subject data to moving forward.

Table of Contents

| | |
|---|-----------|
| <i>Acknowledgements</i> | 3 |
| <i>Abstract</i> | 4 |
| <i>List of Tables</i> | 7 |
| <i>List of Figures</i> | 8 |
| <i>Abbreviations</i> | 12 |
| Chapter 1. Introduction | 13 |
| 1.1. Introduction | 13 |
| 1.2. Purpose | 15 |
| 1.3. Scope | 15 |
| 1.4. Assumptions | 16 |
| 1.5. Hypothesis | 17 |
| 1.6. Significance..... | 18 |
| 1.7. Definitions..... | 18 |
| Chapter 2. Manuscript | 20 |
| <i>Abstract</i> | 20 |
| 2.1. Introduction | 21 |
| 2.2. Methods | 26 |
| 2.2.1. Participants | 26 |
| 2.2.2. Procedure..... | 27 |
| 2.2.3. Data Acquisition..... | 28 |
| 2.2.3.1. Motion Capture and Force Plates..... | 28 |
| 2.2.3.2. Coordinate Systems..... | 30 |
| 2.2.4. Data Analysis..... | 31 |
| 2.2.4.1. Signal Preprocessing | 32 |
| 2.2.4.2. Approximate Entropy..... | 33 |
| 2.2.4.3. Velocity | 36 |
| 2.2.4.4. Power Spectral Density | 37 |
| 2.2.4.5. Regression | 38 |
| 2.2.4.6. Statistical Analysis..... | 39 |
| 2.3. Results..... | 40 |
| 2.3.1. COP and COM Relationship | 43 |
| 2.3.2. Approximate Entropy | 47 |
| 2.3.3. Velocity | 55 |
| 2.3.4. Regression..... | 63 |
| 2.4. Discussion | 67 |
| 2.4.1. COP and COM Correlation..... | 68 |
| 2.4.2. Postural Control and Changing Stability Conditions | 70 |
| 2.4.2.1. Center of Pressure Irregularity | 70 |

| | | |
|---|--|------------|
| 2.4.2.2. | Oscillation Velocity | 71 |
| 2.4.2.3. | Baseline Models | 72 |
| 2.4.3. | Comparison of Analysis Methods..... | 72 |
| 2.4.4. | Limitations and Future Considerations..... | 73 |
| 2.5. | Conclusion | 74 |
| Chapter 3. Extended Review of Literature and Extended Methodology..... | | 76 |
| 3.1. | Extended Review of Literature | 76 |
| 3.1.1. | Quiet Standing | 76 |
| 3.1.2. | Postural Control..... | 77 |
| 3.1.2.1. | Postural Sway..... | 79 |
| 3.1.2.2. | Strategies | 80 |
| 3.1.2.3. | Inverted Pendulum Model..... | 83 |
| 3.1.3. | Brain Health and Postural Control | 84 |
| 3.2. | Extended Methodology..... | 85 |
| 3.2.1. | Participants | 85 |
| 3.2.2. | Experimental Procedure | 86 |
| 3.2.3. | Data Acquisition..... | 88 |
| 3.2.3.1. | Subject Preparation | 88 |
| 3.2.3.2. | Instrumentation | 88 |
| 3.2.4. | Data Analysis..... | 89 |
| 3.2.4.1. | Signal Preprocessing | 89 |
| 3.2.4.2. | Approximate Entropy..... | 90 |
| 3.2.4.3. | Velocity | 92 |
| 3.2.4.4. | Power Spectral Density..... | 93 |
| 3.2.4.5. | Regression | 95 |
| Appendix A. Figures | | 98 |
| Appendix B. Code..... | | 102 |
| B.1. | Correlation Calculations..... | 102 |
| B.2. | Entropy Calculations..... | 104 |
| B.3. | Velocity Calculations..... | 110 |
| B.4. | Regression Calculations | 116 |
| B.5. | Function Library | 119 |
| References | | 127 |

List of Tables

| | |
|--|----|
| Table 2.1. Quiet standing balance conditions | 27 |
| Table 2.2. Pearson's Correlation Coefficient for one trial from each stability condition in all subjects in AP direction | 46 |
| Table 2.3. Pearson's Correlation Coefficient for one trial from each stability condition in all subjects in ML direction | 46 |
| Table 3.1. Subject Characteristics | 85 |
| Table 3.2. Quiet standing balance conditions | 86 |

List of Figures

| | |
|--|----|
| Figure 2.1. Center of pressure, center of mass, and base of support locations, adapted from [26] | 22 |
| Figure 2.2. Center of pressure oscillations at five points in time where the COP location is represented by R, the COM location is represented by W, angular velocity is represented by ω , and angular acceleration is represented by α [2] | 24 |
| Figure 2.3. Subject stance for feet together (left) and feet tandem (right) trials | 28 |
| Figure 2.4. Modified Full-Body Plug-in-Gait model [32] | 29 |
| Figure 2.5. Feet orientation adapted from [32] | 30 |
| Figure 2.6. Orientation of coordinate systems | 31 |
| Figure 2.7. Signal processing function block diagram | 32 |
| Figure 2.8. Graphical interpretation of $C_i^m(r)$ in ApEn, adapted from [39] | 35 |
| Figure 2.9. Difference in approximate entropy values between a periodic signal and white noise, adapted from [39] | 36 |
| Figure 2.10. COP data for eyes open, feet together trial | 40 |
| Figure 2.11. COP data for eyes closed, feet tandem, dominant foot in front trial | 41 |
| Figure 2.12. COM data for eyes open, feet together trial | 42 |
| Figure 2.13. COM data for eyes closed, feet tandem, dominant foot in front trial | 42 |
| Figure 2.14. COP and COM signals for baseline eyes open, feet together condition in subject 1 | 43 |
| Figure 2.15. COP and COM signals for eyes closed, feet tandem, dominant foot in front condition in subject 1 | 44 |
| Figure 2.16. Autocorrelation and cross-correlation for baseline eye open, feet together trial in subject 1 | 45 |
| Figure 2.17. Autocorrelation and cross-correlation for eyes closed, feet tandem, dominant foot in back trial in subject 1..... | 45 |
| Figure 2.18. Velocity of an eyes open, feet together trial from subject 1 | 47 |

| | |
|---|----|
| Figure 2.19. Velocity of an eyes closed, feet tandem, dominant foot in front trial from subject 1 | 48 |
| Figure 2.20. Approximate entropy of each condition for subject 1 | 49 |
| Figure 2.21. Approximate entropy of each condition for subject 2 | 49 |
| Figure 2.22. Approximate entropy of each condition for subject 3 | 50 |
| Figure 2.23. Approximate entropy of each condition for subject 4 | 50 |
| Figure 2.24. Approximate entropy of each condition for subject 5 | 51 |
| Figure 2.25. Approximate entropy of each condition for subject 6 | 51 |
| Figure 2.26. Difference in approximate entropy between each condition and eyes open, feet together for subject 1 with Dunnett's post-hoc test results shown | 52 |
| Figure 2.27. Difference in approximate entropy between each condition and eyes open, feet together for subject 2 with Dunnett's post-hoc test results shown | 53 |
| Figure 2.28. Difference in approximate entropy between each condition and eyes open, feet together for subject 3 with Dunnett's post-hoc test results shown | 53 |
| Figure 2.29. Difference in approximate entropy between each condition and eyes open, feet together for subject 4 with Dunnett's post-hoc test results shown | 54 |
| Figure 2.30. Difference in approximate entropy between each condition and eyes open, feet together for subject 5 with Dunnett's post-hoc test results shown | 54 |
| Figure 2.31. Difference in approximate entropy between each condition and eyes open, feet together for subject 6 with Dunnett's post-hoc test results shown | 55 |
| Figure 2.32. Velocity of an eyes open, feet together trial from subject 1 | 56 |
| Figure 2.33. Velocity of an eyes closed, feet tandem, dominant foot in front trial from subject 1 | 56 |
| Figure 2.34. PSD of velocity signal of an eyes open, feet together trial from subject 1 | 57 |
| Figure 2.35. PSD of velocity signal of an eyes closed, feet tandem, dominant foot in front trial from subject 1 | 57 |
| Figure 2.36. Average velocity and total power of each condition for subject 1 with 1-way ANOVA results shown | 58 |

| | |
|--|----|
| Figure 2.37. Average velocity and total power of each condition for subject 2 with 1-way ANOVA results shown | 58 |
| Figure 2.38. Average velocity and total power of each condition for subject 3 with 1-way ANOVA results shown | 59 |
| Figure 2.39. Average velocity and total power of each condition for subject 4 with 1-way ANOVA results shown | 59 |
| Figure 2.40. Average velocity and total power of each condition for subject 5 with 1-way ANOVA results shown | 59 |
| Figure 2.41. Average velocity and total power of each condition for subject 6 with 1-way ANOVA results shown | 60 |
| Figure 2.42. Difference in velocity and total power between each condition and eyes open, feet together for subject 1 with Dunnett’s post-hoc test results shown | 61 |
| Figure 2.43. Difference in velocity and total power between each condition and eyes open, feet together for subject 2 with Dunnett’s post-hoc test results shown | 61 |
| Figure 2.44. Difference in velocity and total power between each condition and eyes open, feet together for subject 3 with Dunnett’s post-hoc test results shown | 61 |
| Figure 2.45. Difference in velocity and total power between each condition and eyes open, feet together for subject 5 with Dunnett’s post-hoc test results shown | 62 |
| Figure 2.46. Difference in velocity and total power between each condition and eyes open, feet together for subject 6 with Dunnett’s post-hoc test results shown | 62 |
| Figure 2.47. Regression model for all eyes open, feet together trials | 63 |
| Figure 2.48. Regression model for all eye closed, feet together trials | 64 |
| Figure 2.49. Regression model for all eyes open, feet tandem, dominant foot in back trials | 64 |
| Figure 2.50. Regression model for all eyes open, feet tandem, dominant foot in front trials | 65 |
| Figure 2.51. Regression model for all eyes closed, feet tandem, dominant foot in back trials ... | 65 |
| Figure 2.52. Regression model for all eyes closed, feet tandem, dominant foot in front trials ... | 66 |
| Figure 2.53. Regression model for all trials | 67 |
| Figure 3.1. Quiet standing foot positioning, adapted from [46] | 76 |

| | |
|---|-----|
| Figure 3.2. COP, COM, and BOS for human body, adapted from [48] | 78 |
| Figure 3.3. COM and COP oscillations during quiet standing, adapted from [50] | 79 |
| Figure 3.4. Three postural control strategies [52] | 81 |
| Figure 3.5. Single (left) and double (right) inverted pendulum models adapted from [55] | 83 |
| Figure 3.6. Combination of two individual COPs into one resultant COP | 90 |
| Figure 3.7. Power spectral density of a 2 Hz sine wave | 93 |
| Figure 3.8. Power spectral density of a 2 Hz sine wave added to a 5 Hz cosine wave | 94 |
| Figure 3.9. Polynomial regression example, adapted from [61] | 95 |
| Figure A.1. COP data for eyes closed, feet together trial | 98 |
| Figure A.2. COP data for eyes open, feet tandem, dominant foot in back trial | 98 |
| Figure A.3. COP data for eyes open, feet tandem, dominant foot in front trial | 99 |
| Figure A.4. COP data for eyes closed, feet tandem, dominant foot in back trial | 99 |
| Figure A.5. COM data for eyes closed, feet together trial | 100 |
| Figure A.6. COM data for eyes open, feet tandem, dominant foot in back trial | 100 |
| Figure A.7. COM data for eyes open, feet tandem, dominant foot in front trial | 101 |
| Figure A.8. COM data for eyes closed, feet tandem, dominant foot in back trial | 101 |

Abbreviations

COP – center of pressure

COM – center of mass

FT – feet together

TanDB – tandem feet, dominant foot back

TanDF – tandem feet, dominant foot forward

EO – eyes open

EC – eyes closed

CNS – central nervous system

BOS – base of support

EMG – electromyography

FB PiG – full body plug-in-gait

AP – anterior/posterior

ML – medial/lateral

ApEn – approximate entropy

PSD – power spectral density

ANOVA – analysis of variance

SIP – single inverted pendulum

DIP – double inverted pendulum

Chapter 1. Introduction

1.1. Introduction

The physiological processes involved with keeping a human upright are complex and dynamic. In mechanics, balance is a term used to describe a state where the sum of all forces acting on an object are zero [1]. In terms of human physiology, those forces are the elements of body posture that keep a person from falling [2]. Postural control relates to this concept in that it is the act of maintaining balance during all activities [1].

Standing humans have a few different metrics that allow for balance and postural control to be analyzed quantitatively. The two most commonly used are center of pressure (COP) and center of mass (COM). These are often used interchangeably. However, clinically the two metrics are distinct. The COP is the point location of the resultant ground reaction force occurring where the body makes contact with the ground. It is located in the position of the weighted average of all of the pressures that are being exerted on the body by the ground, where the sum of the moments of each individual pressure is equal to the moment of the resultant ground reaction force vector acting at the COP [2]. When a person has both feet planted on the ground, each foot has a separate COP, which can be combined to create one resultant COP for the entire body. The COM is the point location on the body that is representative of all of its mass, where the moment of the COM is equivalent to the sum of the moments of the weight acting at every point on the body [2]. This metric is in a relatively constant location in the center of the body, about one-half to two-thirds of the way up between the feet and the highest point of the body [2]

Another metric that is important to consider is the base of support (BOS). This is an area underneath the body defined by the perimeter around all points of contact with the ground. It defines the limits of motion for which a person can be stable without stepping [3]. Therefore, the BOS boundaries are considered boundaries of stability as well since the COP can only move within them in an attempt to keep the COM within the same limits [4]. Movement of the COP outside the BOS results in the COM following beyond the limits of the BOS, leading to a loss of postural control and, thereby, balance.

Many studies have analyzed the methods of postural control in humans during quiet standing for the purpose of understanding the way that the body maintains balance [2], [4]–[21]. These studies have provided much insight into the way that the human body stays upright. One main takeaway is the general oscillatory pattern that the COP and COM can be expected to follow under typical neurologic function, where the COP oscillates about the COM to counteract a potential fall that could otherwise be caused by the COM moving too far in any direction.

In addition to COP oscillations, the postural control mechanism utilizes ankle and hip strategies while maintaining balance [22]. The ankle strategy compensates for a perturbation of balance by adjusting the angle that the ankle creates between the foot and the leg as opposed to compensating by moving the upper body. This is often thought of as a single inverted pendulum model [2], [23], [24]. When the body utilizes the hip strategy, the angle of the hips relative to the upper and lower body is adjusted in a similar way to how the ankle strategy works. It is useful for strong perturbations [13]. This is often thought of as a double inverted pendulum model [2], [23], [24].

Correlation, approximate entropy, velocity magnitude, velocity power spectrum density, and regression are all useful tools for understanding more about the functioning of the postural control system. Correlation provides information about the similarity of signals, approximate entropy provides information about the regularity of a signal, velocity indicates the rate of change of a signal, power spectral density indicates the frequencies at which a signal occurs, and regression gives a model to predict the relationship between a signal and time. This study utilized these analyses to determine patterns and indices present in postural control for neurotypical subjects in quiet standing positions for eventual comparison with the same data from concussed subjects.

1.2. Purpose

The aim of this study was to examine the relationship between center of pressure (COP) and center of mass (COM). These signals were chosen as they represent functionality of the complex postural control mechanism used to maintain balance. The goal was to determine patterns and indices present in correlation, approximate entropy, velocity, and power spectrum metrics as well as to determine an estimated baseline signal for different stability conditions. This information could be useful in tracking neurological deficits, such as concussion in athletes.

1.3. Scope

This study analyzed patterns and indices present in COP and COM signals during quiet standing of healthy, adult subjects. The two signals were analyzed using the bivariate technique of cross-correlation to determine the relationship between the two signals to gain an understanding of if and how the relationship between the two signals changes with various

stability conditions. Six different stability conditions were considered: feet together (FT), feet tandem with the dominant foot back (TanDB), and feet tandem with dominant foot forward (TanDF), for both eyes open (EO) and eyes closed (EC).

Additionally, the two signals were analyzed using univariate techniques to determine if a single signal can provide useful information. These techniques include autocorrelation, approximate entropy, velocity, power spectral density, and regression. The autocorrelation signal was compared to other correlation signals to determine relationships between signals. For approximate entropy, velocity, and power spectral density, a single value was calculated that could be compared between balance conditions. Regression analysis provided a baseline signal that could approximate what different stability conditions looked like, as well as an R squared value that could be compared between those stability conditions. One-way ANOVA testing was completed to compare the values of these analyses between the baseline conditions (EOFT) with the other conditions to determine the statistical significance of the findings.

It was also considered whether or not changes in the COP and COM signals are linked to specific frequency bands which are associated with neuronal activity. The frequency bands considered were the delta (0.5 – 4 Hz), theta (4 – 8 Hz), alpha (8 – 13 Hz), beta (13 – 30 Hz) and gamma (30 – 100 Hz) bands.

1.4. Assumptions

The assumption that very similar postural control mechanisms exist in all humans, but each individual has postural control that is unique from all others as it can be improved throughout one's life with different experiences was used throughout this study [25]. Therefore, the postural control in different people would function similarly at the base level but may be

more finely tuned in some than others. Because of this assumption, each subject was analyzed against themselves between different stability conditions so as to negate any bias due to differences in the postural control mechanism from one subject to another. It was also assumed that the EOFT condition would be the most stable among the six conditions tested. Accordingly, this was what the rest of the conditions were compared against for determining results. Finally, it was assumed that a resultant COP, as opposed to considering the individual COPs of each foot, would provide the information needed for this analysis.

1.5. Hypothesis

Studies have shown that the COP oscillates about the COM in order to maintain balance. Based upon this understanding, it was hypothesized that COP would show a delay in recovery from finding itself beyond the COM, in any direction, in trials performed under a less stable condition when compared to trials performed under a more stable condition. It was also hypothesized that both COP and COM would display a higher approximate entropy in less stable conditions due to postural control behavior being more erratic while attempting to keep up with increased perturbations to balance. Along with approximate entropy being higher, it was hypothesized that the R-squared value of regression would be lower in low stability conditions as a model would be able to accurately approximate less of the information in the signals. Furthermore, it was hypothesized that velocity of the signals would increase as stability decreased, considering lower stability requires more adjustments from the postural control mechanism in the same amount of time.

1.6. Significance

Determining the relationship between COP and COM signals provides crucial information about the necessary monitoring that needs to be completed in order to adequately assess postural control functionality. As it becomes known what information is most indicative of the functionality of the human postural control mechanism, the additional information gained from univariate analysis on those signals should provide insight into patterns and indices that are characteristic of a healthy brain and how it works to maintain balance. Understanding how a healthy brain works to keep a person upright during different stability conditions is invaluable for future research with subjects that have suffered from a traumatic brain injury such as a concussion. Understanding how a healthy brain reacts to different stability conditions and the way that the body moves in response to that reaction will allow for comparison to the way an unhealthy brain reacts to the same conditions and eventual conclusive testing for concussion diagnosis.

1.7. Definitions

Quiet Standing: standing position where a person has both feet on the ground

Center of Pressure: location of the resultant pressure under a person's points of contact with the ground

Center of Mass: point location representing the weighted average of the body's entire mass

Approximate Entropy: measure of the amount of uncertainty in a signal

Power Spectral Density: measure of the spectral content of a signal

Regression: approximates a function for a set of data

Pearson's Correlation Coefficient: measures the linear relationship between two variables

ANOVA: determines if the difference between signals is statistically significant

Dunnett's Post-Hoc Test: compares all signals to one baseline signal and determines which are significantly different

Chapter 2. Manuscript

Abstract

The body's postural control mechanism is responsible for responding to perturbations of balance and keeping the body upright. One of the main ways that this is completed during quiet standing, where both feet are planted on the ground, is through center of pressure oscillations. In these oscillations, the center of pressure circles around the center of mass, constantly counteracting any lean that exists in the body. These oscillations can be recorded with floor-embedded force plates and center of mass can be recorded with a motion capture system. In this research, these signals were recorded for stances with feet together and feet tandem with eyes opened and eyes closed with neurotypical subjects. Center of pressure and center of mass were compared to determine if they provide the same information as one another. Through different correlation measures, it was shown that they generally have a very strong relationship to one another, and that COP provides as much information as COM.

From there, center of pressure was further analyzed using approximate entropy, velocity measures, and regression. This analysis showed evidence of increased irregularity, increased velocity, and increased frequency content in center of pressure oscillations during standing conditions with lower stability. ApEn indicated significant differences between the most stable eyes open, feet together condition and all of the less stable feet tandem trials for eyes open and eyes closed in nearly every subject. Velocity, however, only indicated significant differences between the most stable condition and the least stable eyes closed, feet tandem trials. Regression analysis showed a decrease in the content that could be explained by the model as stability decreased. Regression also provided a general illustration of what each stability condition may

be expected to look like, which can be used to compare future data against. The results of this study will be useful to compare non-neurotypical subject data to moving forward.

2.1. Introduction

The physiological processes involved with keeping a human upright are complex and dynamic. In mechanics, balance is a term used to describe a state where the sum of all forces acting on an object are zero [1]. Postural control is the act of maintaining balance during all activities [1]. Anticipatory and reactive processes help maintain postural control and keep a person from falling during both expected and unexpected perturbations of their balance [1]. In these processes, sensory neurons work with the central nervous system (CNS) to trigger motor neurons which contract muscles in the lower body to counteract extrinsic and intrinsic forces that impede balance [5]. The information monitored by sensory neurons to make the necessary changes includes tracking the center of mass (COM) and center of pressure (COP) of the body, in relation to its base of support (BOS) [25].

Standing humans have a few different metrics that allow for balance and postural control to be analyzed quantitatively. The two most commonly used are COP and COM. These are often used interchangeably. However, clinically the two metrics are distinct. The COP is the point location of the resultant ground reaction force where the body makes contact with the ground. It is located in the position of the weighted average of all of the pressures that are being exerted on the body by the ground, where the sum of the moments of each individual pressure is equal to the moment of the resultant ground reaction force vector acting at the COP [2]. When a person has both feet planted on the ground, each foot has a separate COP, which can be combined to create one resultant COP for the entire body. The COM is the point location on the body that is

representative of all of its mass, where the moment of the COM is equivalent to the sum of the moments of the weight acting at every point on the body [2]. This metric is in a relatively constant location in the center of the body, about one-half to two-thirds of the way up between the feet and the highest point of the body [2].

Another metric that is important to consider is the BOS. This is an area underneath the body defined by the perimeter around all points of contact with the ground. It defines the limits of motion for which a person can be stable without stepping [3]. Therefore, the BOS boundaries are considered boundaries of stability as well since the COP can only move within them in an attempt to keep the COM within the same limits [4]. Movement of the COP outside the BOS results in the COM following beyond the limits of the BOS, leading to a loss of postural control and, thereby, balance. An illustration of the three described metrics is seen in Figure 2.1.

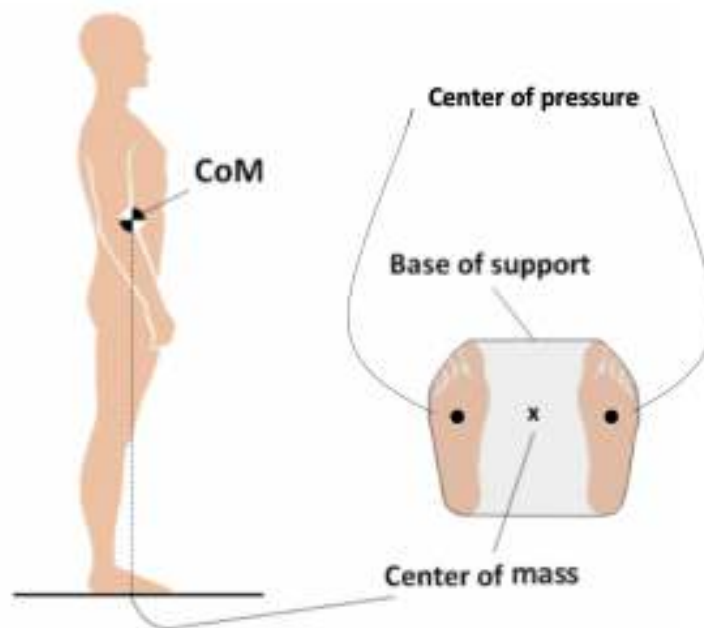


Figure 2.1. Center of pressure, center of mass, and base of support locations, adapted from [26]

Many studies have analyzed the methods of postural control in humans during quiet standing for the purpose of understanding the way that the body maintains balance [2], [4]–[21]. These studies have provided much insight into the way that the human body stays upright. One main takeaway is the general oscillatory pattern that the COP and COM can be expected to follow under typical neurologic function. For example, if the COP moves behind the COM, a person would fall backward without intervention. As the COP moves farther from the COM, angular acceleration and velocity increase, causing the body to fall more quickly. In order to stop this motion and an eventual fall, the body pivots about the ankle, causing an anterior angular velocity and acceleration of the body and moving the COP in the anterior direction due to the moment resulting from the weight acting downward at the COM and the ground reaction force acting upward at the COP. While the body sways forward, the COP and COM line up and the person is no longer at risk of falling backward. At this point, the angular acceleration shifts and begins acting in the posterior direction, due to a change in direction of the moment, while the velocity continues moving anteriorly. When the COP has moved in front of the COM, the body must pivot about the ankle to avoid a forward fall and the angular velocity shifts directions, leading to posterior rotation and causing the body to sway backward. This postural control pattern of the COP oscillating around the COM continues while a person maintains quiet standing and is depicted in Figure 2.2.

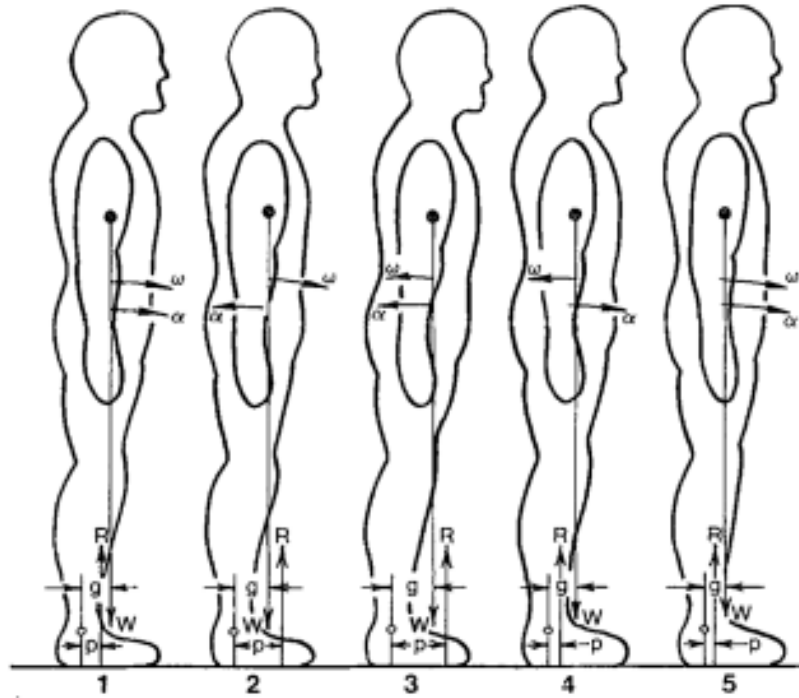


Figure 2.2. Center of pressure oscillations at five points in time where the COP location is represented by R , the COM location is represented by W , angular velocity is represented by ω , and angular acceleration is represented by α [2].

While many researchers have studied the methods of postural control, no studies were found that utilized both COP and COM signals to characterize postural control in neurotypical subjects during changes in stability conditions of quiet standing. There have been a number of studies that analyzed the postural control mechanism in subjects suffering from a concussion while completing trials that involved walking coupled with a cognitive test such as answering questions [6], [9], [27], [28]. While the information gained from these studies is important, it would be difficult to apply outside of a lab environment set up with multiple permanent force plates to ensure uniform data recording while the subject moves as variables are more difficult to control with a moving subject. In quiet standing, changing stability conditions can result from a different standing position or be due to neurological changes that affect the functionality of the body's postural control. In this case, manual changes in standing position were implemented

with neurotypical subjects in order to develop indices that could be useful in tracking neurological deficiencies, such as concussion in athletes.

There are many analyses that can aid in learning more about the patterns of the dynamic COP and COM signals. As the COP and COM of a person with typical neurological functionality can be expected to follow a relatively regular pattern, approximate entropy - a measure that quantifies the regularity of a signal [29], can be useful in identifying changes due to loss of stability. A high stability scenario will be expected to show quite regular movement of those entities, so entropy should be quite low. However, if the scenario is less stable or a person has neurologic functionality that has been negatively affected, irregularity and, therefore, entropy, should increase.

The velocity of these metrics can give information about how quickly a person sways back and forth in attempt to maintain balance. The first derivative of the COP and COM signals provides this knowledge. Comparing the changing velocity between trials of different stability conditions may help identify useful indices for quantifying loss of postural control, independent of the cause – i.e. due to postural changes or neurological changes. In addition to comparing the magnitude of velocity between conditions, the power spectral density (PSD) is another method that may help identify changing postural control by providing information about the frequency content in a signal. Identifying objective metrics from the COP and COM signals could lead to better outcomes when screening for concussive damage.

While every person will have COP and COM responses to quiet standing conditions that look different from those of another, it is possible to develop a neurotypical baseline of these signals using regression. This method considers the relationship between, in this case, the COP

or COM signals and the time over which the signals were recorded [30]. Therefore, it can allow for clear indication of what a certain condition should look like within a certain amount of error.

The purpose of this study was to examine the patterns and indices present in COP and COM signals as well as the relationship between COP and COM signals during quiet standing conditions for healthy adults. Identifying the way that these signals interact at various levels of stability in a neurotypical subject would allow for baseline patterns and behavior to be determined. As these patterns and behavior are understood, the knowledge of how COP and COM look for a healthy individual can be compared to those signals for an individual under suspicion of abnormal neurological functioning, such as a concussion, to provide insight into how the person is responding to postural control requirements.

2.2. Methods

2.2.1. Participants

This study included data from healthy adults of varying levels of physical activity with no history of neurological or muscular disorders or injuries. Two males and four females, between the ages of 18-34, voluntarily provided their signed informed consent prior to participation in this study. Before collection of data commenced, foot dominance for each subject was determined based upon the leg with which they preferred to kick a ball. If a subject was unable to provide a preference for that, they were asked to stand on one leg to determine which they were most steady on. This data collection was approved by the Institutional Review Board at Grand Valley State University (18-246-H) for previous research. The approval was extended to allow for further analysis of the data in this study.

2.2.2. Procedure

Five, 30-second trials of six different balance conditions were completed with each subject as shown in Table 2.1. To obtain a stable baseline condition to compare data for other balance conditions to, the eyes open, feet together (EOFT) condition was considered to be the most stable configuration and completed first. The subject then progressed through increasingly unstable balance conditions. Between each trial, a 30-second break was allowed, with a longer 2-minute break between each balance condition. Conditions were completed in the same order listed in the table for all subjects.

Table 2.1. *Quiet standing balance conditions*

| Order | Balance Condition | Description |
|--------------|--------------------------|--|
| 1 | EOFT | Eyes open, feet together (most stable, baseline) |
| 2 | ECFT | Eyes closed, feet together |
| 3 | EOTanDB | Eyes open, feet tandem, dominant foot in back |
| 4 | ECTanDB | Eyes closed, feet tandem, dominant foot in back |
| 5 | EOTanDF | Eyes open, feet tandem, dominant foot in front |
| 6 | ECTanDF | Eyes closed, feet tandem, dominant foot in front |

The self-reported foot dominance was used for each subject to satisfy the description of relevant conditions. Balance tasks were performed barefoot with the arms positioned with the index finger pointed towards the shoulder on the same side of the body and the elbows pulled in. An image of one of the subjects performing feet together and feet tandem tasks are shown below in Figure 2.3 as generated by the Nexus software.

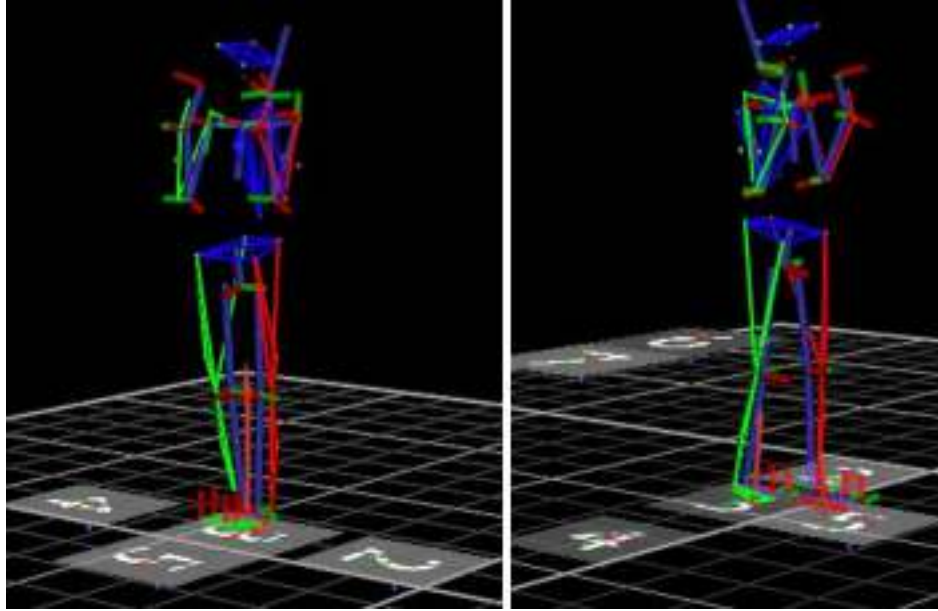


Figure 2.3. *Subject stance for feet together (left) and feet tandem (right) trials*

For feet together conditions, both feet were placed on one force plate while feet tandem conditions utilized two force plates, with each foot fully on an individual force plate. The subject was asked to hold the quiet standing position for the full thirty seconds without moving their body or stepping out of position.

2.2.3. Data Acquisition

2.2.3.1. Motion Capture and Force Plates

To track the movement trajectories of a modified Full-Body Plug-in-Gait (FB PiG) model, 16 Vicon MX cameras (Oxford Metrics, Oxford, UK) were used. Data were collected at a sampling frequency of 120 Hz during quiet standing balance tasks. Recording of this data resulted in three separate COM signals for each trial, including the x, y, and z axes for the location of the COM. Of those signals, the x and y axis data were used for analysis, which represents the anterior/posterior (AP) and medial/lateral (ML) directions for the subject,

respectively. Vicon Nexus motion capture software v2.8 (Oxford Metrics, Oxford, UK) calculated the COM from the output of the motion capture cameras using Dempster’s anthropometric data to compute segmental centers of mass and inertial properties to compute joint kinetics as described in [31]. The modified FB PiG model included additional fifth metatarsal (5thMet) and medial knee markers. The set of markers were placed on the subject as shown in Figure 2.4.

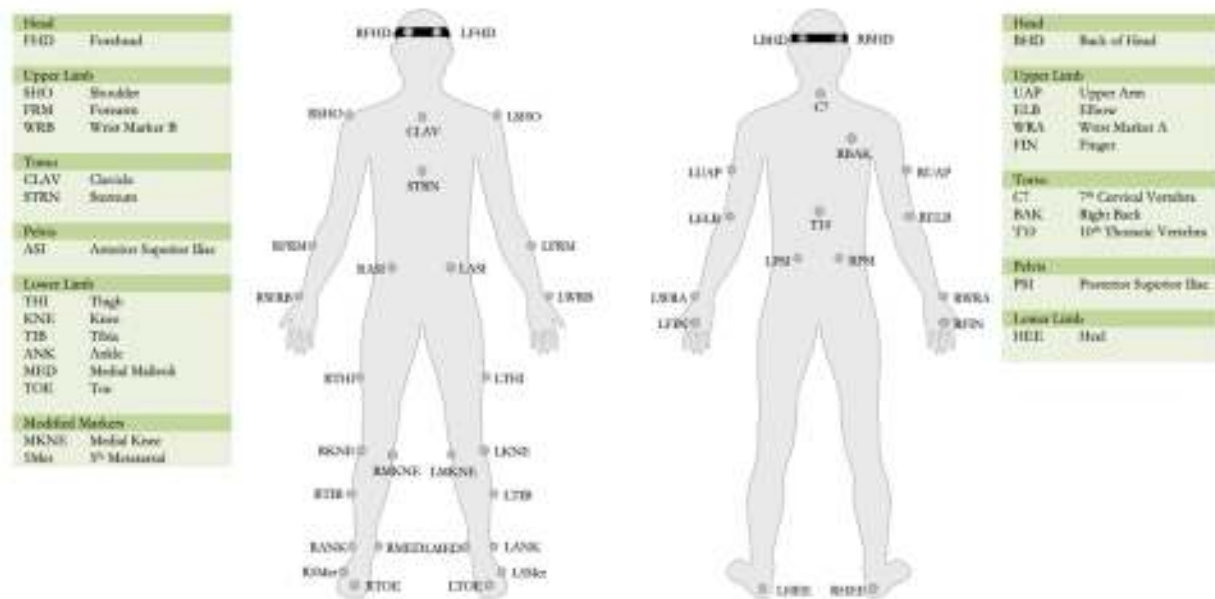


Figure 2.4. Modified Full-Body Plug-in-Gait model [32]

For collection of ground reaction forces during quiet standing balance tasks, two floor-embedded AMTI (Advanced Mechanical Technology Inc., Watertown, MA) force plates were used. These collected data at a sampling frequency of 1200 Hz. They were oriented one directly in front of the other. For feet together tasks, both feet were placed on one force plate. The second force plate was implemented to measure separate ground reaction forces when the feet were positioned in a tandem stance [32]. Similar to the COM data, this data collection resulted in three separate COP signals for each force plate used, for each trial. These include the x, y, and z axis

points for the location of the COP. Of those signals, the x and y axis data were used for analysis, as they represent the AP and ML directions for the subject, respectively. COP and COM signals were synchronized using Vicon Nexus motion capture software v2.8 (Oxford Metrics, Oxford, UK). The orientation of the feet on the force plates is illustrated in Figure 2.5.

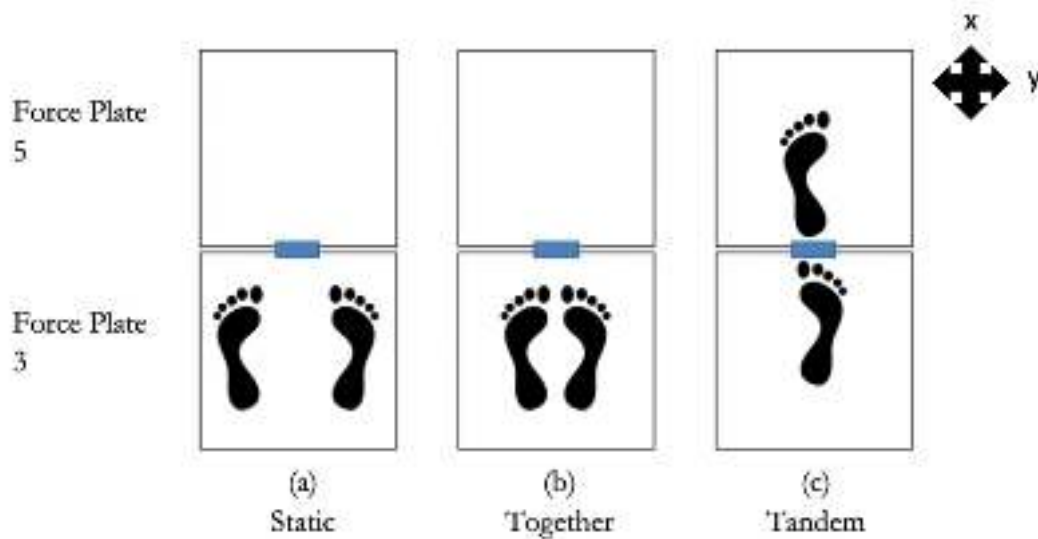


Figure 2.5. Feet orientation adapted from [32]

2.2.3.2. Coordinate Systems

The coordinate systems that the COP and COM signals were recorded in are two separate systems. The COP signal was recorded in the force plate coordinate system, where the origin was located in force plate two, which was not used in recording. In this system, the x-axis ran in the AP direction with respect to the subject where positive x was anterior. The y-axis ran in the ML direction where positive y was to the right of the subject. The COM signal, on the other hand, was recorded in the laboratory coordinate system, where the origin was located in a corner of the room, as opposed to being associated with the force plates. In this system, the x-axis also ran in the AP direction with respect to the subject, however, positive x was posterior for this system.

The y-axis was the same as the force plate coordinate system where it ran in the ML direction and positive y was to the right of the subject. These coordinate systems are illustrated in Figure 2.6.

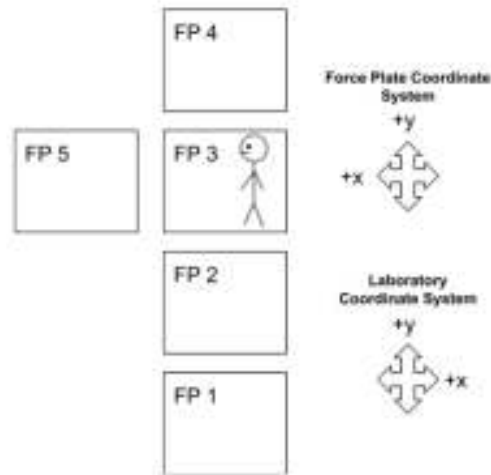


Figure 2.6. Orientation of coordinate systems

While the coordinate systems that the two signals were recorded in were different, the Vicon Nexus motion capture software v2.8 (Oxford Metrics, Oxford, UK) converted the COP data into the laboratory coordinate system. Therefore, data that was analyzed had x and y-axis data that were in the same direction as one another in relation to the subject. This final form had a positive x-axis in the posterior direction and a positive y-axis to the right of the subject.

2.2.4. Data Analysis

The COP and COM data were analyzed using both bivariate and univariate measures in the time and frequency domains using Python 3.7.6 (Python Software Foundation, <https://www.python.org/>). As all people have a slightly different postural control system, each subject was analyzed separately so as to not have data skewed by differences in magnitude or

behavior of data from one subject to the next. The process for this analysis is illustrated in Figure 2.7.

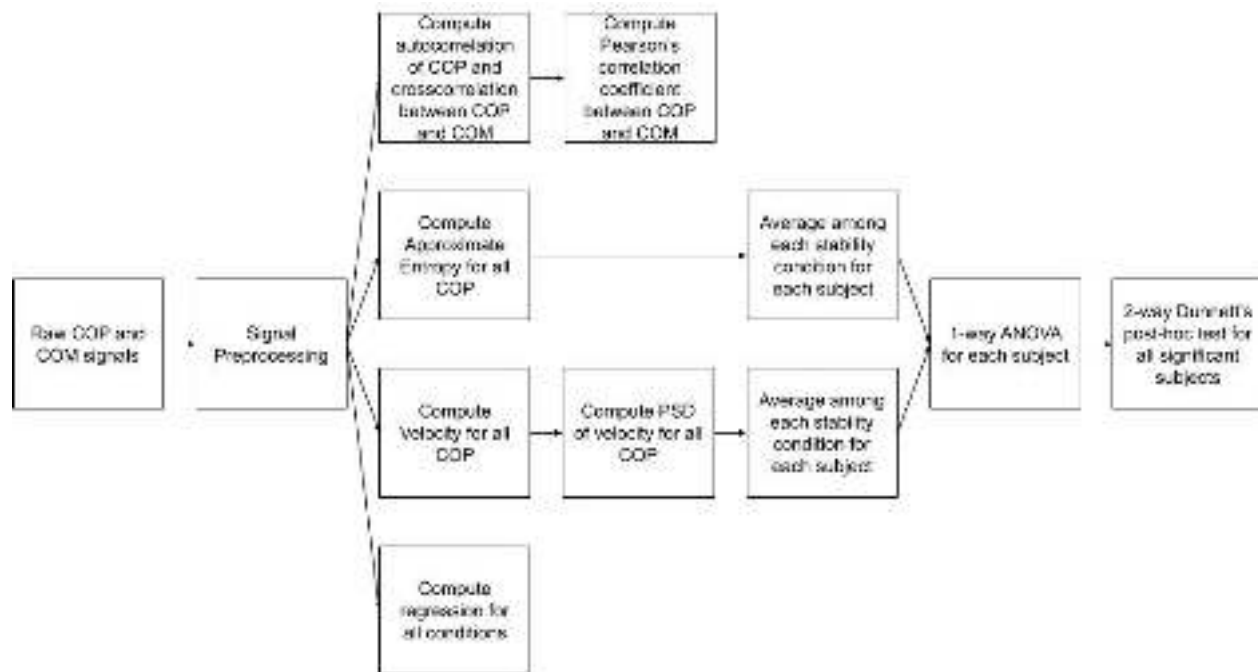


Figure 2.7. Signal processing function block diagram

2.2.4.1. Signal Preprocessing

A Fast Fourier Transform was applied to the COP signal of the baseline condition for all subjects to allow for analysis of the frequency content of the raw data. Upon completion of this, a fourth-order, zero-lag, low-pass Butterworth filter was applied with a cutoff frequency of 6 Hz via Nexus motion capture software v2.8 (Oxford Metrics, Oxford, UK) to eliminate any noise present in the signal that could not be attributed to each subject’s postural control mechanism. This cutoff frequency was chosen because numerous studies on the frequency content of postural sway have shown that its signal content exists at or below 5 Hz [33]–[35]. This value was corroborated by the frequency analysis performed on the current study’s data.

The movement trajectories collected via motion capture cameras were filtered by the Nexus motion capture software v2.8 (Oxford Metrics, Oxford, UK) using a Woltring filter with a 15 Hz cutoff [36]. This is the recommended course of action for movement trajectory collection in the Nexus software. The movement trajectories are what were used to calculate the COM.

In addition to the application of these filters, the two separate COP signals for tandem balance conditions had to be combined into one resultant COP so that it could be directly compared to the feet together conditions. As stated previously, feet together trials were completed using only one force plate while feet tandem trials were completed using two force plates, where each plate collected data for one foot, respectively. Therefore, the feet together data resulted in only one COP signal, while the feet tandem data resulted in two COP signals. In order to compare the two condition types, the two COP signals for the feet tandem trials were combined into one resultant COP for the entire body as follows [2], [37], [38]:

$$COP_{net} = COP_L \frac{F_{zL}}{F_{zL} + F_{zR}} + COP_R \frac{F_{zR}}{F_{zL} + F_{zR}} \quad (2.1)$$

Where COP_L and COP_R are the values of the COP signal from the left and right foot, respectively, and F_{zL} and F_{zR} are the vertical forces exerted on the force plates under the left and right foot, respectively.

2.2.4.2. *Approximate Entropy*

Approximate entropy (ApEn) quantifies the regularity of a time-series signal [29]. It is well suited for small data sets, which nicely frames the measure to be used on small windows of a larger dataset to obtain a moving representation of the regularity of a signal. ApEn is defined as follows [29]:

$$-ApEn = \Phi^{m+1}(r) - \Phi^m(r) \quad (2.2)$$

Where m and r are fixed values, m being the length of compared runs and r is a filter value, and $\Phi^m(r)$ is defined as:

$$\Phi^m(r) = (N - m + 1)^{-1} \sum_{i=1}^{N-m+1} \ln [C_i^m(r)] \quad (2.3)$$

Where N is the total number of data points and $C_i^m(r)$ is defined as:

$$C_i^m(r) = \frac{\text{number of } j \leq (N-m+1) \text{ such that } d[x(i), x(j)] \leq r}{N-m+1} \quad (2.4)$$

Where $d[x(i), x(j)]$ is the maximum distance between the respective scalar components of vectors $x(i)$ and $x(j)$.

As the meaning behind Equation 2.4 for calculating $C_i^m(r)$ can be difficult to discern, Figure 2.8 has been provided to explain how the numerator is determined if the value of m is set to two, which is what was used in this research. Here, each pair of neighboring data points creates a line segment, $X(i) = [x(i) \ x(i+1)]$. Two darks regions are seen in the figure, which represent the tolerance regions for the calculation. The tolerance bands are separated by a distance of r , to satisfy the requirement in the equation that a line segment have a distance less than or equal to r . The numerator of the equation is equal to the number of line segments for which the first point falls within tolerance region one and the second point falls within tolerance region two [39]. In the case shown below, there are four line segments which satisfy the requirement: $X(8)$, $X(15)$, $X(19)$, and $X(24)$. They are shown in bold.

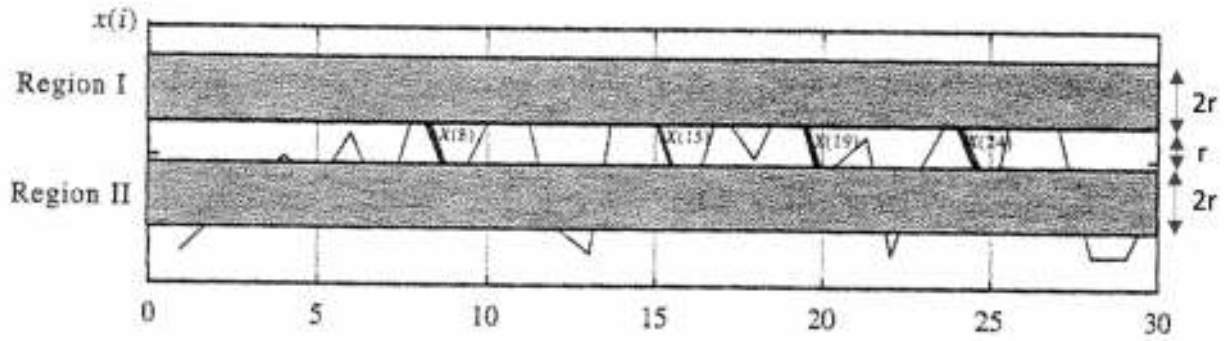


Figure 2.8. Graphical interpretation of $C_i^m(r)$ in ApEn, adapted from [39]

A signal will have an ApEn value of zero if it is entirely predictable. This value increases as the uncertainty in the signal increases. This provides insight into the regularity of the COP oscillations for a subject to determine whether the postural control mechanism is functioning as expected or not. Figure 2.9 shows how the ApEn value of a periodic signal is much lower than that of white noise.

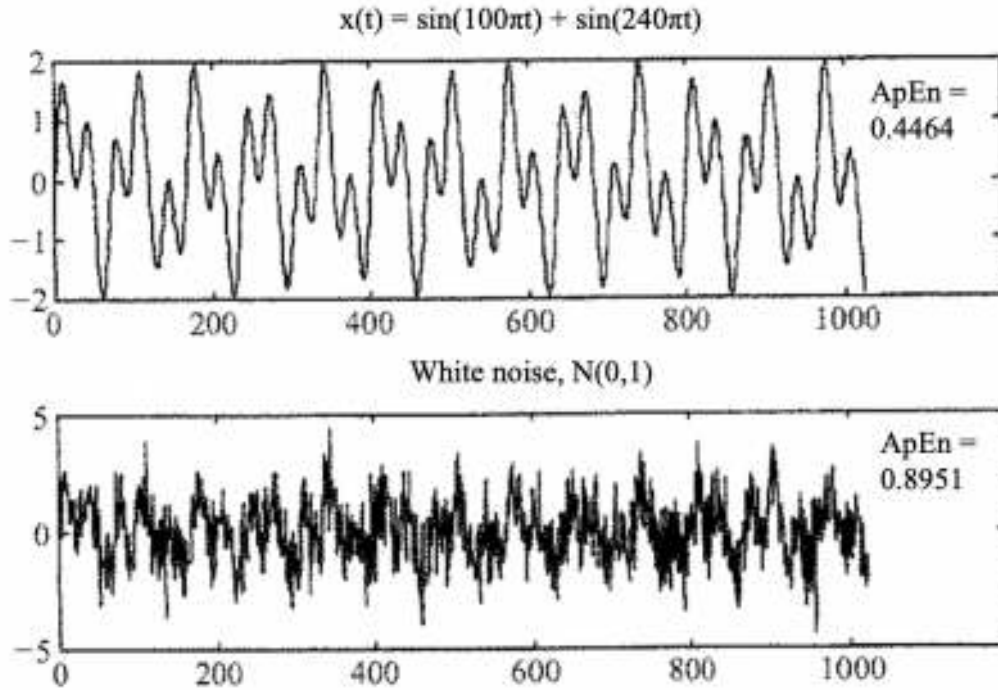


Figure 2.9. Difference in approximate entropy values between a periodic signal and white noise, adapted from [39]

Moving approximate entropy was calculated for all COP trials using windows of size 1800, or 1.5 second intervals, with a 50 percent overlap to create 39 segments. This allowed for visual understanding of how the approximate entropy changed over time, however, these 39 values were averaged to obtain a single approximate entropy value for further calculations. This was done as numerous studies have shown postural sway to be a stationary signal in durations greater than 15 seconds [19], [40], [41].

2.2.4.3. Velocity

The first-derivative velocity provides information about how quickly the position of the COP and COM moves during postural control. This is estimated using the following equation:

$$V(i) = \frac{x(i+1) - x(i)}{t(i+1) - t(i)} \quad (2.5)$$

Where x is the COP or COM signal, t is the time vector, and i is the index equal to the length of the signal. This slope equation gives the rate of change of the signal, providing knowledge about how quickly the body is swaying while maintaining balance.

Velocity was calculated for all COP signals between every two points. This created a new signal with a length equal to the original COP signal. The magnitudes of the data in the new velocity signal were averaged together to create a single value representing the average velocity for each trial, respectively.

2.2.4.4. *Power Spectral Density*

The power spectral density (PSD) of a signal indicates how much content of that signal exists at each frequency. High velocity signals contain more content at higher frequencies than signals that change with low velocity. This measure is defined as follows:

$$S_{xx}(\omega) = \int_{-\infty}^{\infty} R_{xx}(\tau) e^{-j\omega\tau} d\tau \quad (2.6)$$

Where $R_{xx}(\tau)$ is the autocorrelation and is defined as follows:

$$R_{xx}(\tau) = \frac{1}{T_0} \int_0^{T_0} x(t) * x(t + \tau) dt \quad (2.7)$$

Where the signal in question is a finite length, real valued signal, $x(t)$, from $0 \leq t \leq T_0$ and where τ is some amount of lag.

Auto-power, or the PSD of an individual signal, was determined for the velocity signal of all COP data. This was not calculated for the raw COP signal, as numerous studies suggest that content for that signal exists only at frequencies that are 5 Hz and less [33]–[35]. Therefore,

further analysis was unnecessary as the data would have no connection to neural activity and the behavior of content that does exist has been well documented.

In order to calculate the PSD for the velocity signals, Python's *NumPy* tool *correlate* was used to calculate the autocorrelation of the signal. This was followed by the *NumPy* tool *fft.fft* to complete the necessary Fourier transform to obtain the PSD. A summation of all frequency content in a signal was performed to obtain a metric of total power that could be compared between trials.

In addition to the autocorrelation calculation that was completed as a part of the PSD calculation, the cross-correlation between COP and COM signals of the same direction was also performed using the *NumPy correlate* tool. This gave information about the similarity between the two signals. Cross-correlation is defined as follows:

$$R_{xy}(\tau) = \frac{1}{T_0} \int_0^{T_0} x(t) * y(t + \tau) dt \quad (2.8)$$

2.2.4.5. Regression

Regression estimates the relationship between a signal and the time over which it was recorded. This allows for a baseline idea of what a signal can be expected to look like. It is defined as follows:

$$y = \beta_0 + \beta_1 x + \beta_2 x^2 + \beta_3 x^3 + \dots + \beta_n x^n + \varepsilon \quad (2.9)$$

Where each β is a coefficient for the n th power of the independent variable, x , and ε is the error in the regression. This is often calculated in matrix form as shown below:

$$\begin{bmatrix} y_1 \\ y_2 \\ y_3 \\ \vdots \\ y_n \end{bmatrix} = \begin{bmatrix} 1 & x_1 & x_1^2 & \dots & x_1^m \\ 1 & x_2 & x_2^2 & \dots & x_2^m \\ 1 & x_3 & x_3^2 & \dots & x_3^m \\ \vdots & \vdots & \vdots & \ddots & \vdots \\ 1 & x_n & x_n^2 & \dots & x_n^m \end{bmatrix} \begin{bmatrix} \beta_0 \\ \beta_1 \\ \beta_2 \\ \vdots \\ \beta_m \end{bmatrix} + \begin{bmatrix} \varepsilon_0 \\ \varepsilon_1 \\ \varepsilon_2 \\ \vdots \\ \varepsilon_n \end{bmatrix} \quad (2.10)$$

This was calculated using the *LinearRegression* and *PolynomialFeatures* tools from the *scikit-learn* machine learning library for Python. It was done to represent the relationship between the time over which the data were recorded and an average of COP signals in the AP and ML directions, from groupings of all trials from each respective stability condition. The average COP signals were found by, first, converting all data to a delta value, where each data point represented the deviation from the starting position of the signal. This allowed for all signals to be on the same scale, starting at zero, as opposed to having a magnitude that changed significantly based on subject. The mean value of the new signals of delta values was then taken. This allowed for a visualization of what each condition can be expected to look like, in general, and not be subject specific.

2.2.4.6. Statistical Analysis

Each subject was considered independent from one another due to the assumption of unique postural control mechanisms. Furthermore, trials and stability conditions were considered independent of one another due to the breaks given between each of them. The subject's ability to rest and then reset allow for this assumption. This allowed for a one-way analysis of variance (ANOVA) test to be completed for each subject in both the AP and ML directions. This was done velocity magnitude, velocity PSD, and ApEn.

The ANOVA testing resulted in information about whether there were statistically significant differences between different stability conditions for each of the listed analyses. If

ANOVA determined that there were significant differences between conditions, a two-sided Dunnett's post-hoc test was completed to determine which conditions varied significantly from one another. This test compared the baseline EOFT condition to every other, less stable, condition.

2.3. Results

Examples of the COP data that were analyzed are illustrated in Figures 2.10 and 2.11, which display raw data from subject 1 for the most stable EOFT condition and one of the least stable conditions, ECFTanDF, respectively. Raw COP data examples from the remaining stability conditions can be found in Appendix A.

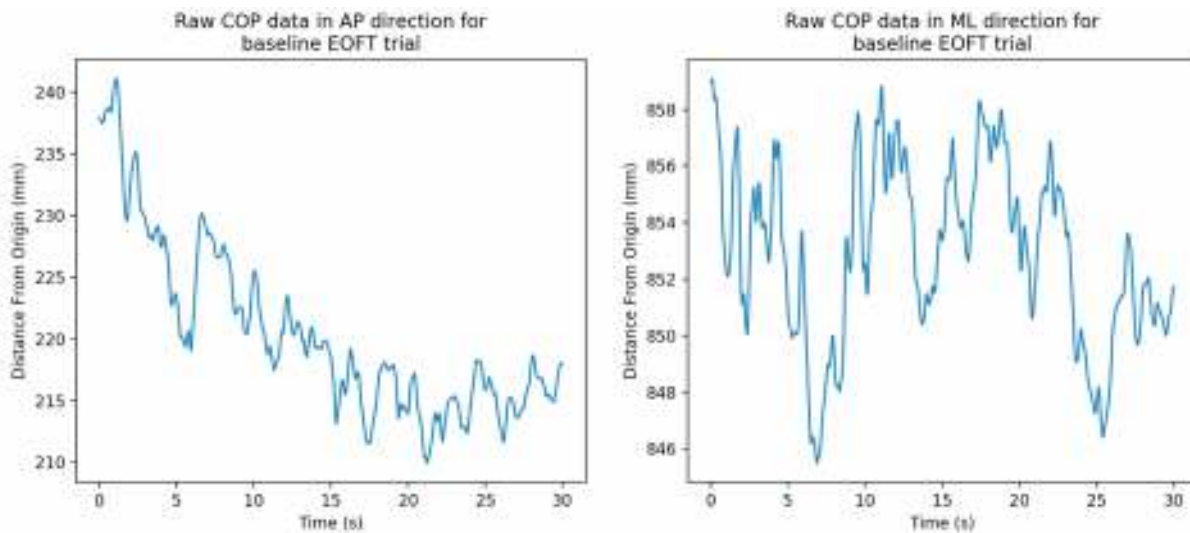


Figure 2.10. COP data for eyes open, feet together trial

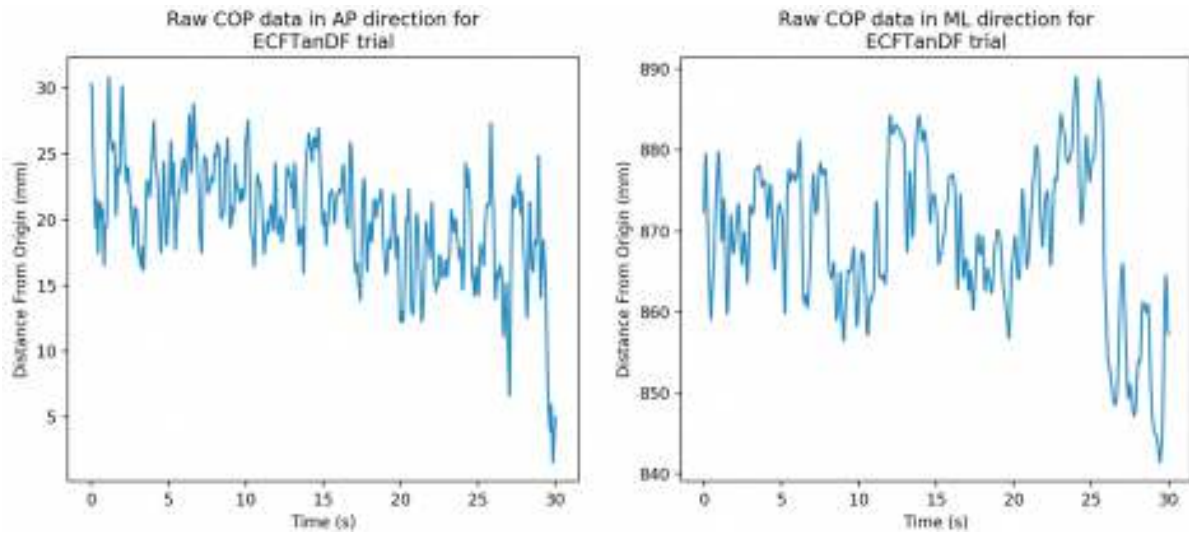


Figure 2.11. COP data for eyes open, feet tandem, dominant foot in front trial

While there are clear differences in the appearance of the COP in very stable conditions versus very unstable conditions, as less-stable conditions have less-smooth signals, there is no easy way to distinguish between each condition where the amount of stability differs only slightly.

Examples of the COM data that were analyzed are shown in Figures 2.12 and 2.13, which illustrate raw data from subject 1 during the EOFT condition and the ECFTanDF condition, respectively. Raw COM data from the remaining stability conditions can be found in Appendix A.

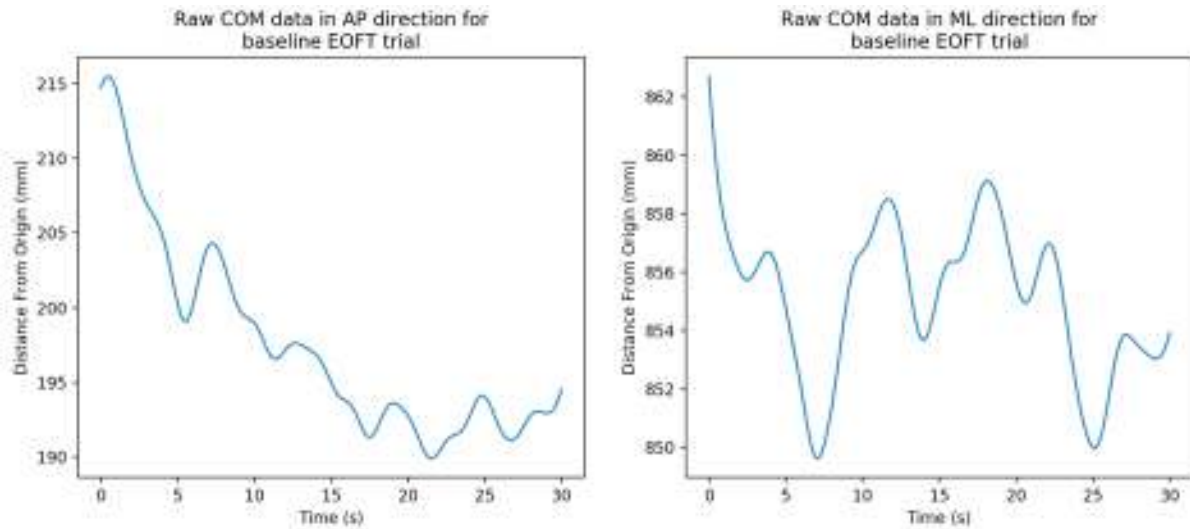


Figure 2.12. COM data for eyes open, feet together trial

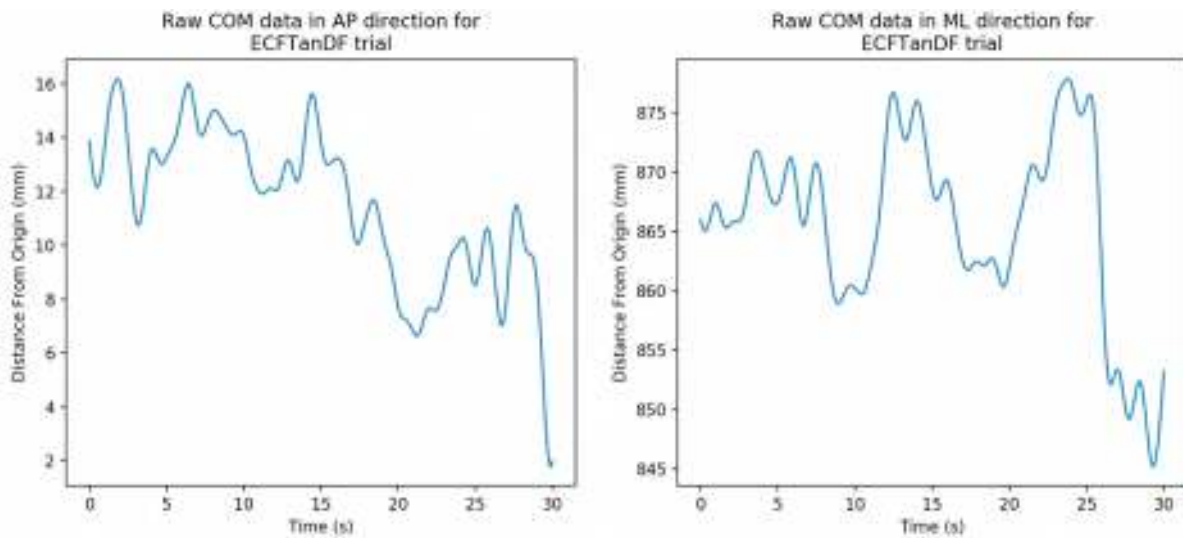


Figure 2.13. COM data for eyes closed, feet tandem, dominant foot in front trial

The COM signals appear to have very similar shapes to their coordinating COP signal. These signals are much smoother, however, and changes in signal appearance between stability conditions are much less significant than with the COP signals. Once again, there is no easy way to distinguish between conditions.

2.3.1. COP and COM Relationship

The COP and COM signals look very similar when compared between the same trial for each subject. An example of the two signals plotted together for a baseline EOFT trial for subject 1 is shown in Figure 2.14. Another example for an EOFTanDF trial is shown in Figure 2.15. As the two signals were recorded with different instruments, their signals had different magnitudes. Therefore, they were both standardized to have a mean of zero and a standard deviation of one for comparison.

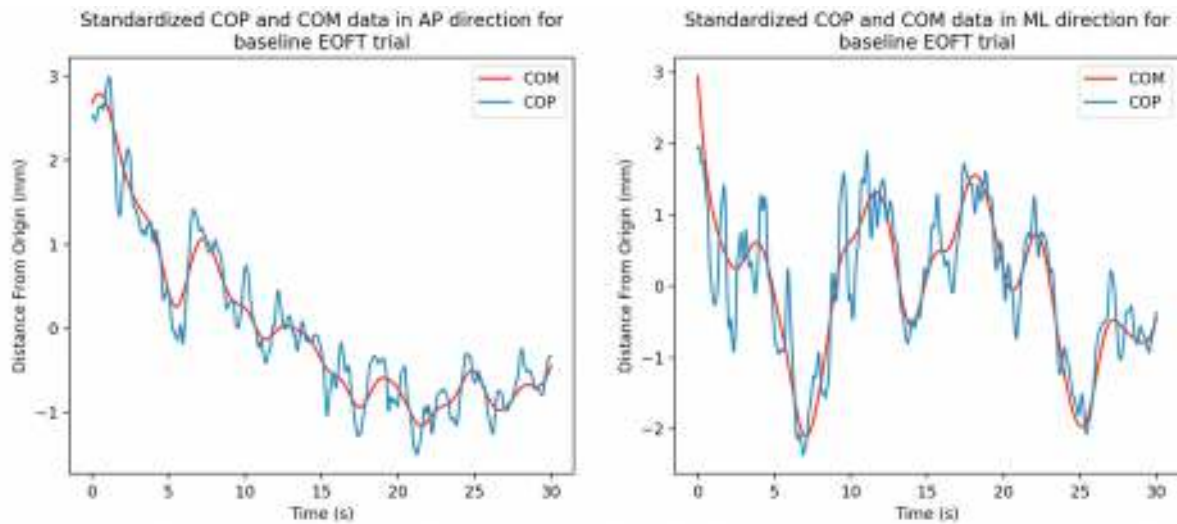


Figure 2.14. COP and COM signals for baseline eyes open, feet together condition in subject 1

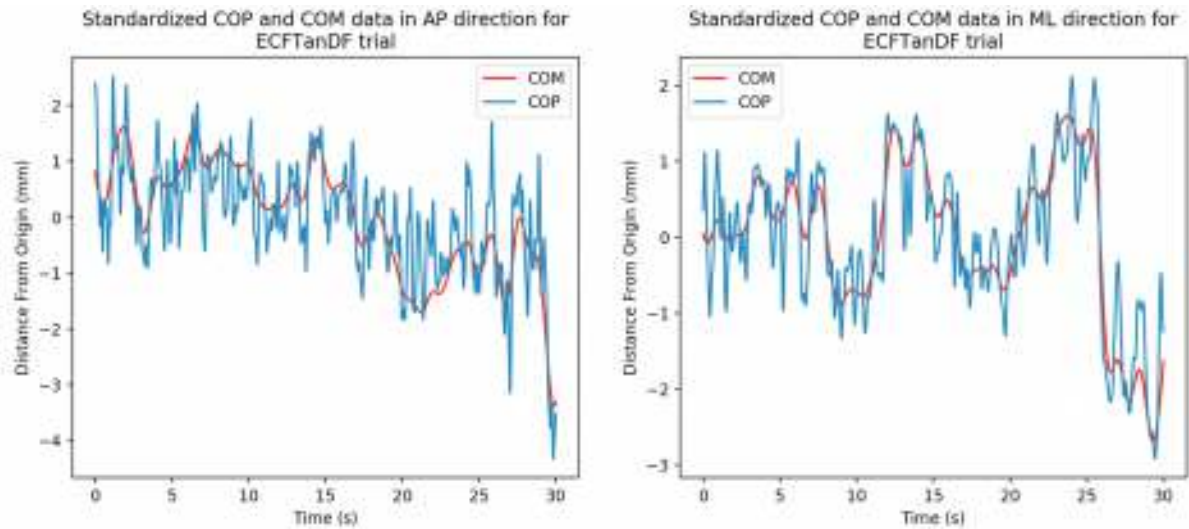


Figure 2.15. *COP and COM signals for eyes closed, feet tandem, dominant foot in front condition in subject 1*

From the above figures, the COP and COM signals follow the same pattern, but the COP signal displays higher frequency and magnitude of oscillations. While the signals appear very similar, it was important to determine how similar they truly were so that it was clear whether one signal could be used moving forward or if each signal provided information that the other did not, indicating that both signals should be used for further analysis. To do this, the autocorrelation of the COP signal was compared to the cross-correlation between the COP and COM signals of the same trial. An example of what this plot looks like is shown in Figure 2.16 for an EOFT trial and 2.17 for an ECFTanDF trial.

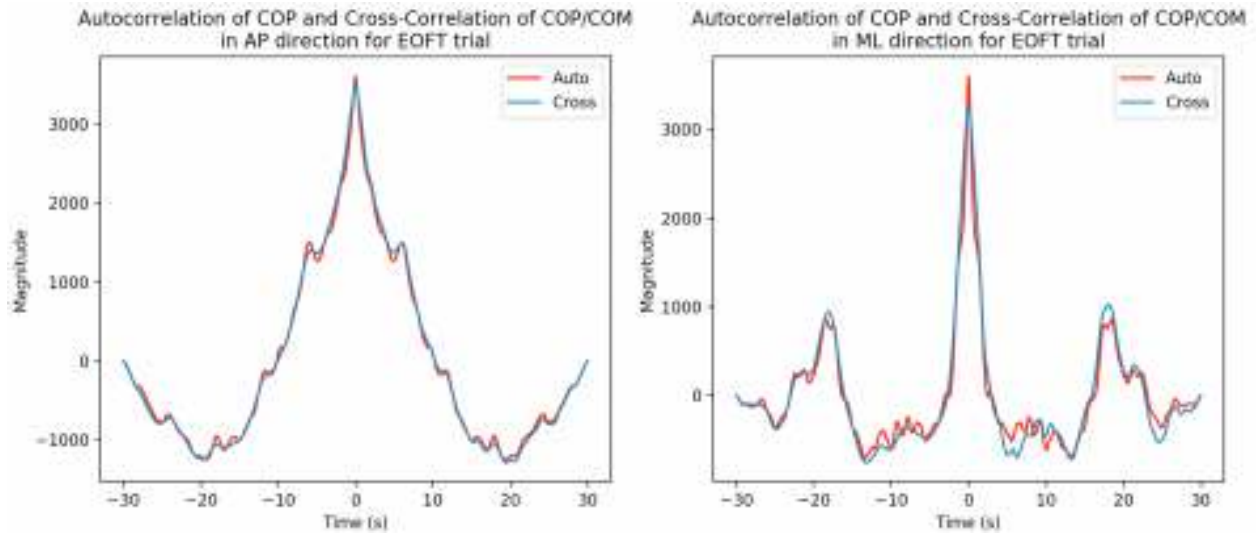


Figure 2.16. Autocorrelation and cross-correlation for baseline eyes open, feet together trial in subject 1

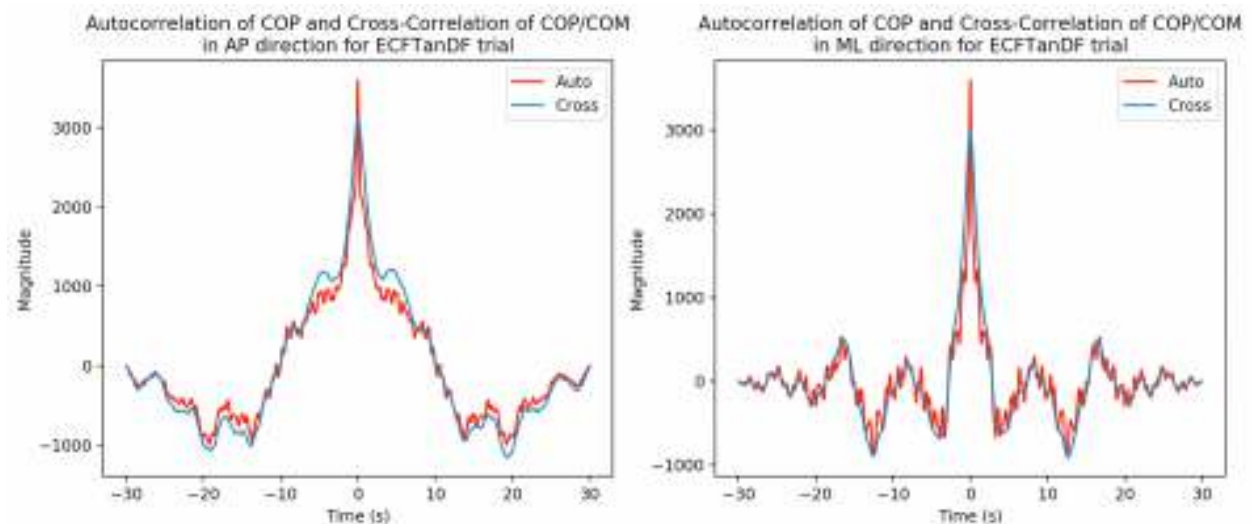


Figure 2.17. Autocorrelation and cross-correlation for eyes closed, feet tandem, dominant foot in front trial in subject 1

By completing autocorrelation and cross-correlation analysis it has shown that both COP and COM signals look very similar across all time lags. This further verifies the prediction that was made upon looking at the raw data that the two signals may be providing the same information. In order to determine exactly how similar the signals are and if it is reasonable to assume that they will provide the same information and to eliminate one of them from further

analysis, the Pearson's correlation coefficient was calculated between COP and COM signals for one trial from each stability condition for every subject. The results for the AP direction are seen in Table 2.2 and the results for the ML direction are seen in Table 2.3.

Table 2.2. *Pearson's Correlation Coefficient for one trial from each stability condition in all subjects in AP direction*

| Condition Subject | EOFT | ECFT | EOFTanDB | ECFTanDB | EOFTanDF | ECFTanDF |
|----------------------|-------|-------|----------|----------|----------|----------|
| 1 | 0.974 | 0.981 | 0.838 | 0.923 | 0.869 | 0.866 |
| 2 | 0.951 | 0.922 | 0.863 | 0.792 | 0.819 | 0.845 |
| 3 | 0.958 | 0.788 | 0.755 | 0.665 | 0.648 | 0.787 |
| 4 | 0.929 | 0.923 | 0.527 | 0.892 | 0.705 | 0.919 |
| 5 | 0.966 | 0.939 | 0.944 | 0.877 | 0.921 | 0.828 |
| 6 | 0.942 | 0.870 | 0.863 | 0.948 | 0.698 | 0.866 |

Table 2.3. *Pearson's Correlation Coefficient for one trial from each stability condition in all subjects in ML direction*

| Condition Subject | EOFT | ECFT | EOFTanDB | ECFTanDB | EOFTanDF | ECFTanDF |
|----------------------|-------|-------|----------|----------|----------|----------|
| 1 | 0.908 | 0.866 | 0.930 | 0.843 | 0.863 | 0.828 |
| 2 | 0.944 | 0.834 | 0.754 | 0.850 | 0.857 | 0.870 |
| 3 | 0.909 | 0.881 | 0.925 | 0.838 | 0.750 | 0.852 |
| 4 | 0.886 | 0.896 | 0.818 | 0.820 | 0.863 | 0.843 |
| 5 | 0.976 | 0.937 | 0.900 | 0.901 | 0.901 | 0.903 |
| 6 | 0.955 | 0.887 | 0.868 | 0.848 | 0.824 | 0.825 |

It has been suggested that a Pearson correlation coefficient that is greater than 0.7 indicates a strong relationship between two variables and a value greater than 0.9 indicates a very strong relationship [42]. Based upon those numbers, it is clear that the COP and COM signals have a strong or very strong relationship in most cases.

2.3.2. Approximate Entropy

Approximate entropy was analyzed for all COP data. A representative view, from subject 1 of the moving ApEn signal for a baseline EOFT condition in the AP and ML directions is seen in Figure 2.18 and a view of the moving ApEn of a much less stable, ECFTanDF trial is seen in Figure 2.19. The less stable condition in Figure 2.19 has a maximum magnitude that is much greater than the stable, baseline condition.

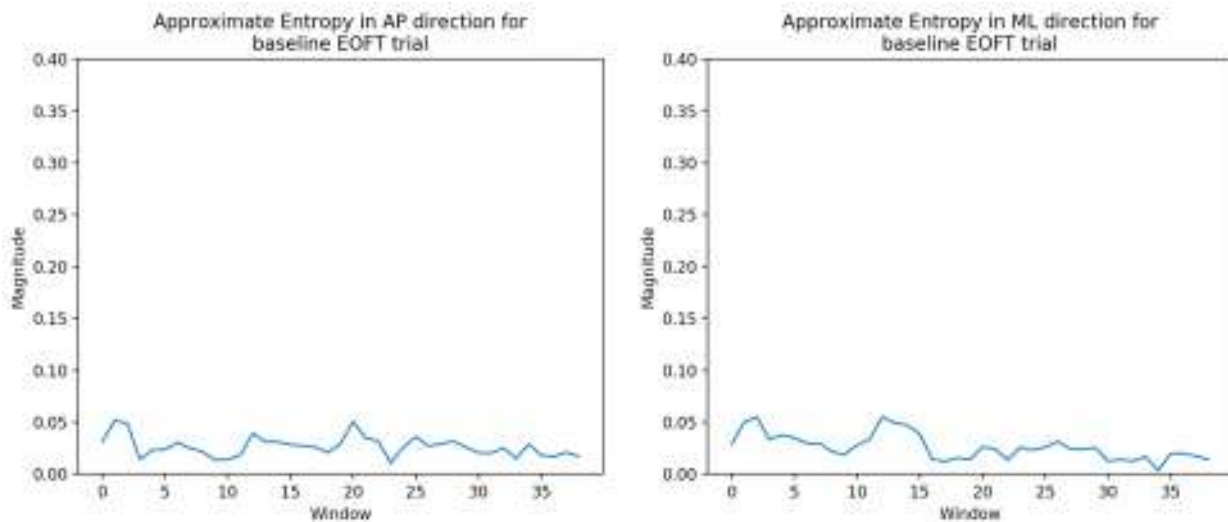


Figure 2.18. Approximate entropy of an eyes open, feet together trial from subject 1

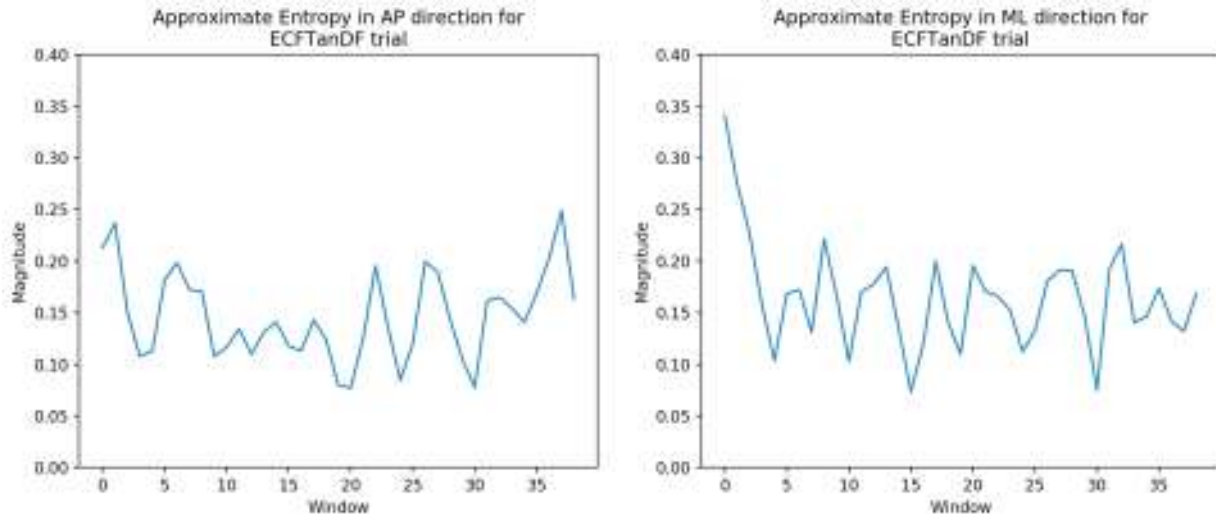


Figure 2.19. *Approximate entropy of an eyes closed, feet tandem, dominant foot in front trial from subject 1*

Figures 2.20 – 2.25 show the comparison of the average ApEn between each stability conditions for all subjects in both the AP and ML directions. As the conditions become less stable, the signals become more irregular and ApEn increased in both AP and ML directions. Additionally, the results of individual one-way ANOVA tests are indicated above each plot with *significance at $p < 0.05$, **significance at $p < 0.01$, and ***significance at $p < 0.001$.

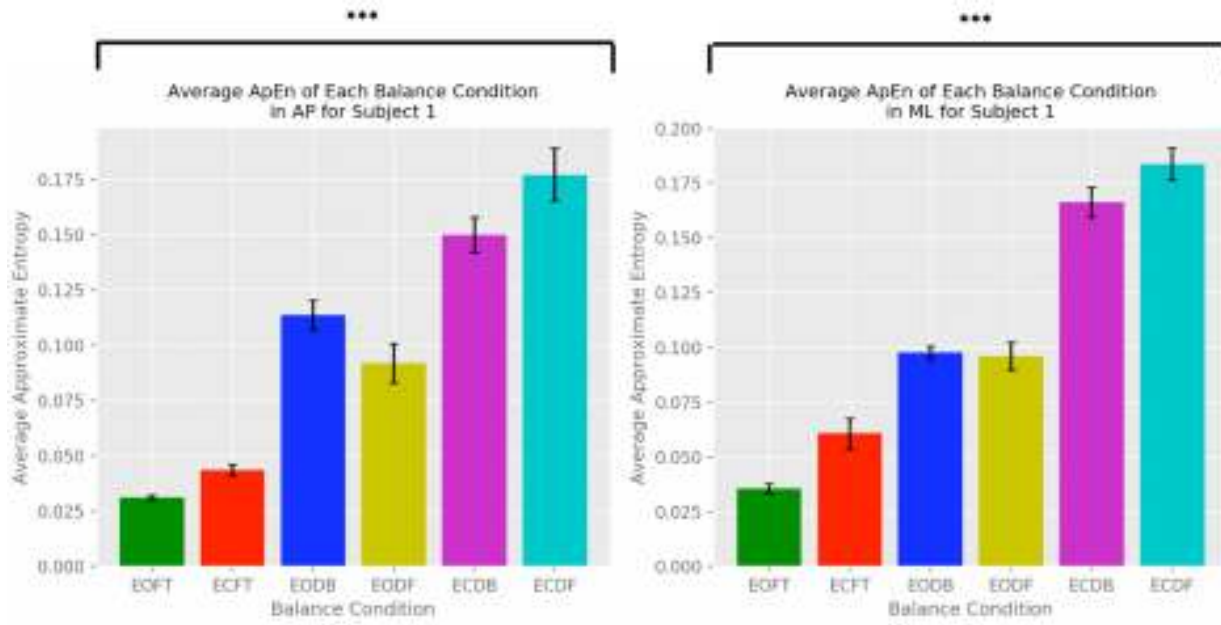


Figure 2.20. Approximate entropy of each condition for subject 1

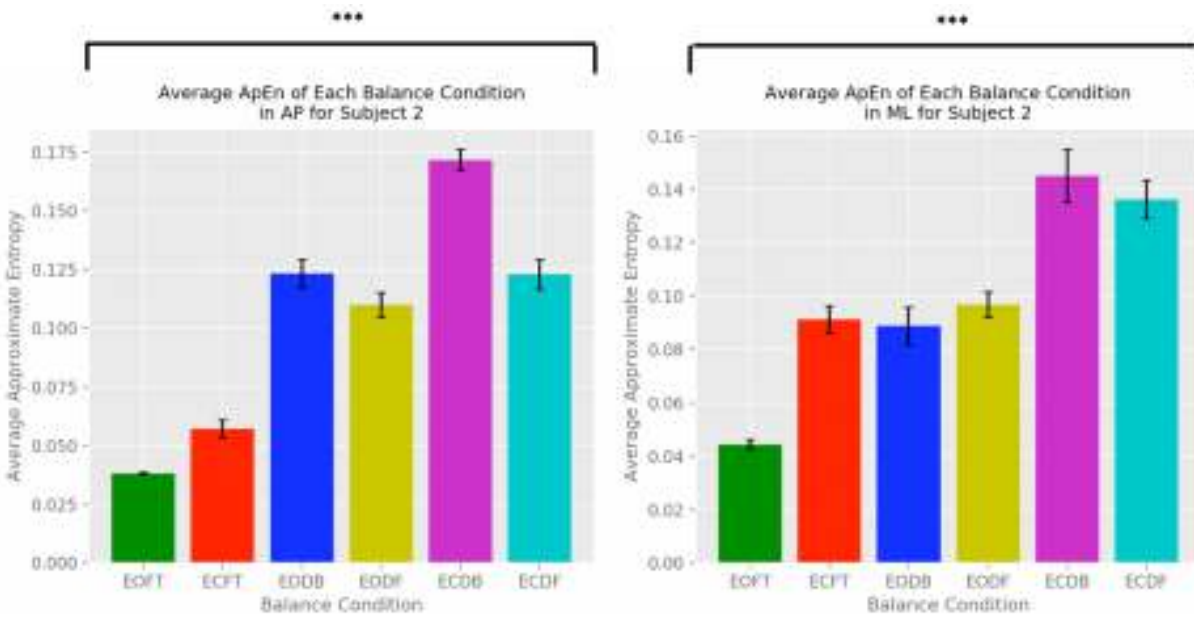


Figure 2.21. Approximate entropy of each condition for subject 2

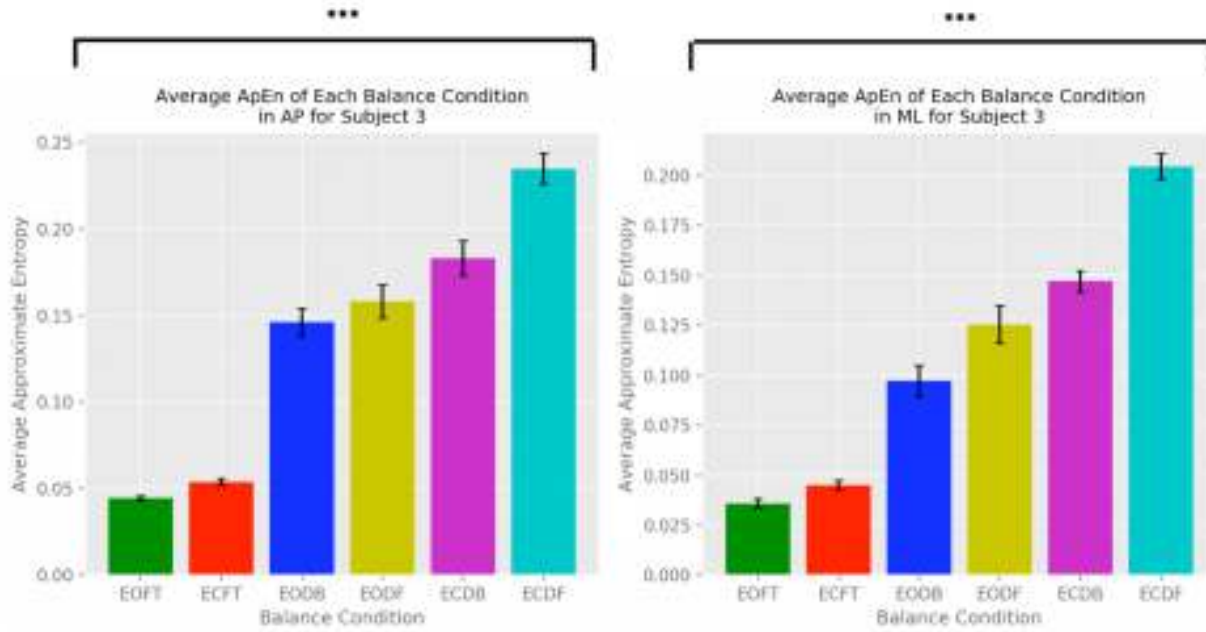


Figure 2.22. Approximate entropy of each condition for subject 3

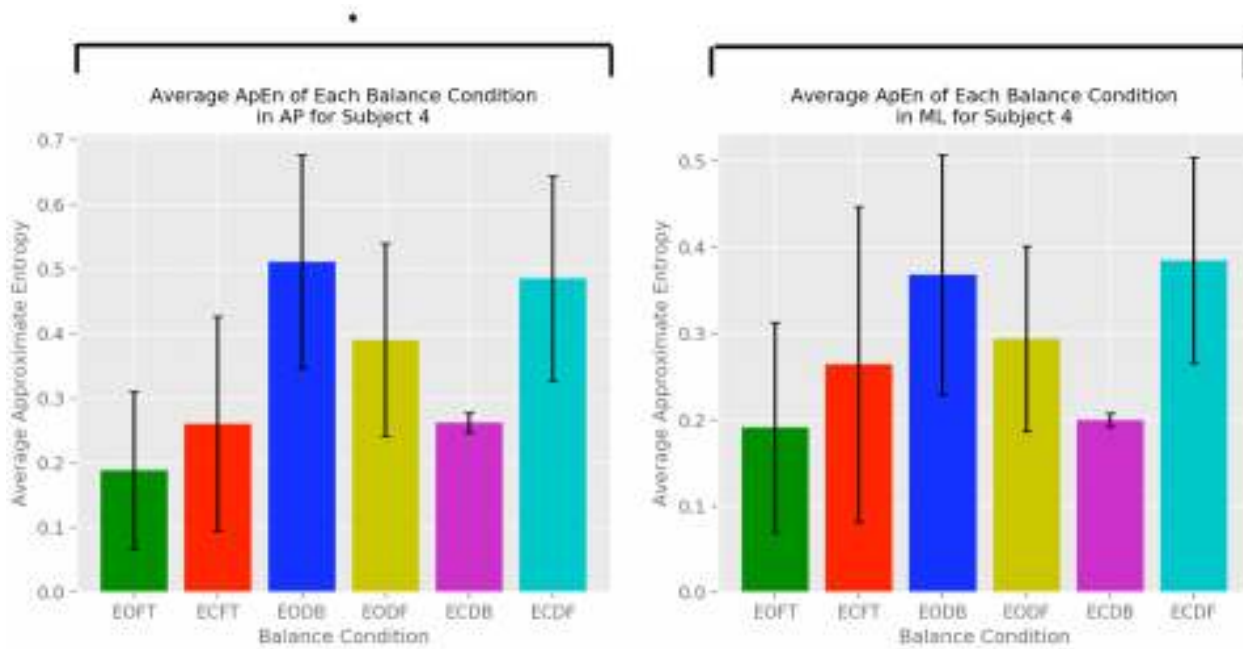


Figure 2.23. Approximate entropy of each condition for subject 4

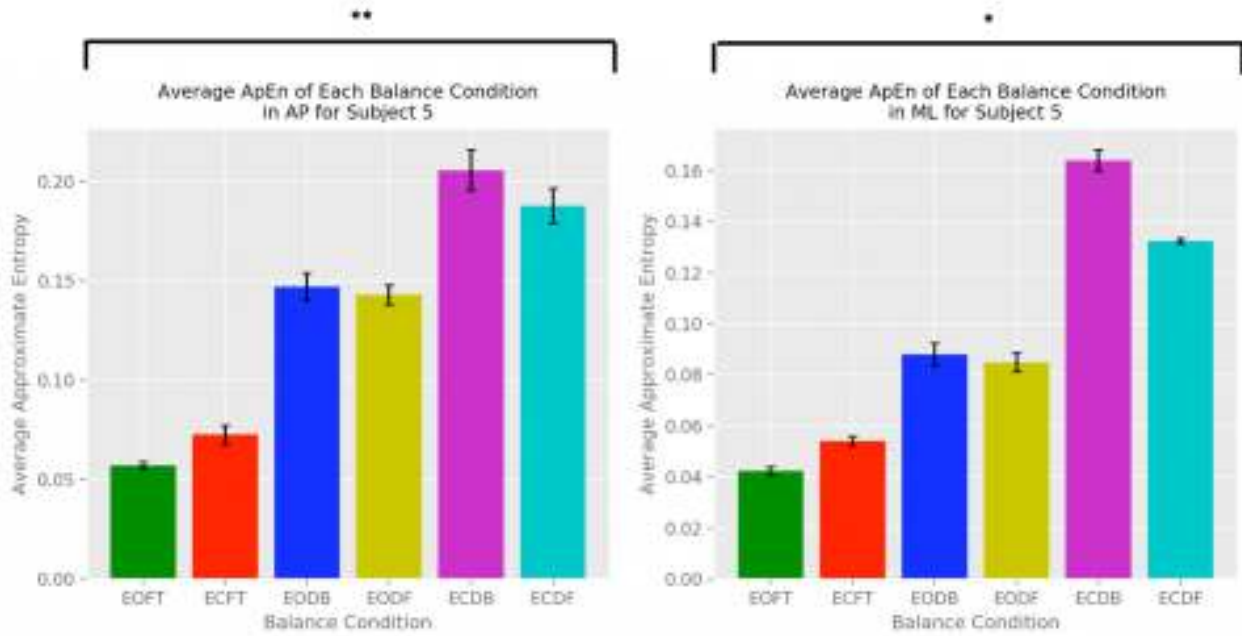


Figure 2.24. Approximate entropy of each condition for subject 5

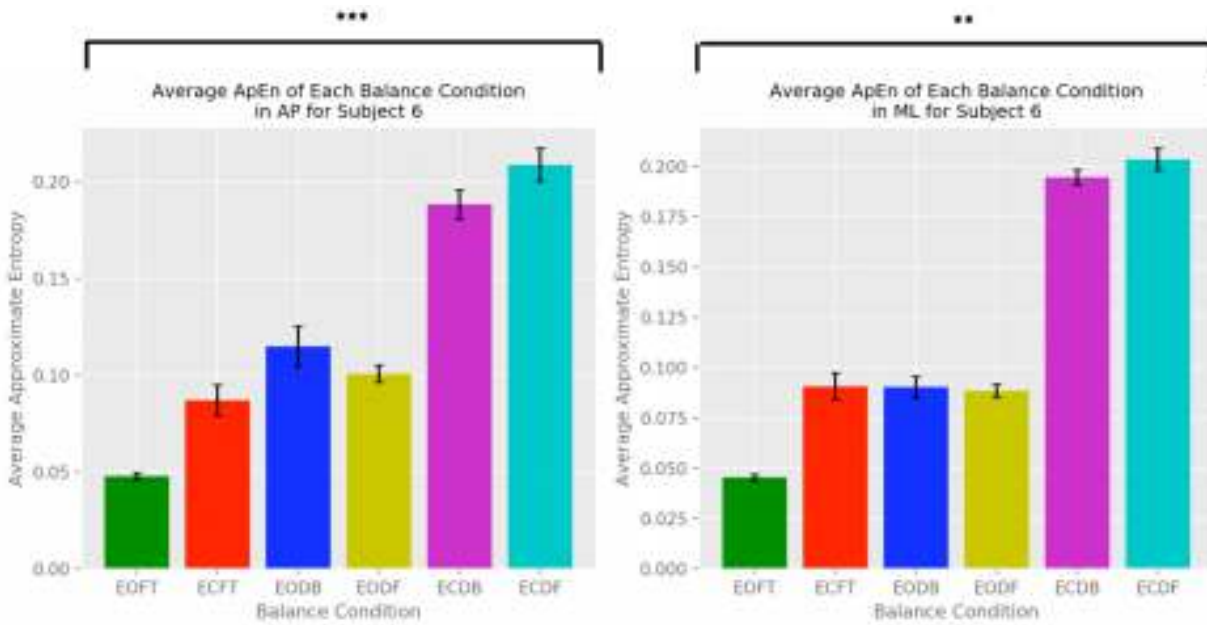


Figure 2.25. Approximate entropy of each condition for subject 6

In most cases, the ECFTan trials showed the highest approximate entropy of all of the conditions. The only subject for which that did not apply was subject 4, shown in Figure 2.23,

which showed much higher variability between trials of the same conditions than other subjects, affecting their results.

A 2-sided Dunnett’s post-hoc test was performed for all subjects and directions that resulted in a significant ANOVA test. This test compares all conditions to the baseline EOFT condition and indicates which differ significantly. Those results are seen in Figure 2.26 – 2.31, indicated by *significance at $p < 0.05$, **significance at $p < 0.01$, and ***significance at $p < 0.001$. These are seen on plots showing the difference in ApEn between the EOFT condition and every other condition.

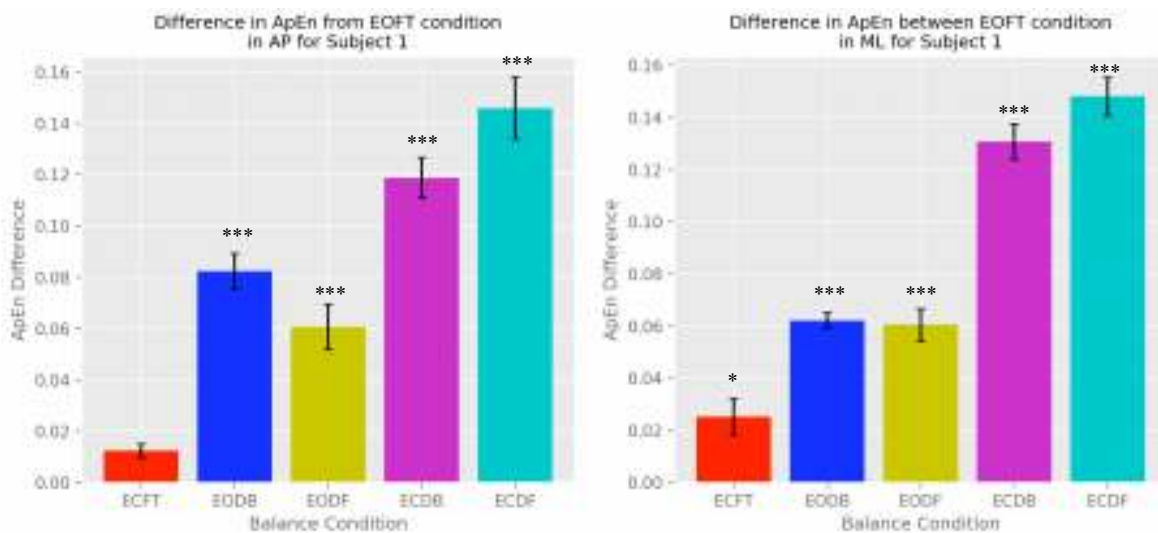


Figure 2.26. Difference in approximate entropy between each condition and eyes open, feet together for subject 1 with Dunnett’s post-hoc test results shown

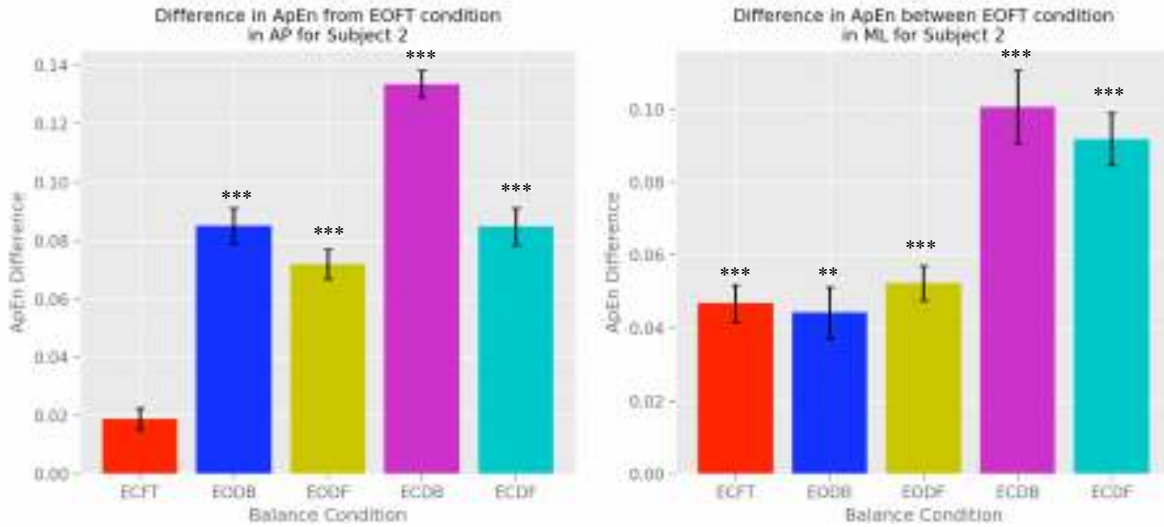


Figure 2.27. Difference in approximate entropy between each condition and eyes open, feet together for subject 2 with Dunnett's post-hoc test results shown

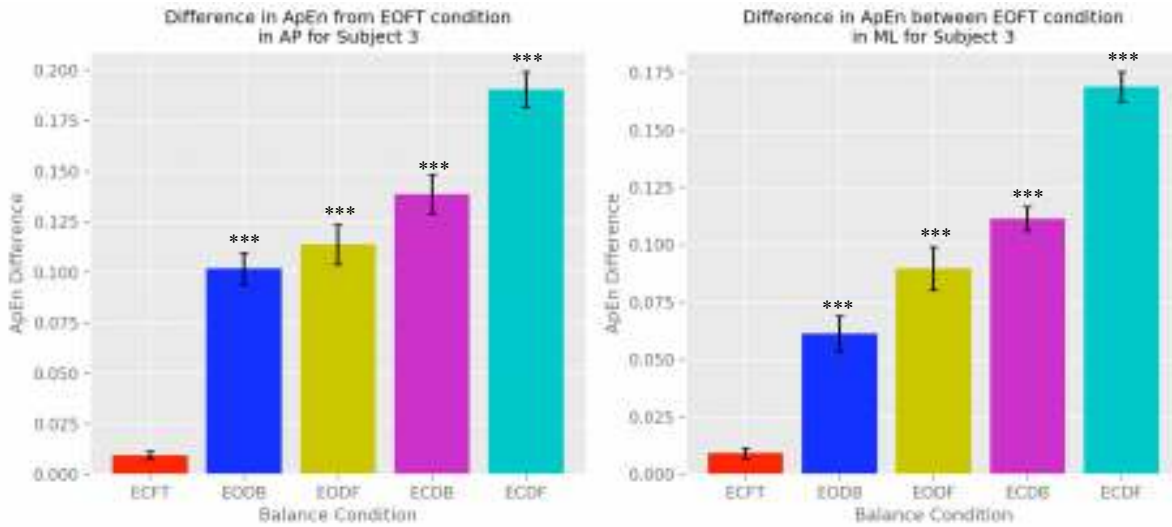


Figure 2.28. Difference in approximate entropy between each condition and eyes open, feet together for subject 3 with Dunnett's post-hoc test results shown

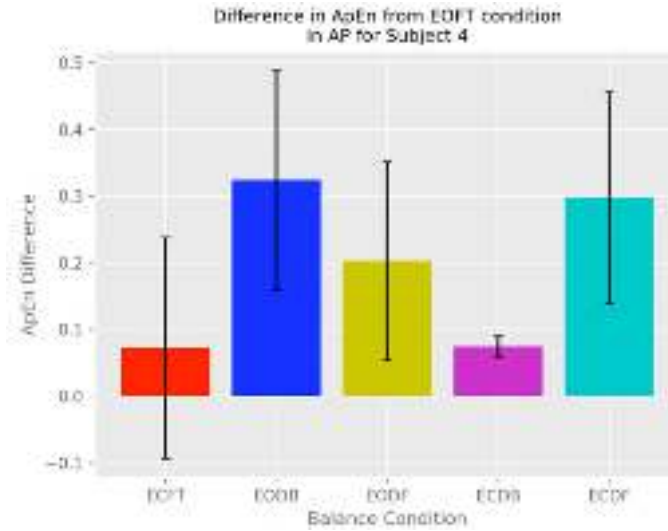


Figure 2.29. Difference in approximate entropy between each condition and eyes open, feet together for subject 4 with Dunnett's post-hoc test results shown

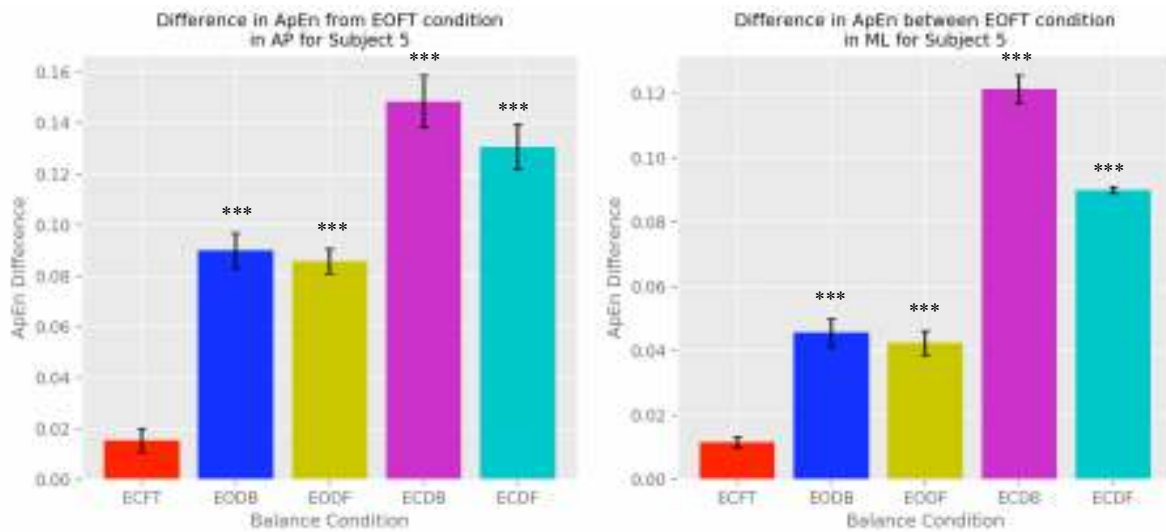


Figure 2.30. Difference in approximate entropy between each condition and eyes open, feet together for subject 5 with Dunnett's post-hoc test results shown

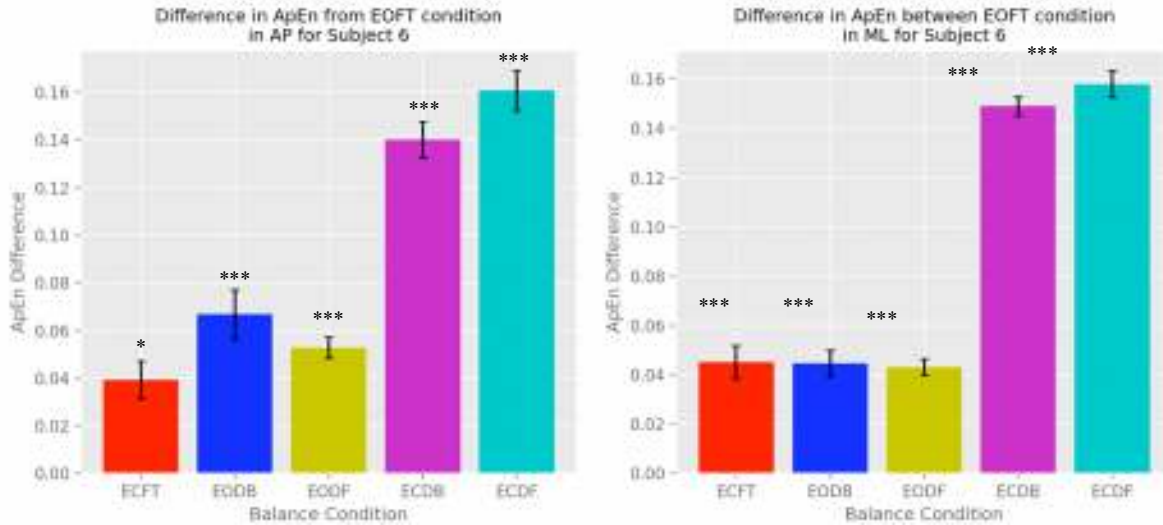


Figure 2.31. Difference in approximate entropy between each condition and eyes open, feet together for subject 6 with Dunnett's post-hoc test results shown

Post-hoc analysis showed that there is a significant difference from the baseline EOFT condition for all remaining stability conditions aside from ECFT in all subjects, excluding subject 4. In addition to that, subjects 1, 2 and 6 showed significant difference in the ECFT condition in at least one direction as well.

2.3.3. Velocity

Magnitude of velocity and PSD of velocity were both analyzed for all COP data. A representative view, from subject 1, of the velocity signal of the baseline EOFT condition in the AP and ML directions is seen in Figure 2.32 and a view of the velocity of a much less stable, ECFTanDF trial is seen in Figure 2.33. The less stable condition in Figure 2.33 has a maximum magnitude greater than the stable, baseline condition. Additionally, for both stability conditions, the velocity in the ML direction has a maximum magnitude that is higher than the AP direction.

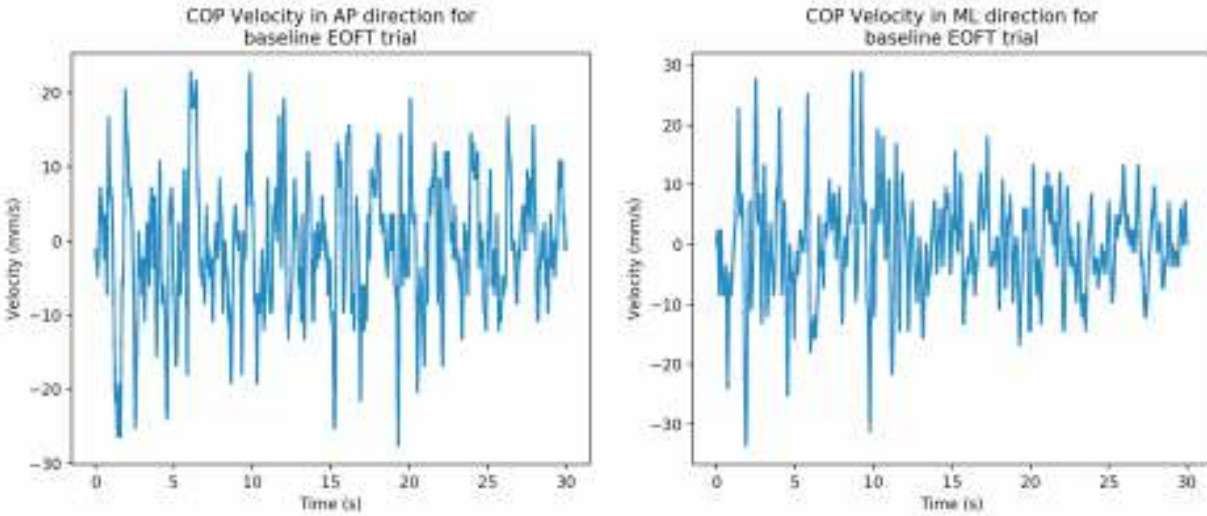


Figure 2.32. Velocity of an eyes open, feet together trial from subject 1

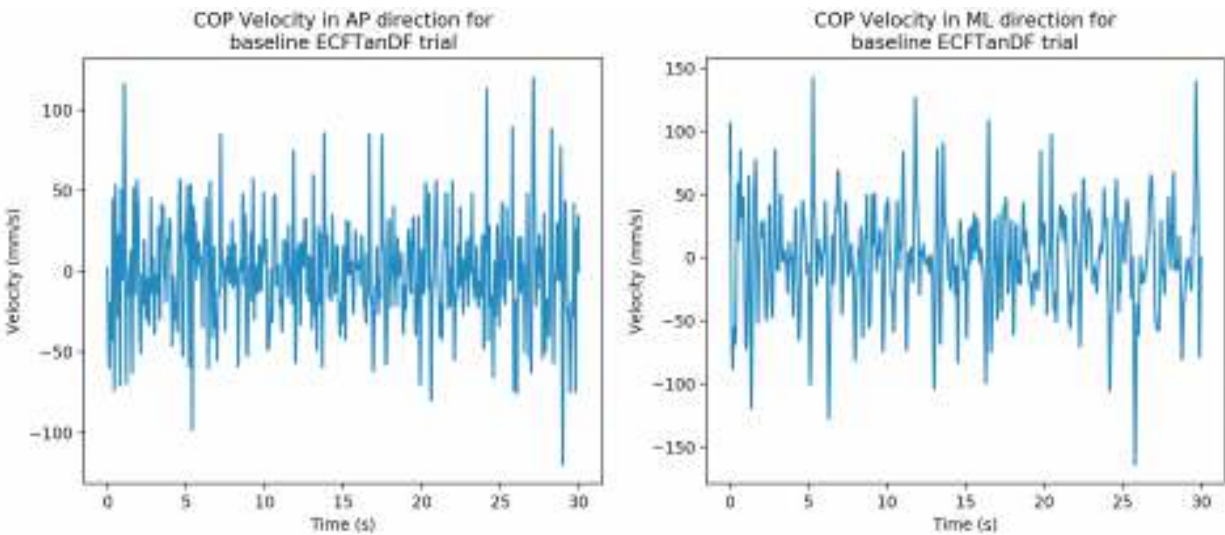


Figure 2.33. Velocity of an eyes closed, feet tandem, dominant foot in front trial from subject 1

A representative view of the PSD of the velocity signals seen in Figures 2.32 and 2.33 are shown below in Figures 2.34 and 2.35, respectively. For the EOFT trial in Figure 2.34, the AP and ML directions show content up to around 6 Hz. For the ECFTanDB trial in Figure 2.35, both directions show content up to a higher frequency, with the AP direction having content until around 10 Hz and the ML direction having content until around 8 Hz. In addition to having

content at higher frequencies, the magnitude of the content was also greater by an order of magnitude in the less stable condition in Figure 2.35.

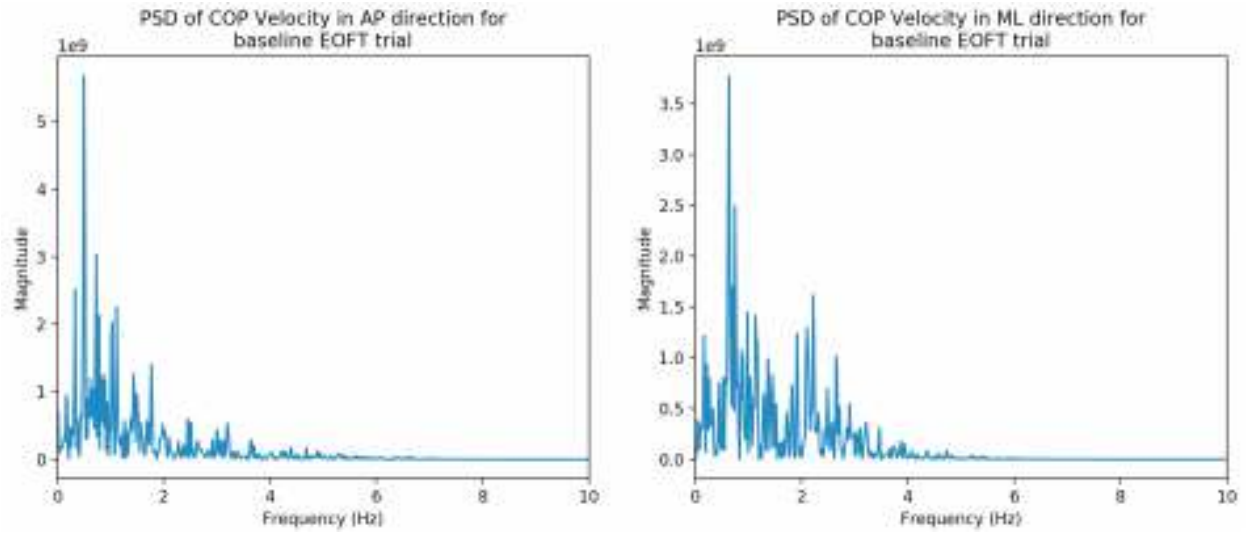


Figure 2.34. PSD of velocity signal of an eyes open, feet together trial from subject 1

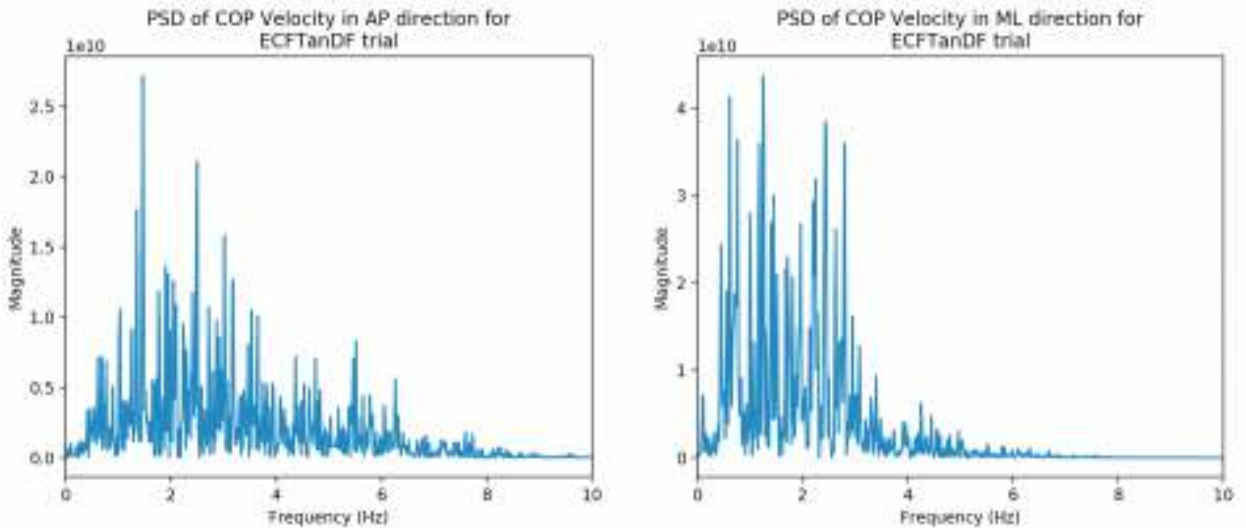


Figure 2.35. PSD of velocity signal of an eyes closed, feet tandem, dominant foot in front trial from subject 1

Figures 2.36 – 2.41 show the results for each stability condition in the AP and ML directions with the average velocity magnitude in the leftmost plots and the average total power in the rightmost plots. The magnitude of velocity was observed to be greater as stability

decreased as all conditions with decreased stability from baseline had a greater average velocity than the EOFT stance in all subjects. Additionally, total power also increased as stability decreased. While there are some slight differences between subjects and how much each stability condition affected them, all subjects showed the same trend of increasing velocity and PSD of velocity as conditions became less stable. Standard error bars are shown for each stability condition to indicate the amount of variability in the data. The results of individual one-way ANOVAs are indicated above each plot with *significance at $p < 0.05$, **significance at $p < 0.01$, and ***significance at $p < 0.001$.

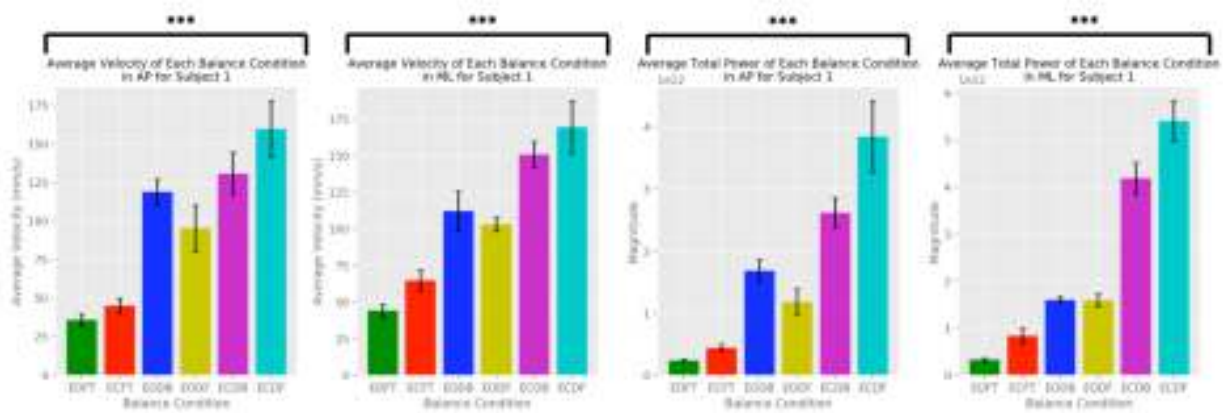


Figure 2.36. Average velocity and total power of each condition for subject 1 with 1-way ANOVA results shown

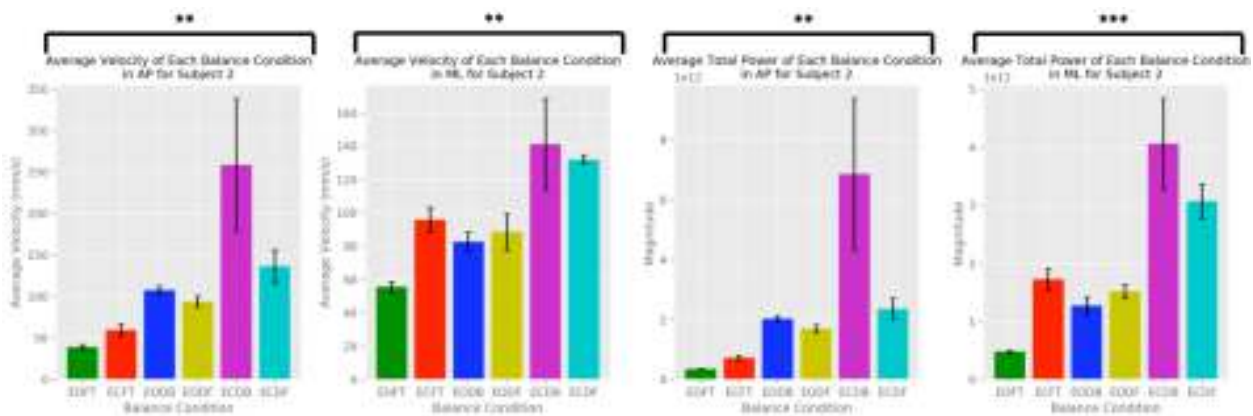


Figure 2.37. Average velocity and total power of each condition for subject 2 with 1-way ANOVA results shown

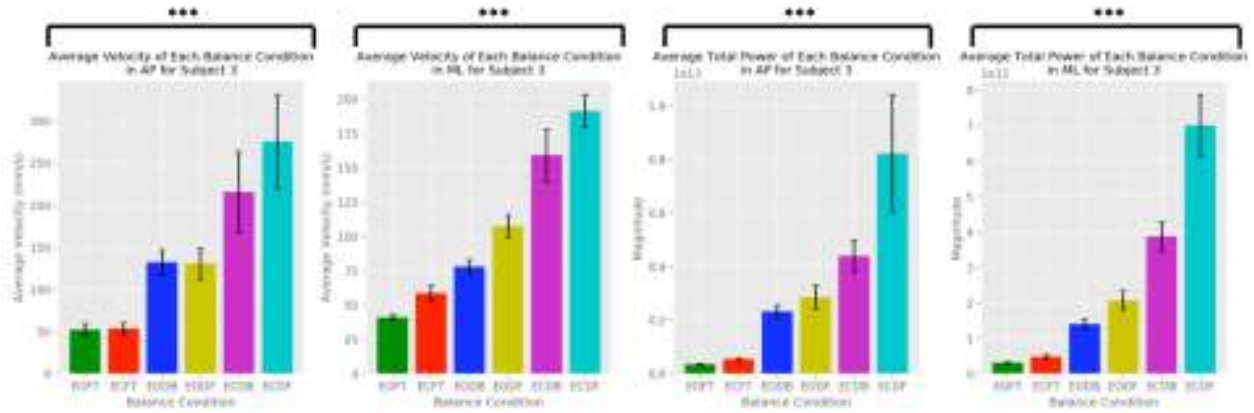


Figure 2.38. Average velocity and total power of each condition for subject 3 with 1-way ANOVA results shown

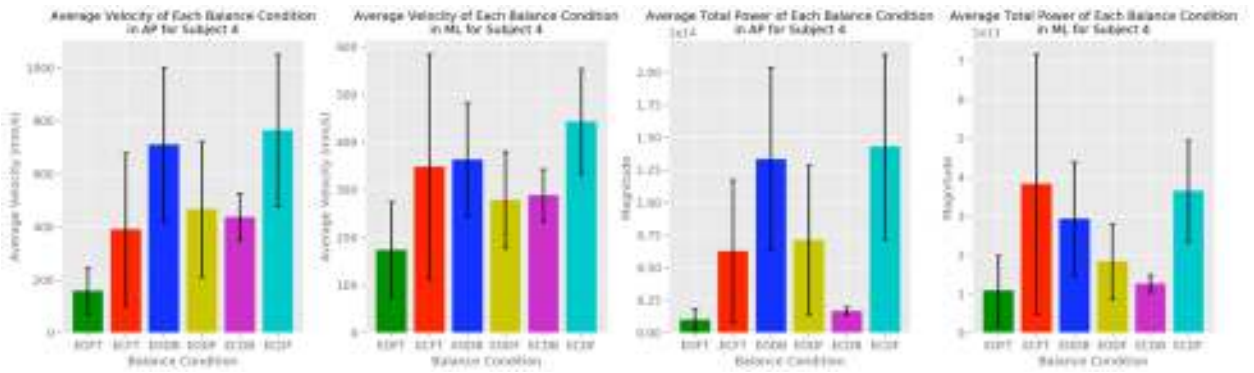


Figure 2.39. Average velocity and total power of each condition for subject 4 with 1-way ANOVA results shown

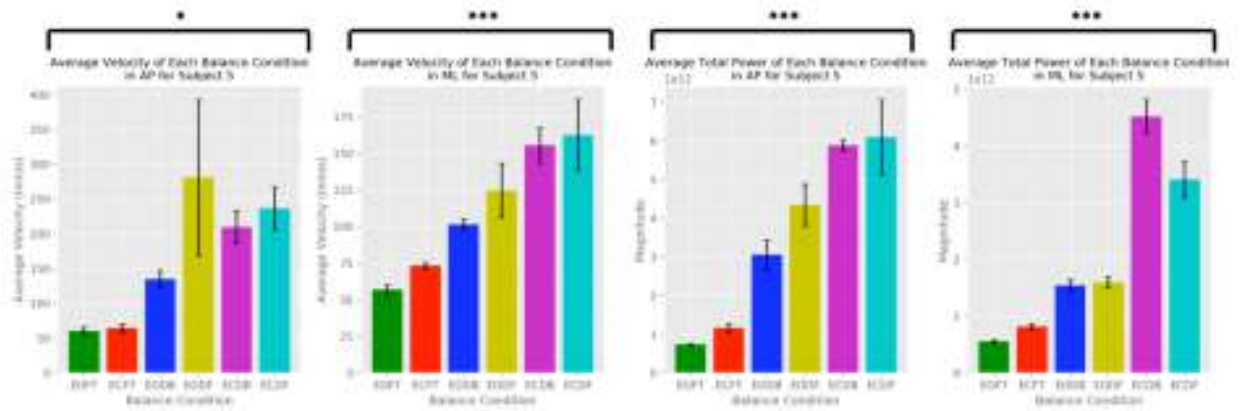


Figure 2.40. Average velocity and total power of each condition for subject 5 with 1-way ANOVA results shown

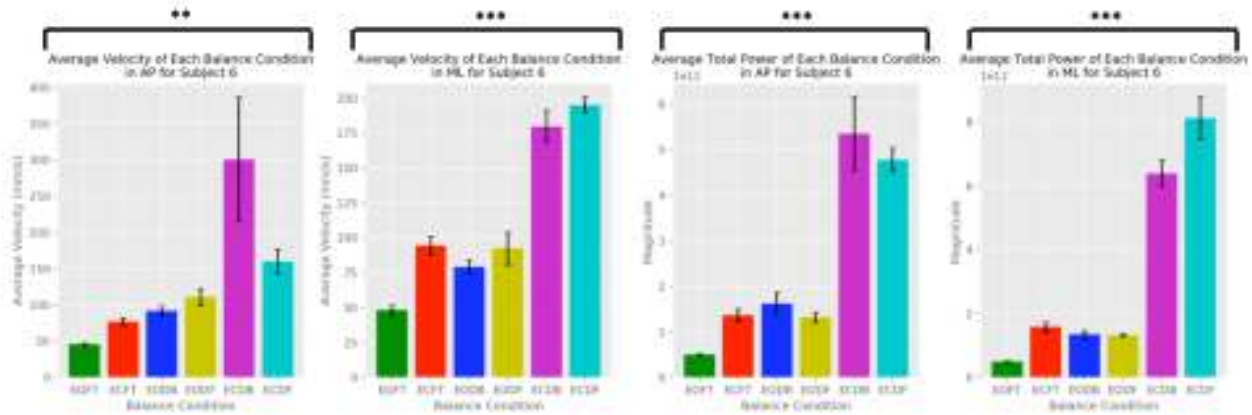


Figure 2.41. Average velocity and total power of each condition for subject 6 with 1-way ANOVA results shown

In most cases seen in Figures 2.36 – 2.41, the ECFTan trials showed the highest velocity and total power of all conditions. Whether having the dominant foot forward or backward resulted in more instability varied by subject.

A 2-sided Dunnett’s post-hoc test was performed for all subjects and directions that resulted in a significant ANOVA test. This test indicates which conditions differ significantly from the baseline EOFT condition. Those results are seen in Figure 2.42 – 2.46, indicated by *significance at $p < 0.05$, **significance at $p < 0.01$, and ***significance at $p < 0.001$. These are seen on plots showing the difference between the baseline EOFT condition and the remaining conditions from results shown above in Figures 2.36 – 2.41. As subject 4 was the only subject whose ANOVA test was not significant, a difference plot was left out.

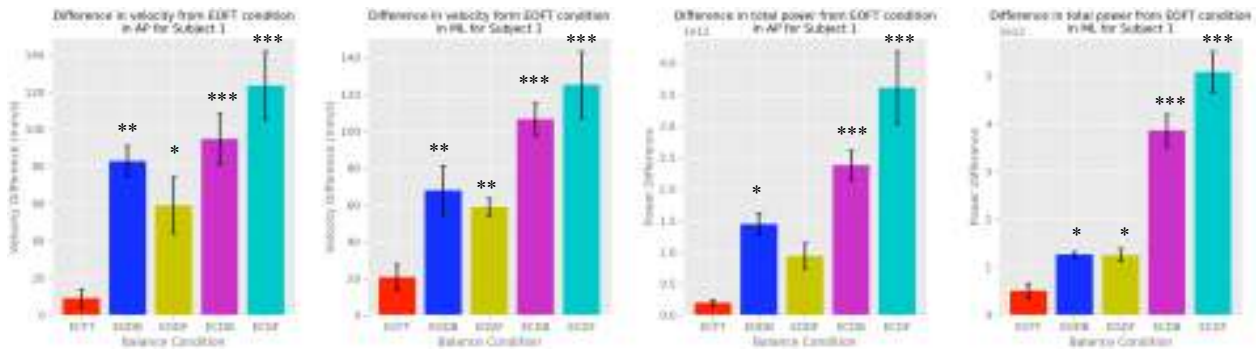


Figure 2.42. Difference in velocity and total power between each condition and eyes open, feet together for subject 1 with Dunnett's post-hoc test results shown

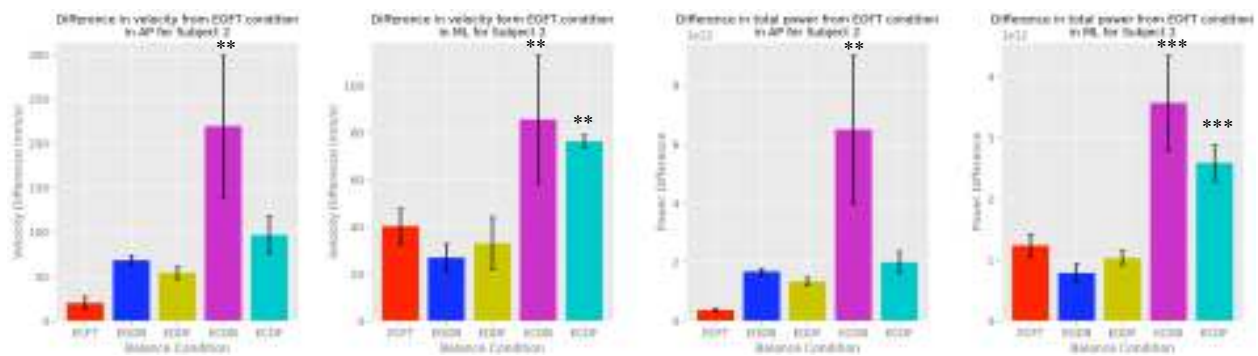


Figure 2.43. Difference in velocity and total power between each condition and eyes open, feet together for subject 2 with Dunnett's post-hoc test results shown

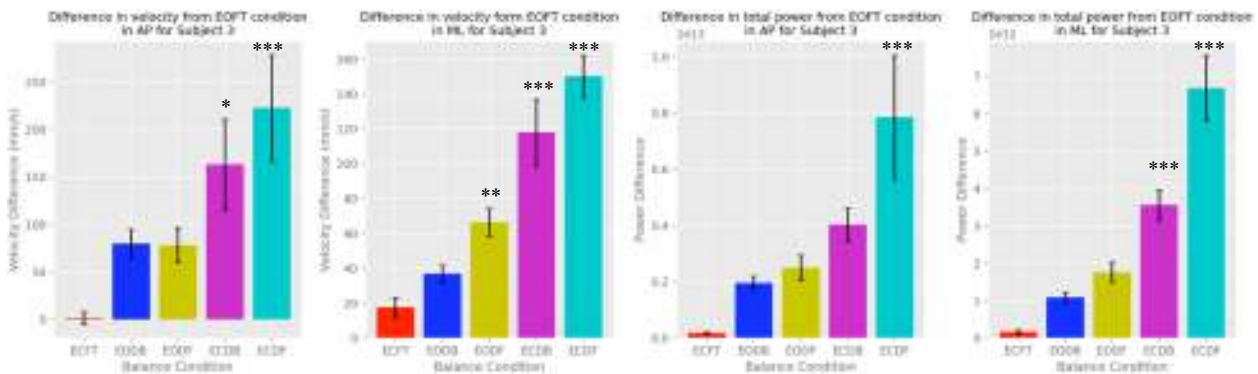


Figure 2.44. Difference in velocity and total power between each condition and eyes open, feet together for subject 3 with Dunnett's post-hoc test results shown

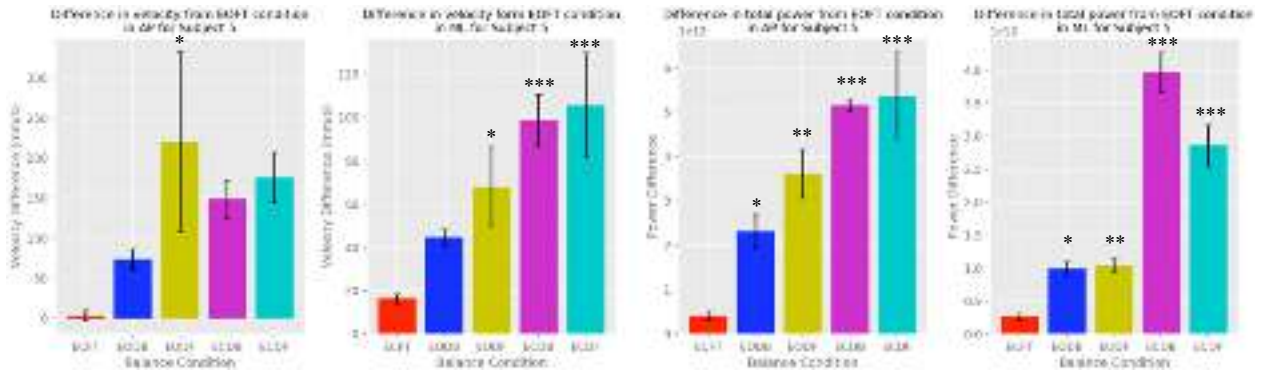


Figure 2.45. Difference in velocity and total power between each condition and eyes open, feet together for subject 5 with Dunnett’s post-hoc test results shown

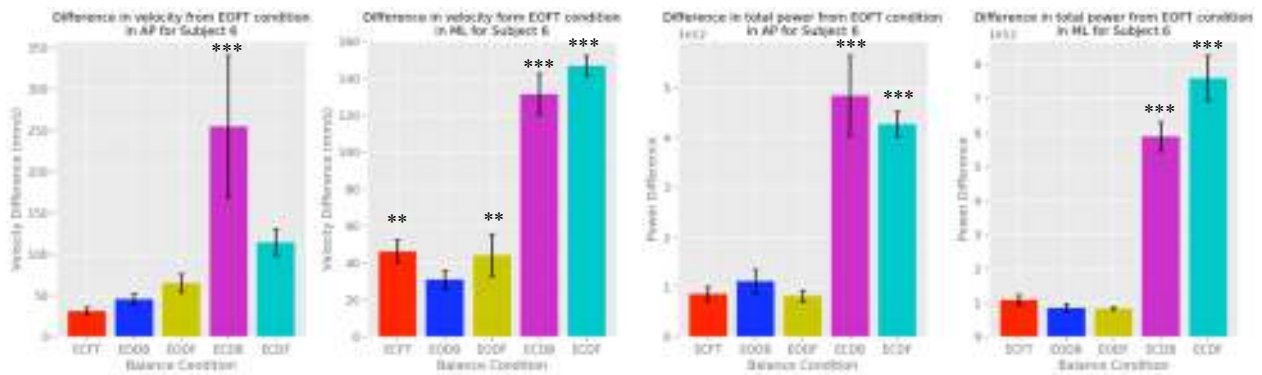


Figure 2.46. Difference in velocity and total power between each condition and eyes open, feet together for subject 6 with Dunnett’s post-hoc test results shown

Post-hoc analysis illustrates that the ECFTan conditions showed statistically significant differences from the baseline EOFT conditions more often than the others. Aside from subject 4, all subjects showed significant differences in at least one of those conditions for magnitude of velocity and velocity PSD except for one instance where subject 5 did not show significance in either of them for magnitude of velocity in the AP direction. Comparatively, for all instances except one, which was velocity magnitude in the ML direction for subject 6, the ECFT condition did not show a statistically significant difference from the baseline EOFT condition. The EOFTan conditions showed a significant difference from baseline about half of the time for both velocity magnitude and PSD.

2.3.4. Regression

Regression analysis was completed on groups of trials of the same stability condition across all subjects, resulting in models of what any one condition may generally look like. These are shown in Figures 2.57 – 2.52, where the blue line is the average of all trials for the given stability condition, the purple line is the regression model, and the red lines represent the 95 percent prediction interval.

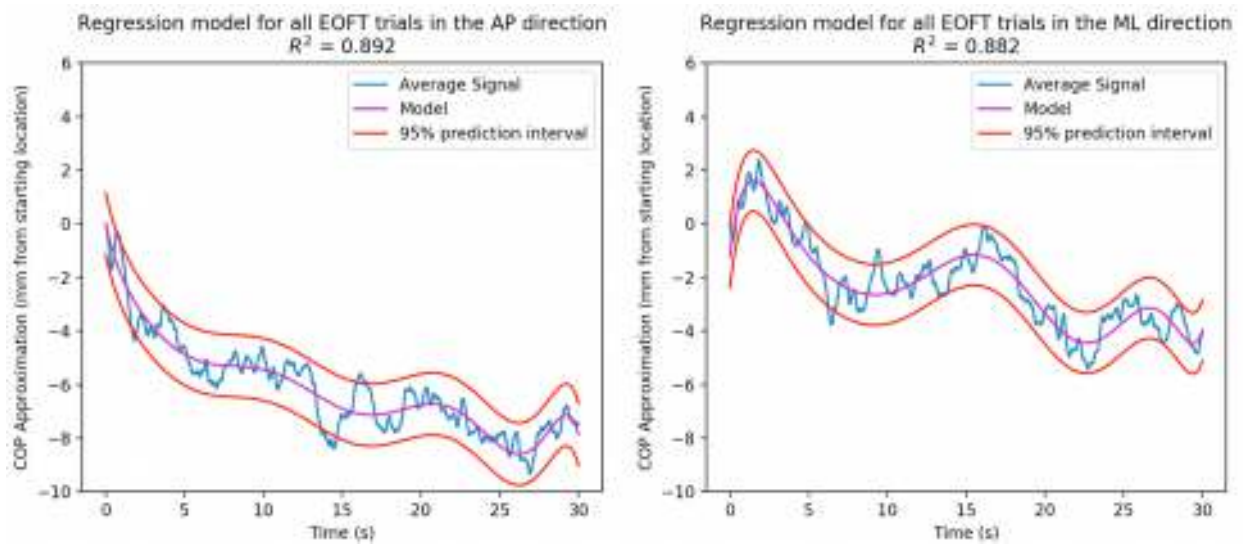


Figure 2.47. Regression model for all eyes open, feet together trials

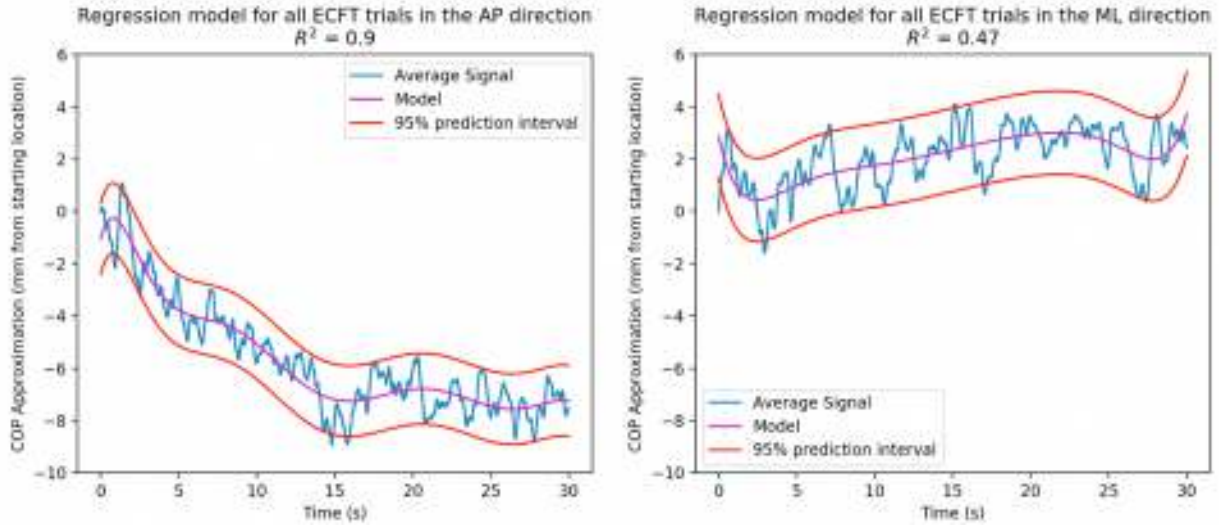


Figure 2.48. Regression model for all eyes closed, feet together trials

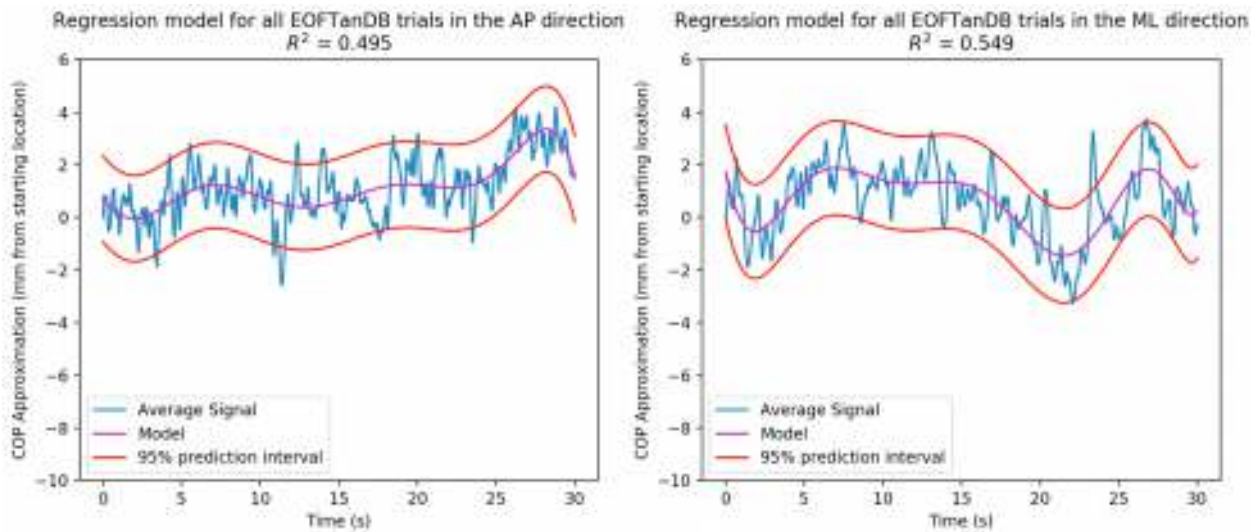


Figure 2.49. Regression model for all eyes open, feet tandem, dominant foot in back trials

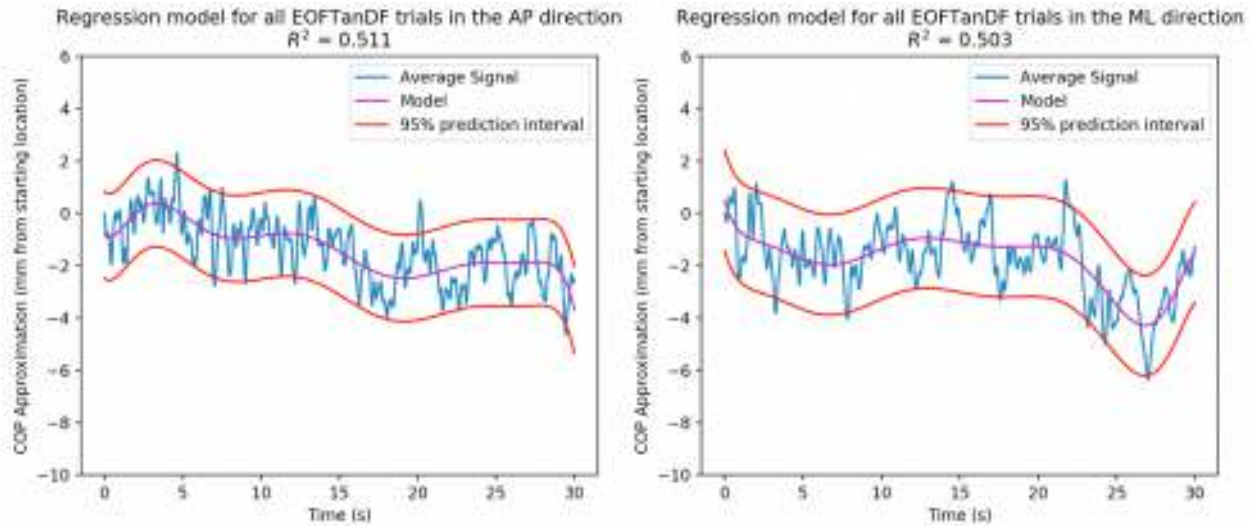


Figure 2.50. Regression model for all eyes open, feet tandem, dominant foot in front trials

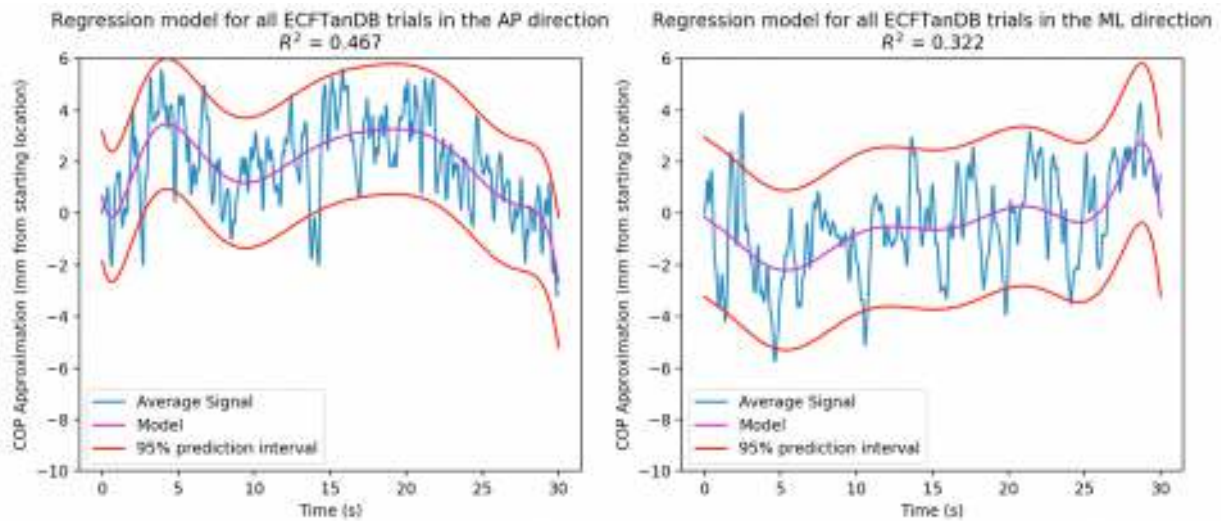


Figure 2.51. Regression model for all eyes closed, feet tandem, dominant foot in back trials

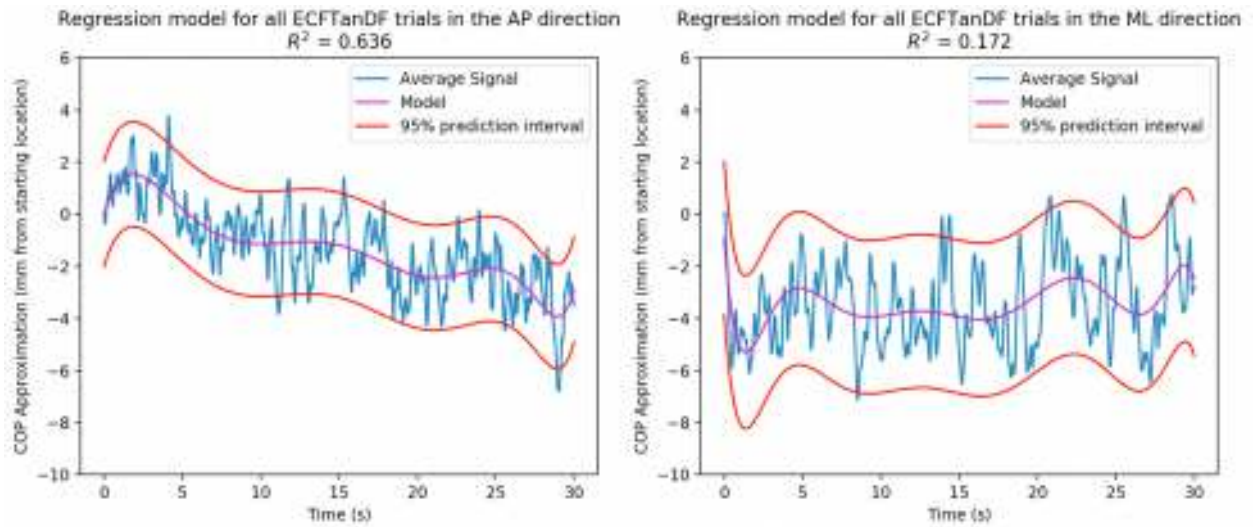


Figure 2.52. Regression model for all eyes closed, feet tandem, dominant foot in front trials

A pattern is seen in the above figures where trials of less stability have a wider 95 percent prediction interval and the R^2 value is lower. Furthermore, in all conditions except for EOFTanDB, the R^2 value is greater in the AP direction than the ML direction.

In addition to models for each individual stability condition, regression was completed for all trials of all subjects to create a model for a neurotypical subject in quiet standing. This is shown in Figure 2.53.

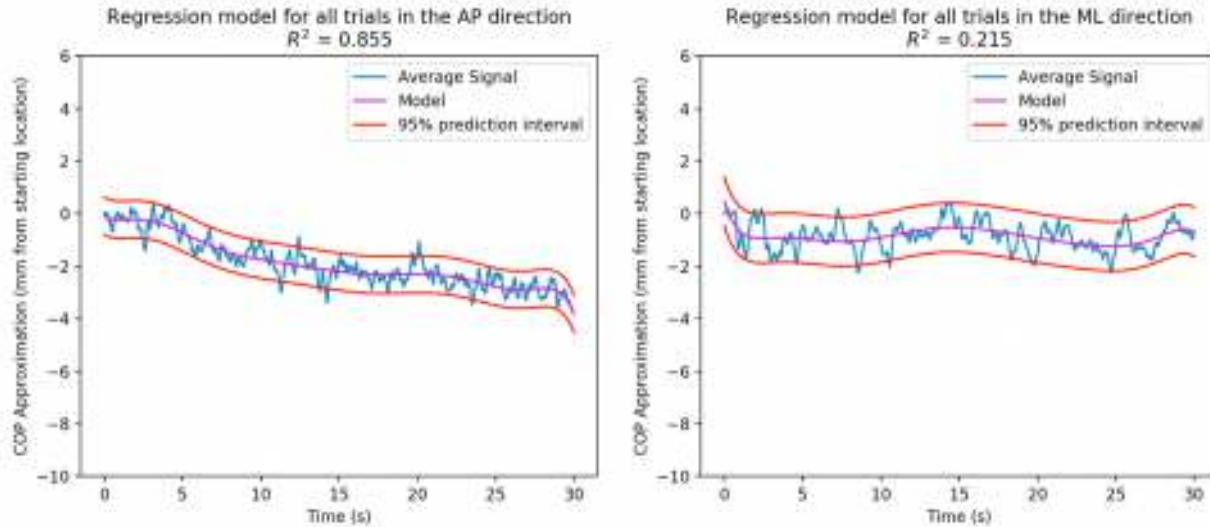


Figure 2.53. Regression model for all trials

In Figure 2.53, it can be observed that the R^2 value of the AP direction is much higher than the R^2 value for the ML direction and the 95 percent prediction interval is approximately twice as wide with a width of nearly two versus a width of one in the AP direction.

2.4. Discussion

Postural control is a fine-tuned system in the human body that is very adept at keeping a person upright, particularly during quiet standing. It is important to understand the processes that affect this mechanism, and the degree to which it is affected. For this study, it was assumed that while postural control is mostly equivalent for all individuals, every person's postural control mechanism is unique, due to learned experiences [25]. Therefore, it is necessary to consider that each person's response to changing conditions may be slightly different. In previous studies, EMG signals in the lower leg muscles were assessed for changes in connectivity with increasing instability to understand the neural mechanisms responsible for postural control [32]. In the current study, signals from COP and COM measurements were assessed under the same

increasingly unstable conditions in an effort to develop indices of interest that can help accurately identify the degree of postural stability. These indices may be used to screen for conditions like concussion in a more objective manner. Results showed that ApEn, velocity analysis, and regression were clearly and significantly changed between very stable and less stable quiet standing positions for each subject.

Additionally, results, along with literature, show that COP and COM are not effective measures for determining neural activity based on frequency bands. As previous studies have shown, and as was corroborated in this study, COP and COM data have content at frequencies which are limited to about 5 Hz and less [33]–[35]. This range encompasses only the delta (0 – 4 Hz) and very beginning of the theta (4 – 8 Hz) neural bands. These are associated with deep sleep and very slow brain activity, such as that which occurs during daydreaming. As postural control occurs in a much more involved state of neural activity, it is clear that COP and COM cannot accurately represent neural activity using frequency analysis. This is because the two signals are not measuring an immediate and direct response from the brain. Instead, they measure body movement which only occurs as needed to keep a person's balance. Therefore, the frequencies at which the COP and COM signals occur cannot be related to the frequency at which neural activity is occurring.

2.4.1. COP and COM Correlation

The COP and COM signals look very similar when they are standardized to have a mean of zero and a standard deviation of one and compared directly. The main difference was that the COP signal displays many more spikes than the COM signal, with a greater magnitude. This relates to the COP oscillations that occur during quiet standing. Since the COP moves more

significantly in all directions than the COM, it is expected to have a greater magnitude. Additionally, since the COP moves in order to keep the COM in a relatively steady location, it would be expected for the COP to make many small movements so as to keep the COM steady and avoid many movements in that signal. Further analysis was necessary to determine if the differences seen are indicative of a difference in the information that they provide, or if they truly provide the same information.

Autocorrelation shows how similar a signal is to itself at different amounts of lag. Similarly, cross-correlation shows how similar one signal is to another signal at different amount of lag. Therefore, if an autocorrelation signal looks the same as a cross-correlation signal, where one of the signals correlated was the same as the signal used for autocorrelation, that means the two signals look the same over the time that they were recorded. A comparison of the autocorrelation of the COP signal and the cross-correlation of the COP and COM signals shows that the two look very similar. Both high stability and low stability conditions displayed this same result. There are slight differences between the two correlation results where the autocorrelation has more spikes and the cross-correlation is a smoother line, but the overall shapes of the curves are the exact same.

Given the knowledge gained by the auto and cross-correlation analysis that COP and COM signals are, in fact, highly correlated, it was necessary to quantify just how similar the COP and COM signals were. An important factor of similarity is whether or not the two signals are dependent. Pearson's correlation coefficient provided insight into this by assigning a value between negative one and one to the pair of signals, where the high and low values of that range show a perfect linear relationship between the two variables in either the negative or positive

direction and a value of zero shows no relationship whatsoever. This coefficient was calculated between COP and COM signals for one trial from every stability condition and for each subject in both AP and ML directions. Of the pairs that were tested, 37.5 percent displayed a very strong relationship, 56.9 percent displayed a strong relationship, and only 5.6 percent displayed a moderate relationship. Given the large number of strong and very strong relationships, it was reasonable to assume that COP and COM signals provide very similar information and it was not necessary to consider both in further analysis. As COP is an easier signal to record, this metric was used for all further analysis.

2.4.2. Postural Control and Changing Stability Conditions

2.4.2.1. Center of Pressure Irregularity

A very clear pattern emerged with ApEn analysis. All subjects displayed an increase in ApEn while under increasingly unstable conditions when compared to baseline EOFT. Aside from subject 4, all subjects showed the highest ApEn in the two ECFTan trials. Subject 4 was different from the rest due to increased variability among trials of the same condition. This is evidenced by the error bars seen in Figure 2.23. Due to this variability, it is not unexpected that the patterns of the subject may look different than those of other, more consistent subjects.

Furthermore, in all subjects aside from subject 4, all stability conditions except for ECFT showed significant difference from the baseline EOFT condition based on Dunnett's post-hoc testing. On some occasions, even the ECFT condition showed statistically significant difference in ApEn from the baseline condition, despite the fact that the condition does not display a large difference in stability. This shows that ApEn can be a very sensitive and useful metric for

analyzing postural control. Changes in ApEn did not appear to differ between the AP direction and ML direction.

2.4.2.2. *Oscillation Velocity*

Both magnitude and frequency content of the velocity of COP oscillations were shown to increase as quiet standing stances became less stable. This means that as a subject was less stable, their COP moved from behind to in front of their COM more quickly when they were less stable and that it did so more frequently. This pattern was consistent across both AP and ML directions. This is reasonable because when a perturbation to balance is more extreme, the postural control mechanism must act more significantly and with stronger force in order to counteract the impedance to balance. With less stability comes a higher number of balance perturbations, as well, increasing the necessary frequency of oscillations.

Dunnett's post-hoc testing showed that the only conditions that were consistently statistically significant in their difference from the baseline EOFT condition were the two ECFTan conditions. This may be EC and FTan are the two characteristics that were assumed to decrease stability the most in this research. Therefore, it would be expected that the conditions with the lowest stability would most often show statistical significance in their results when compared to the most stable condition.

Velocity analysis was not able to identify a significant result from ECFT trials aside from one instance with magnitude of subject 6 in the ML direction. In addition to that, it was only able to identify significant results from EOFTan conditions around half of the time. This shows that velocity analysis of COP oscillations may not be sensitive to small amounts of instability. However, it has shown that it is reliable when stability conditions are significantly affected.

2.4.2.3. *Baseline Models*

Baseline models developed using regression were useful in corroborating results that were obtained using other analysis methods. These models showed a general trend of decreased R^2 values as stability decreased. This is important as it illustrates the fact that lower stability results in less consistent COP data with more variability, leading to information held in the signal that could not be explained by the regression model. This agrees with what ApEn and velocity analyses determined. Regression, however, was the metric that displayed the most difference between the two directions. A pattern of much larger R^2 values among models in the AP direction than models in the ML direction was evident, showing that ML motion has more variability. This difference in variability is likely linked to the fact that muscles that facilitate flexion and extension are much stronger than muscles that facilitate abduction and adduction [43], [44]. Increased strength in the AP direction would allow for more control of the body and its posture when moving in that direction than in the ML direction, leading to less irregularity and, therefore, larger R^2 values when adjusting front-to-back.

The models may be more useful moving forward. Having a model of what each stability condition looks like, on average, along with what quiet standing of a neurotypical subject looks like will be invaluable. It may show differences between subjects with and without concussions. The 95 percent prediction interval may allow ease of identifying largely different behavior in future research.

2.4.3. Comparison of Analysis Methods

Postural stability affected all methods used for analysis and the computed indices showed significant differences resulting from changes in stability based on COP oscillation data

recordings. When all conditions were compared to baseline using Dunnett's post-hoc analysis, ApEn was able to find significant changes with much more sensitivity than velocity magnitude, velocity PSD, and regression. While that analysis was able to find significant differences in nearly all stability conditions, the velocity measures were only able to indicate significant deviances with consistency in the two least stable conditions, ECFTan.

Velocity analysis was only able to find significant differences in the ECFT and EOTan conditions about half of the time. It is likely that the velocity analysis is limited in its usefulness due to the limits that the body has as far as how quickly it can move. ApEn is not limited by the ability of the human body while velocity of motion is constrained by physiologic limitations of muscle activation kinetics.

While regression analysis did show changes in R^2 values as stability decreased, these were not consistent and not significant to justify the use of regression analysis for quantifying changing conditions. A general pattern existed, which corroborated results from the other analyses, however, it would not be of much use on its own to determine the stability of one's postural control system.

2.4.4. Limitations and Future Considerations

This study was limited by the small number of subjects that were involved in data collection. Having a larger pool of volunteers would be beneficial to determine whether the findings that were obtained are applicable to a wider range of people. Additionally, it would have allowed for any outliers to become obvious, as opposed to potentially be factored into the results.

Future work on this data should analyze the angular acceleration of the COP and COM signals to identify how COP oscillations pivot as the two signals move toward and away from one another. Namely, considering the distance between the COP and COM over time could lead to interesting findings as it is directly proportional to the angular acceleration, but does not require any derivative calculations. Future analysis should also consider non-neurotypical subjects. Particularly, it should consider subjects who are suffering from a concussion. The same data collection procedure could be completed on those subjects to determine if analysis of their COP displays significantly different results than a neurotypical subject. This analysis could be the next step in developing a definitive diagnostic tool for concussions. Additionally, future analysis should involve an increase in sample size of both neurotypical and non-neurotypical subjects. This will allow for results that can be applied to a larger and more varied population.

2.5. Conclusion

Analysis of COP and COM signals showed that the two signals provide very similar information. Therefore, it was unnecessary to consider both throughout the entirety of the analysis and all research could be performed on only the COP signal. This is important as collection of COP data is much simpler and more inexpensive than collection of COM data. Not needing a COM signal for performance of this analysis will allow for collection of all necessary data in future studies and in a potential concussion diagnostic tool to be completed in many different locations. For example, this could be completed at the site of a suspected concussion as opposed to in a well-equipped laboratory.

Further analysis of COP oscillations in quiet standing of neurotypical subjects provides insight into how the body compensates for small amounts of instability. Strong evidence has

been found to suggest that variability, velocity, and frequency of the COP all increase as stability also increases. All three of those analyses were able to consistently indicate significant differences between a baseline EOFT condition and much less stable ECFTan conditions. ApEn was more sensitive than the other techniques and was able to identify significant differences between baseline and all tandem stances, while also indicating significance between EO and EC of the feet together stance. Regression models corroborated other findings and will provide a resource to compare further research to when concussed subjects are being studied. The results of this study will be useful as a thorough understanding of how the postural control system functions under baseline, neurotypical conditions. Having this knowledge will make it possible to compare subjects with concussions and potentially identify multiple metrics that can more objectively link brain functionality to postural control.

Chapter 3. Extended Review of Literature and Extended Methodology

3.1. Extended Review of Literature

3.1.1. Quiet Standing

Quiet standing is the act of standing upright on two feet [45]. As most humans are able to perform this from a very young age, it is an easy stance to that can serve as a baseline for stability research. Additionally, quiet standing is quite stable, which allows for data collected in this position to indicate the innate postural control that humans utilize to keep from falling in the absence of direct perturbances to their balance. Examples of foot orientation for different quiet standing stances are shown in Figure 3.1. Of these, the feet apart stance was used for the static trial for instrumentation calibration, and feet together and full tandem were used for data collection trials in this research.

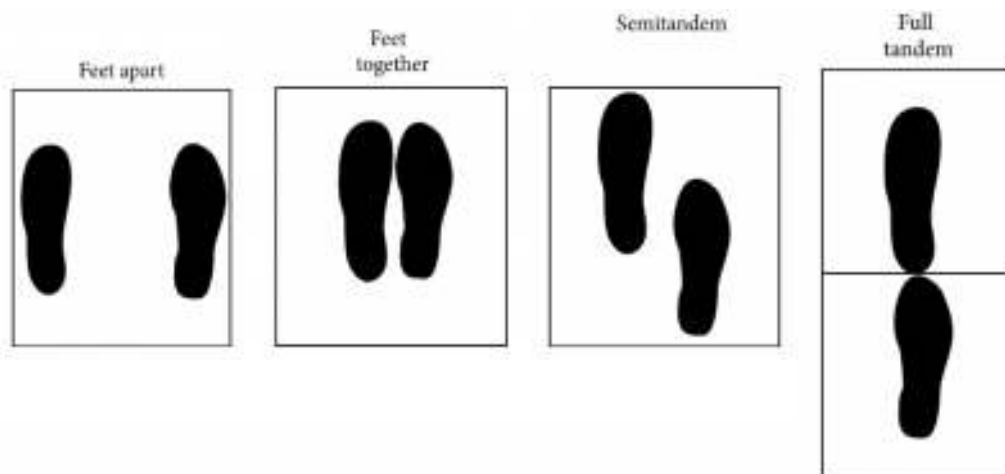


Figure 3.1. Quiet standing foot positioning, adapted from [46]

While quiet standing is relatively stable and the postural control mechanism does not have to account for external perturbances that may be encountered while moving such as unstable surfaces or physical pushing, there are still certain mechanisms that do affect balance. Gravitational force always plays a role as it acts on all parts of the body. If it pulls more on one side of the COM than another due to body positioning, the postural control mechanism must account for those forces [47]. Additionally, internal perturbances such as the natural respiratory oscillation affect balance as well [3]. In the case of respiration, the cyclical movement of the diaphragm and lung expansion slightly alter the COM location, requiring a postural control response.

3.1.2. Postural Control

There are three important metrics that are involved with describing postural control including center of pressure (COP), center of mass (COM), and base of support (BOS). The COP is the point location of the resultant ground reaction force where the body makes contact with the ground and where the moment of the COP is equivalent to the sum of the moments of all ground reaction forces exerted on the body by the ground [2]. The COM is the point location on the body that is representative of all of its mass, where the moment of the COM is equivalent to the sum of the moments of the weight acting at every point on the body, located approximately one-half to two-thirds of a person's body height above the ground [2]. The BOS is the perimeter created around the bounds of the parts of the body that are touching the ground, typically the feet [2]. COP, COM, and BOS are illustrated in Figure 3.2.

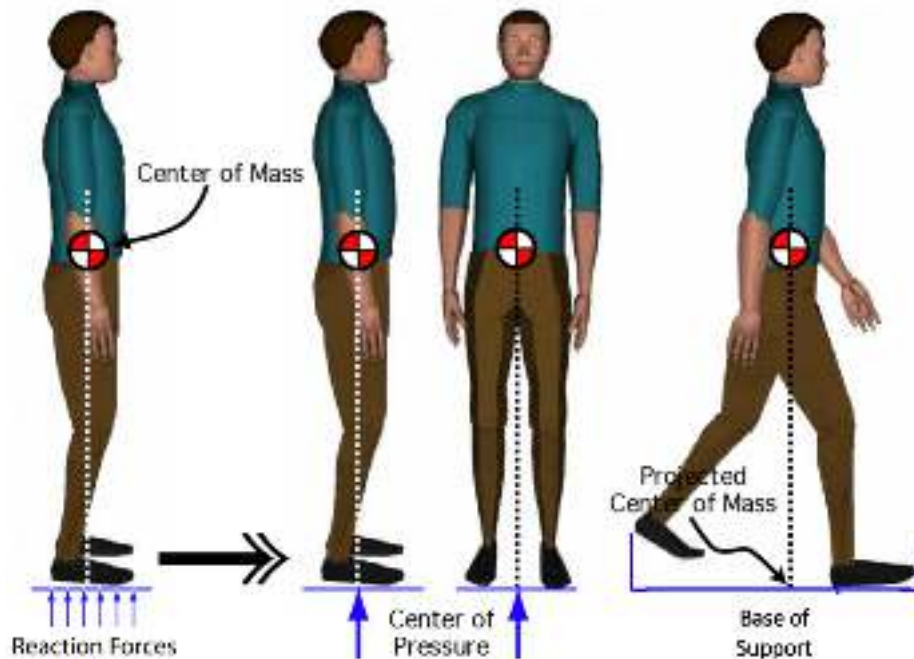


Figure 3.2. COP, COM, and BOS for human body, adapted from [48]

Postural control involves accounting for external and internal forces on the body, such as gravity, wind, physical pushing, respiratory cycles, and more in order to maintain equilibrium of balance where the COM remains within the bounds of the BOS [49]. As the BOS can only safely accommodate a few degrees of sway of the COM before balance is lost, movements associated with postural control are often very minute [49]. For bipedal and quadrupedal beings, these small movements are structured in a way that will return the body to a standard reference position [3]. For humans, this is an upright position where the COP and COM are in similar locations on the ground and at the center of the BOS.

3.1.2.1. Postural Sway

As the body engages in quiet standing, postural control mechanisms are continuously engaged in the form of oscillations of the COP and COM, commonly referred to as postural sway [2], [18]. In quiet standing, the COP oscillates about the COM, which also exhibits a small oscillatory pattern. In order for the COP to assist in maintaining a position of the COM that is suitably within the BOS so that a person can be balanced, the amplitude of the COP oscillations is greater than that of the COM [18]. As COP movement is more pronounced, the oscillations of the COM are often overlooked. The sway of COP and COM can be seen in Figure 3.3, where it is clear that COP follows the same general motion of the COM, but to a greater degree of magnitude.

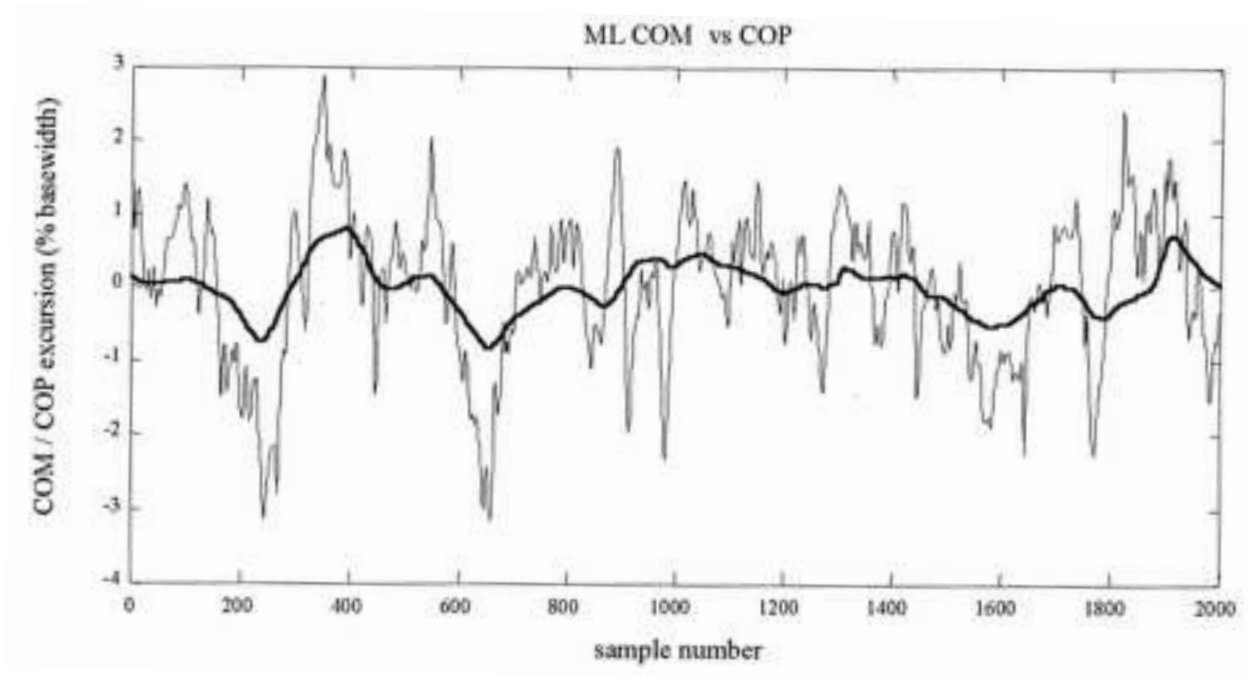


Figure 3.3. COM and COP oscillations during quiet standing, adapted from [50]

Postural sway acts as a constant correction for its own movements. If COP oscillations were to cease, there would be nothing to counteract the movement of the COM, which would result in the person's mass continuing to move in one direction until it has left the bounds of the BOS, causing a fall. Both fatigue of the ankle muscles and absence of vision have been shown to significantly increase sway [20], [51]. This is attributed to the fact that fine control of the COP oscillations has been suppressed in both situations, causing either overcorrection or under correction and the subsequent need for a stronger response.

3.1.2.2. Strategies

When assessing the strategies behind postural control, a neurological factor that must be considered is whether or not the perturbation of stability was foreseen. Postural control can be either predictive or reactive. If the person is aware of the fact that a perturbation to their balance is imminent, subconscious predictive postural control will be activated and may involve a voluntary movement or increase in muscle activity before the expected disturbance occurs [1]. Reactive postural control, however, involves muscular response and movement of the body following an unpredicted disturbance to the balance in order to recover after the fact [1].

Typically, predictive postural control is completed with the ankle strategy [22]. That is where most of the compensation for a perturbation of balance is made via the angle that the ankle creates between the foot and the leg as opposed to compensating by moving the upper body. This allows for low difficulty balance corrections to be made with fine accuracy and without affecting the positioning of the rest of the body significantly.

Reactive postural control is typically completed using the hip strategy. This strategy adjusts the angle of the hips relative to the upper and lower body in a similar way to how the ankle strategy works. It is useful for stronger perturbations as well as those that occur unexpectedly [13]. This is because in both cases, more significant instability occurs requiring a more significant reactive motion of the body to counteract it.

When perturbations are too strong or unexpected for the hip strategy to provide postural control alone, the hip and ankle strategies will work in tandem with one another. In this case, the hip movement accounts for a large amount of reactive activity while the ankle movement may allow the person to have prepared themselves slightly for the perturbation. In the case where the hip and ankle strategies, together, are not enough to keep a person upright, the step strategy will be utilized. This is where the person moves one foot in the direction that they are falling to widen their BOS. These strategies are shown in Figure 3.4.

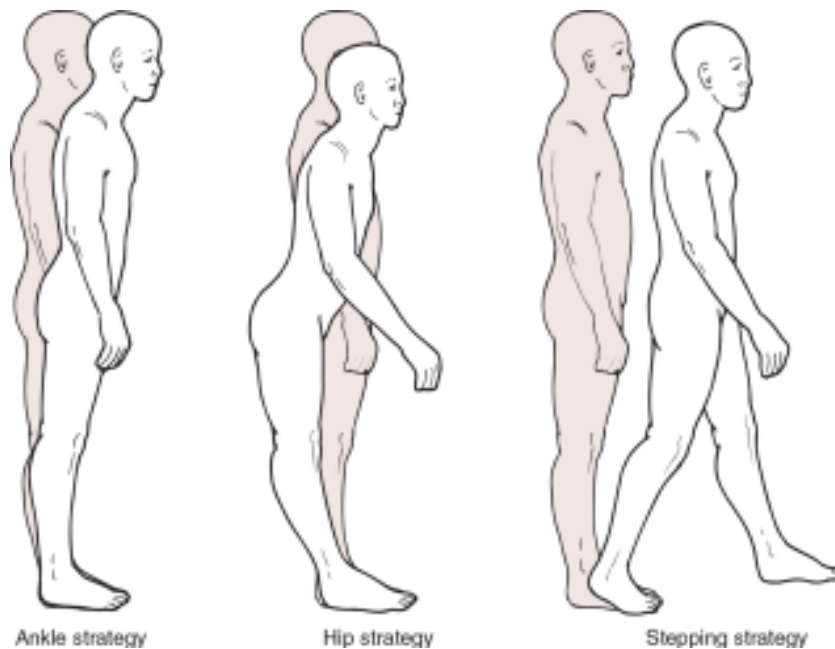


Figure 3.4. Three postural control strategies [52]

The activation of the strategies discussed is not a voluntary reaction. All of postural control is involuntary to ensure a reaction that is as quick as possible to prevent a person from falling. However, these reactions are not the same as a spinal stretch reflex, another involuntary movement of the body, such as the knee jerk reflex. In that movement, the body recognizes when a muscle is stretched beyond the typical amount at a time where it is not expected. When this is sensed, the body immediately contracts the muscle in order to return it to its homeostatic state [53], [54]. There is very little latency between the onset of the muscular stretching and muscle activation. With responses to postural perturbations, however, longer latencies exist. This shows that the CNS has a greater ability to modify the postural responses than it does to modify stretch reflexes. Shorter latencies are associated with decreased involvement of the cerebral cortex [5]. In postural control, a shorter latency could indicate that the perturbation was one that was not very complex to recover from or one that the body is naturally accustomed to dealing with.

In addition to the latency that exists between the CNS and the body's reaction to a balance perturbation, the CNS also has the ability to learn from its past. Studies suggest that the cerebellar-cortical loop can adapt postural control responses based upon prior experiences. They also suggest that the basal ganglia-cortical loop can judge the current context and select postural responses that will be optimal given the known situation [5]. This functionality allows for stability and balance to be improved upon over time as the CNS understands the best way to counteract perturbations after they have previously occurred. When the CNS is required to act from memory, longer latencies between perturbation and action can be expected. This means the reaction to the perturbation may be slightly delayed, however, the action that the body's postural control mechanism is taking will be more efficient and specialized to the current situation, so the latency should not result in a fall.

3.1.2.3. Inverted Pendulum Model

In human mechanics, the ankle and hip strategies described above are often described as an inverted pendulum model. The ankle strategy can be described as a single inverted pendulum (SIP), while the combined ankle and hip strategy is described as a double inverted pendulum (DIP). These models are shown in Figure 3.5, where the distance from the ground to different points on the body as well as angles between these points can be used in mechanics equations to quantify the strategies.

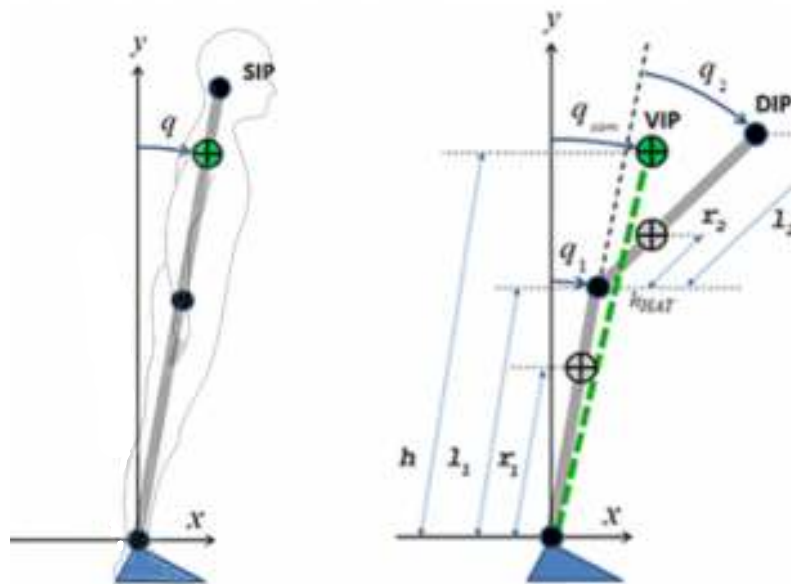


Figure 3.5. Single (left) and double (right) inverted pendulum models adapted from [55]

In the SIP the ankle is the pivot point of the pendulum [2], [24]. In this case, it is assumed that the body detects angular deviation about the ankle pivot point and sensory systems indicate necessary corrections that must be made to eliminate that deviation. Those come in the form of a

corrective torque about the ankle [24]. The DIP functions similarly to the SIP, except for the additional pivot point at the hips [2], [24]. As studies have shown that even during quiet standing the hip strategy is employed, however slightly, the DIP provides a more accurate representation of the human postural control strategy during quiet standing than the SIP [16], [56], [57].

Utilizing these models is useful as they allow for mechanics theorems and equations that have been studied and proven for pendulums, to be applied to the human body. This leads to the ability for quantitative calculations about postural control.

3.1.3. Brain Health and Postural Control

It is widely known that concussion results in symptoms of dizziness and balance impairments. These symptoms are due, in part, to the damage of the vestibular system that are associated with concussions [58]. The vestibular system is responsible for transmitting sensory information about motion, head position, and spatial orientation as well as initiating motor function for maintaining balance and stability. Therefore, impairment of this system can be expected to have a significant effect of postural control, making research on the topic an important step in developing a definitive concussion diagnosis tool.

In addition to vestibular damage, concussions have been shown to damage individual neurons in the brain in differing location, based upon where impact with the head occurred and how strong the impact was [59], [60]. This damage happens when the neurons must change direction in order to accommodate rapid acceleration and deceleration of the brain. Depending on the location of damaged neurons, many systems in the body can be affected, leading to different symptoms in different people.

3.2. Extended Methodology

3.2.1. Participants

Subjects included in this study were all healthy with no history of neurological or muscular disorders. Additionally, volunteers were excluded from participating if they had a history of head trauma resulting in loss of consciousness, a history of reconstructive surgery due to a musculoskeletal injury of the trunk or lower extremities, or any non-weight bearing injury to the lower extremities within the 12 months prior to data collection. To gain an understanding of the subjects' current activity level and their history that could contribute to tuning of their postural control system, all participants were asked to fill out a questionnaire. In addition to the subject provided information, body height (cm), mass (kg), and inter-anterior superior iliac spine (ASIS) distance (cm), as well as leg length (cm), knee width (cm), and ankle width (cm) for the left and right legs were collected prior to subject preparation. The Full-Body Plug-in-Gait (FB PiG) model, which was used for motion capture analysis to obtain center of mass data, required those measurements for normalization of the calculated outputs. Characteristics of each subject are shown in Table 3.1.

Table 3.1. Subject Characteristics

| Subject | Gender | Foot Dominance | Age | Height (cm) | Weight (kg) |
|----------------|---------------|-----------------------|------------|--------------------|--------------------|
| SB01 | F | Right | 26 | 170.4 | 64.5 |
| SB02 | F | Right | 21 | 162.6 | 64.7 |
| SB03 | M | Left | 23 | 174.7 | 63.9 |
| SB04 | M | Left | 28 | 190.0 | 98.2 |
| SB05 | F | Right | 25 | 163.0 | 70.1 |
| SB06 | F | Right | 25 | 164.0 | 63.2 |

3.2.2. Experimental Procedure

Prior to following the experimental protocol for data collection, subjects were asked to perform a static trial to calibrate a Vicon labeling skeleton from an existing Vicon skeletal template. This enabled Nexus to automatically detect a subject and determine the proper reconstruction labels for the subsequent trials for data acquisition. This static trial was performed by having the subject hold a position with their feet shoulder width apart, arms raised slightly at the sides, and with their palms and head facing forward for one second prior to starting the experimental protocol. The calibration process resulting from the combination of the anthropometric measurements of each subject that were collected before subject preparation and the static trial allowed for the system to have the ability to calculate body segments, joint centers, and determine a local reference system for dynamic calculations. Once the static trial was complete, subjects were asked to complete the experimental protocol using stability conditions in the order shown in Table 3.2.

Table 3.2. Quiet standing balance conditions

| Order | Balance Condition | Description |
|--------------|--------------------------|--|
| 1 | EOFT | Eyes open, feet together (most stable, baseline) |
| 2 | ECFT | Eyes closed, feet together |
| 3 | EOTanDB | Eyes open, feet tandem, dominant foot in back |
| 4 | ECTanDB | Eyes closed, feet tandem, dominant foot in back |
| 5 | EOTanDF | Eyes open, feet tandem, dominant foot in front |
| 6 | ECTanDF | Eyes closed, feet tandem, dominant foot in front |

It was assumed that the EOFT condition would be the most stable. This allowed for a control condition that would provide a baseline measure against which the other, less stable, conditions could be compared. To ensure a standardized protocol between subjects as well as to constrain potential effects of fatigue, a 30 second break was required between each trial, with a

2-minute break between each condition. To ensure full recovery, subjects were asked to sit during the 2-minute break.

For stability conditions that utilized a tandem stance, subjects were informed of the COP distribution between their two feet prior to the onset of the trial and were asked to adjust until equal distribution was realized. After the trial had begun, subjects were given no further information about the distribution of their COP.

The use of stepping, arm motions, ankle strategy, and hip strategy were expected during the course of the study. Subjects were instructed to attempt to regain their balance and return to the testing stance as quickly as possible if they ever felt that they were losing their balance during a trial. In the event that a subject moved their feet off the force plate, the trial was redone. Foot orientation on the force plates for each of the positions required are shown in Figure 2.5.

The blue rectangles shown in Figure 2.5 represent 1.5-inch-wide athletic tape, which was used to indicate the junction between force plates. For feet tandem positions, subjects were instructed to place the toe of the back foot and the heel of the front foot on the edges of the tape. This ensured that each foot was entirely on its respective force plate, guaranteeing the COP oscillations for each foot were being collected independently. Additionally, the inclusion of the tape provided standardization of feet position between subjects.

3.2.3. Data Acquisition

3.2.3.1. Subject Preparation

Preparation for the collection COM data required marker placement on the subject following pre-amplifier placement. Highly reflective, spherical markers were placed on the subject as specified by the FB PiG model for motion capture as illustrated in Figure 2.4.

The modified version of this model requires the inclusion of the fifth metatarsal (5th-Met) and a medial knee marker in place of a knee alignment device. The FB PiG 5th – Met model was a predefined model used solely for the purpose of this study. Markers were secured to their necessary locations using double-sided hypoallergenic tape and 3M tape.

3.2.3.2. Instrumentation

COP data were collected with two floor-embedded AMTI (Advanced Mechanical Technology Inc., Watertown, MA) force plates. These measured the forces and moments applied to the ground during quiet standing. Ground reaction forces were collected at a sampling frequency of 1200 Hz. 16 Vicon MX cameras (Oxford Metrics, Oxford, UK) were utilized for COM data acquisition. These cameras tracked movement trajectories of the musculoskeletal system, with the use of the modified FB PiG model for marker location, at a sampling frequency of 120 Hz. For both of these signals, the coordinate system used represents the anterior/posterior (AP) directions of the body on the x-axis and the medial/lateral (ML) directions of the body on the y-axis. Both of those axes were represented with a respective signal to report the location on the coordinate system. Nexus motion capture software v2.8 (Oxford Metrics, Oxford, UK) was used to synchronize the force plate and motion capture data.

3.2.4. Data Analysis

All recorded COP and COM signals were analyzed using time and frequency methods of univariate and bivariate analysis to determine patterns and indices present within them during quiet standing for neuro-normative subjects. This analysis was done using Python 3.7.6 (Python Software Foundation, <https://www.python.org/>).

3.2.4.1. Signal Preprocessing

Numerous studies on the frequency content of postural sway have shown that its signal content exists at or below 5 Hz [33]–[35]. For this reason, it was beneficial to apply a filter to the data so that only the frequencies for which true postural sway content would be found was analyzed. A fourth order, zero-lag, low-pass Butterworth filter was applied with a cutoff frequency of 6 Hz using the Vicon Nexus motion capture software v2.8 (Oxford Metrics, Oxford, UK).

An additional preprocessing step was necessary for the tandem feet trials, as they were recorded using two separate force plates, one under each foot. It was important to record the data in this way to ensure that the force plates registered the activity of each foot, respectively. However, since the feet together trials only had COP data from one force plate, it would be impossible to directly compare the COP data from two separate force plates from the feet tandem trials. In order to avoid this issue, a single resultant COP was calculated for feet tandem trials based on a weighted percentage of the COPs recorded on the two force plates, taking into consideration the amount of force that each foot was exerting on the ground and the position of each COP as defined below:

$$COP_{net} = COP_L \frac{F_{zL}}{F_{zL}+F_{zR}} + COP_R \frac{F_{zR}}{F_{zL}+F_{zR}} \quad (3.1)$$

Where COP_L and COP_R are the positions of the COP for the left and right foot, respectively, and F_{zL} and F_{zR} are the ground reaction force of the left and right foot, respectively. This calculation was repeated twice, once using COP positions in the x direction and once using COP positions in the y direction to obtain both the resultant x and y coordinates for the combined COP. The combining of two individual COPs into one net COP is shown in Figure 3.6.

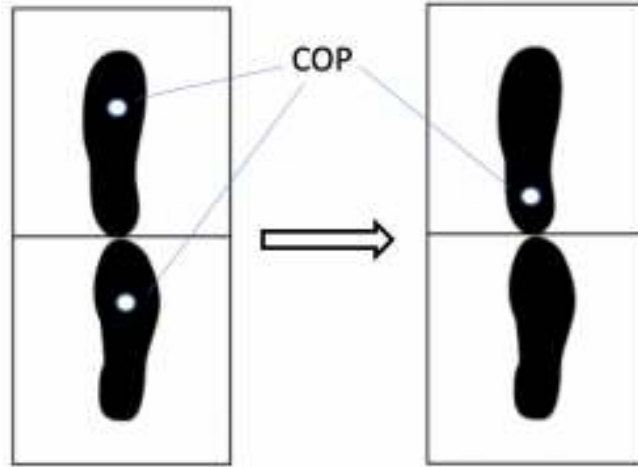


Figure 3.6. Combination of two individual COPs into one resultant COP

3.2.4.2. Approximate Entropy

While there are many different types of entropy, approximate entropy (ApEn) was chosen to determine the uncertainty in all COP signals. Approximate entropy differs from other forms of the metric in important ways. It differs from joint entropy which measures the uncertainty in two random variables, conditional entropy which measures the average uncertainty in one random variable given a second random variable, transfer entropy which describes information transfer between two signals, and cross-approximate entropy which describes the similarity of patterns

between two time-series signals. Comparatively, approximate entropy quantifies the regularity of a single time-series signal and is defined as follows [29]:

$$-ApEn = \Phi^{m+1}(r) - \Phi^m(r) \quad (3.2)$$

Where m and r are fixed values, m being the length of compared runs and r is a filter value, and $\Phi^m(r)$ is defined as:

$$\Phi^m(r) = (N - m + 1)^{-1} \sum_{i=1}^{N-m+1} \ln [C_i^m(r)] \quad (3.3)$$

Where N is the total number of data points and $C_i^m(r)$ is defined as:

$$C_i^m(r) = \frac{\text{number of } j \leq (N-m+1) \text{ such that } d[x(i), x(j)] \leq r}{N-m+1} \quad (3.4)$$

Where $d[x(i), x(j)]$ is the maximum distance between the respective scalar components of vectors $x(i)$ and $x(j)$.

ApEn is especially adept at quantifying regularity in short time-series signals and is good at suppressing noise and resisting outliers. These attributes make it a suitable analysis for this research as it allows for analysis to be completed using a moving technique with small windows of data to account for potential changes in ApEn over time. Additionally, it ensures that small amounts of noise that were not able to be filtered out and outliers that are bound to occur in data do not greatly affect the results. A calculated ApEn result that is lower in value indicates a signal that is more regular. For example, a periodic signal will have a lower ApEn value than random noise. This can provide knowledge about whether postural control becomes more or less regular as stability conditions change.

Moving approximate entropy was calculated for all COP trials using windows of size 1800, or 1.5 second intervals, with a 50 percent overlap to create 39 segments. Performing this calculation across windows allowed for the segments of data to be a suitable length for an ApEn calculation, as the entire time-series signal would have been too long. Additionally, this allowed for visual understanding of how the approximate entropy changed over time. While it was necessary to calculate a moving ApEn, the 39 resulting values were averaged to obtain a single approximate entropy value for further calculations and ease of comparing between different stability conditions.

3.2.4.3. *Velocity*

It is known that the steeper a signal appears when plotted against time, the higher its velocity is. This is because more has changed over a shorter amount of time than in a signal that is flatter. COP data shows many steep spikes due to the quick reaction of the body's postural control system. These spikes appear to be steeper in less stable conditions. It is necessary, however, to complete calculations to quantify the apparent increase in velocity. The changing velocity of a signal can be determined with a first derivative and is estimated using the following equation:

$$V(i) = \frac{x(i+1)-x(i)}{t(i+1)-t(i)} \quad (3.5)$$

Where x is the COP signal, t is the time vector, and i is the index equal to the length of the signal. This slope equation gives the rate of change of the signal, providing knowledge about how quickly the body is swaying while maintaining balance.

Velocity was calculated for all COP signals between every two points. This created a new signal with a length equal to the original COP signal. The data in the new velocity signal was averaged together to create a single value representing the average velocity for each trial, respectively. This average represented the typical oscillation speed of the given trial.

3.2.4.4. Power Spectral Density

Power spectral density (PSD) provides information about the frequencies that exist within a signal. More specifically, it gives a representation of how much of a signal exists at each frequency. For example, the PSD of a 2 Hz sine wave is shown in Figure 3.7. Here, a large spike is shown only at 2 Hz, as that is the only frequency that exists in the signal.

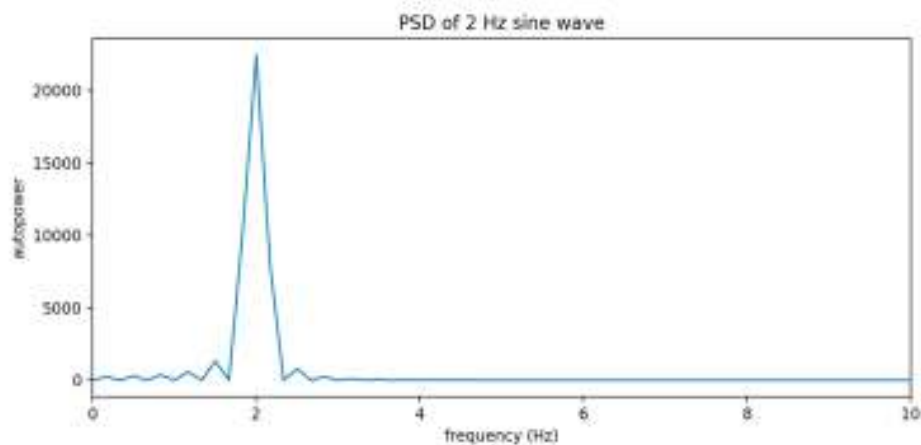


Figure 3.7. Power spectral density of a 2 Hz sine wave

Comparatively, Figure 3.8 shows the PSD of the same 2 Hz sine wave added to a 5 Hz cosine wave. Here, spikes are seen at both 2 Hz and 5 Hz, with the same amplitude, because the signal is made up of equal parts of both frequencies.

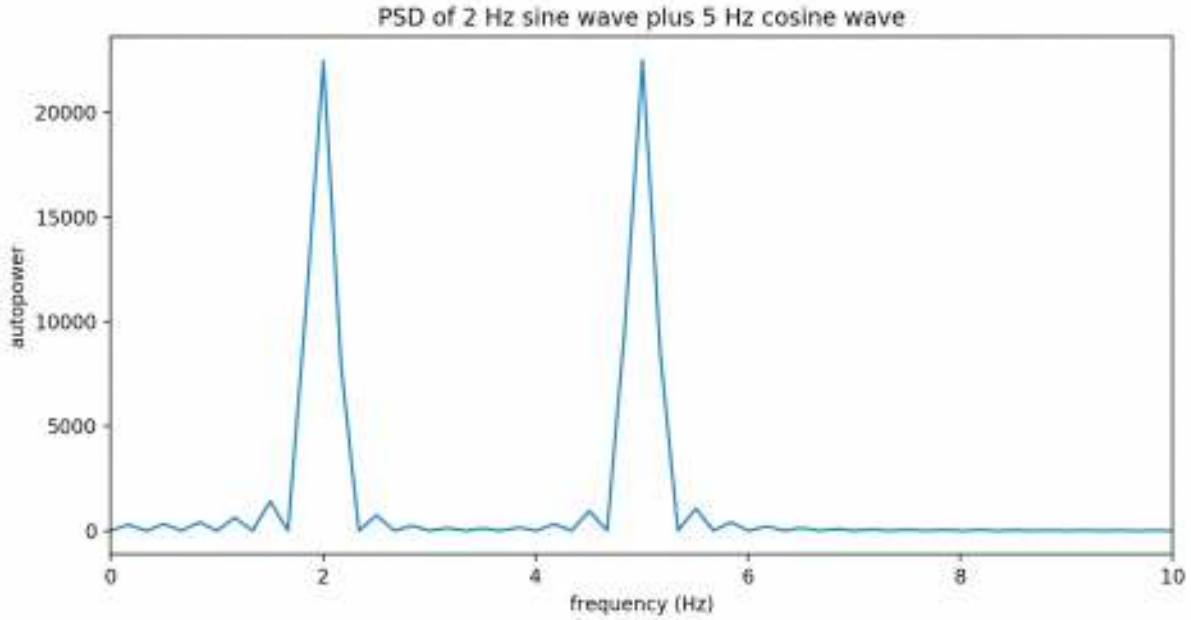


Figure 3.8. Power spectral density of a 2 Hz sine wave added to a 5 Hz cosine wave

PSD is defined as follows:

$$S_{xx}(\omega) = \int_{-\infty}^{\infty} R_{xx}(\tau) e^{-j\omega\tau} d\tau \quad (3.6)$$

Where $R_{xx}(\tau)$ is the autocorrelation and is defined as follows:

$$R_{xx}(\tau) = \frac{1}{T_0} \int_0^{T_0} x(t) * x(t + \tau) dt \quad (3.7)$$

Where the signal in question is a finite length, real valued signal, $x(t)$, from $0 \leq t \leq T_0$ and where τ is some amount of lag.

Auto-power, or the PSD of an individual signal, was determined for the velocity signal of all COP data. In order to do this, the Python *NumPy* tool *correlate* was used to calculate the autocorrelation of the signal. This was followed by the *NumPy* tool *fft.fft* to complete the

necessary Fourier transform to obtain the PSD. A summation of all frequency content in a signal was performed to obtain a metric of total power that could be compared between trials.

In addition to using autocorrelation as a part of the PSD calculation, it was also used on its own with all COP data. Autocorrelation provides information about how strongly a signal is related to itself at different amounts of lag. This autocorrelation was compared to the cross-correlation between COP and COM signals of the same direction. Like autocorrelation, cross-correlation provides information about similarity, but it provides information about how similar one signal is to another signal, as opposed to the same signal, at different amounts of lag. The comparison of autocorrelation of COP to cross-correlation between COP and COM shows how similar the COP and COM signals are to one another. If the autocorrelation of the COP signal looks very similar to the cross-correlation between the COP and COM signals, then it is clear that the signals themselves look similar at all times. Cross-correlation was performed using the same *NumPy correlate* tool as autocorrelation and is defined as follows:

$$R_{xy}(\tau) = \frac{1}{T_0} \int_0^{T_0} x(t) * y(t + \tau) dt \quad (3.8)$$

3.2.4.5. Regression

Regression is a tool used to estimate the relationship between a signal and the time over which it was recorded. It is defined as follows:

$$y = \beta_0 + \beta_1 x + \beta_2 x^2 + \beta_3 x^3 + \dots + \beta_n x^n + \varepsilon \quad (3.9)$$

Where the betas are the coefficients for the nth powers of the independent variable, x, and epsilon is the error in the regression. This is often calculated in matrix form as shown below:

$$\begin{bmatrix} y_1 \\ y_2 \\ y_3 \\ \vdots \\ y_n \end{bmatrix} = \begin{bmatrix} 1 & x_1 & x_1^2 & \dots & x_1^m \\ 1 & x_2 & x_2^2 & \dots & x_2^m \\ 1 & x_3 & x_3^2 & \dots & x_3^m \\ \vdots & \vdots & \vdots & \ddots & \vdots \\ 1 & x_n & x_n^2 & \dots & x_n^m \end{bmatrix} \begin{bmatrix} \beta_0 \\ \beta_1 \\ \beta_2 \\ \vdots \\ \beta_m \end{bmatrix} + \begin{bmatrix} \varepsilon_0 \\ \varepsilon_1 \\ \varepsilon_2 \\ \vdots \\ \varepsilon_n \end{bmatrix} \quad (3.10)$$

This was calculated using the *LinearRegression* and *PolynomialFeatures* tools from the *scikit-learn* machine learning library for python. This was done to create a baseline estimate for what different stability conditions can be expected to look like, similar to the regression line shown in Figure 3.9.

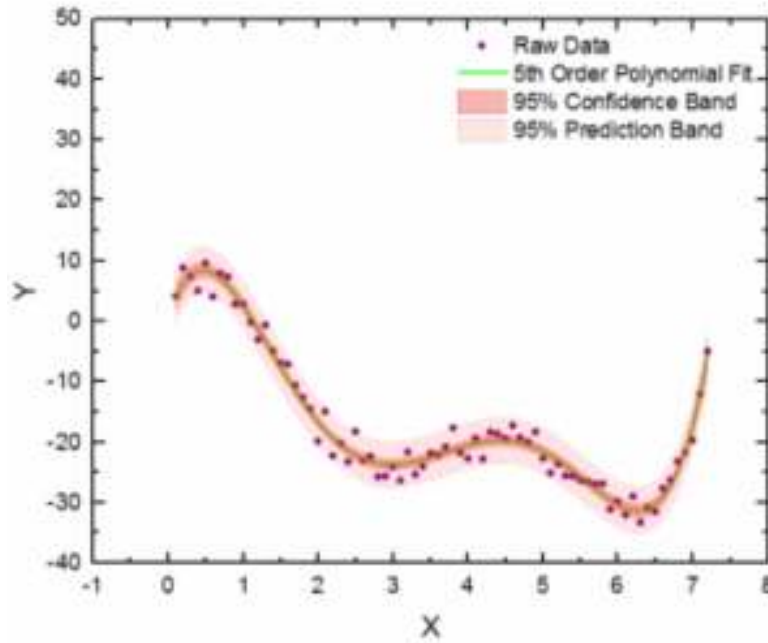


Figure 3.9. Polynomial regression example, adapted from [61]

In order to create regression predictions, the trials from each respective stability condition were averaged among all subjects to obtain one signal for each condition. This was done by taking the average value for each index position. For example, the average was taken of all first data points for all trials of the EOFT condition, and so on. Then, regression was calculated for the resulting average signal. This provided important information, such as what a smooth signal

approximate of that average would look like and where the boundaries were for a 95 percent prediction band. Additionally, an R^2 value of the regression describes how much of the signal was able to be approximated by the calculation. This can provide supporting evidence for approximate entropy, as it is another way to estimate the uncertainty in a signal.

Appendix A. Figures

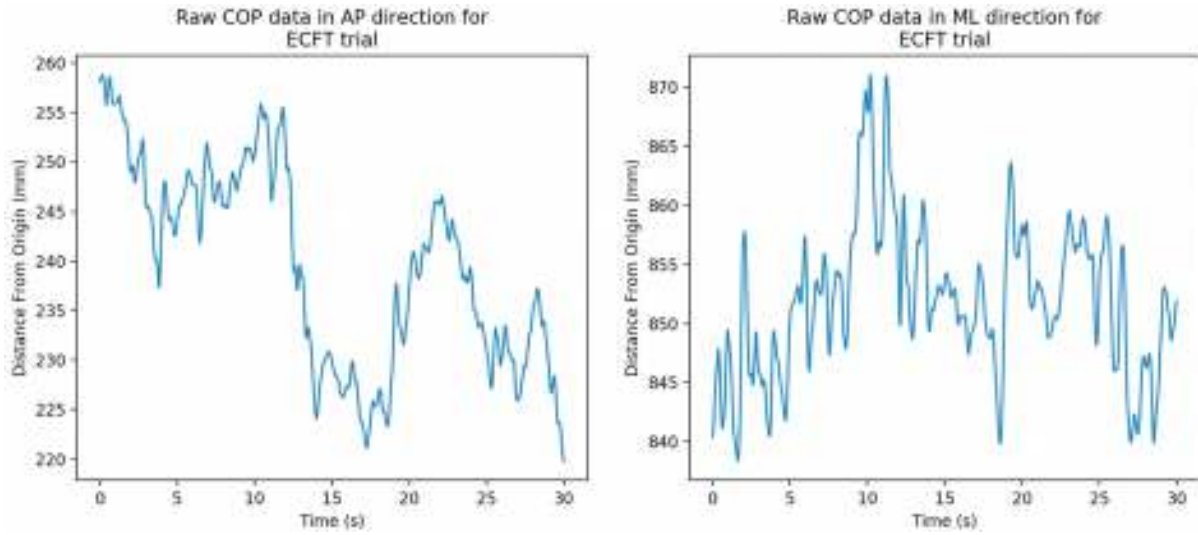


Figure A.1. COP data for eyes closed, feet together trial

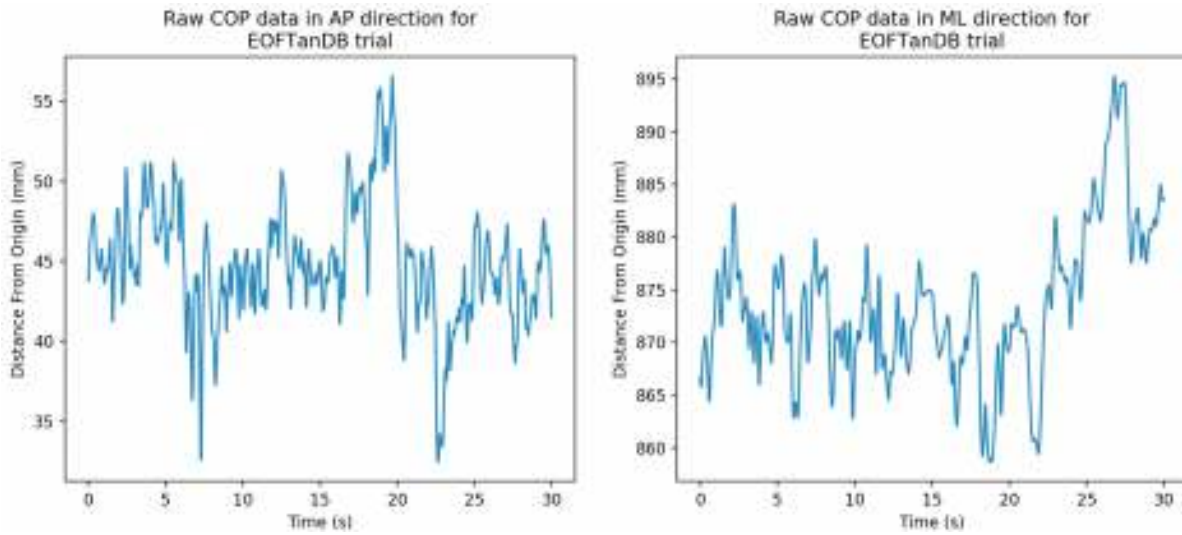


Figure A.2. COP data for eyes open, feet tandem, dominant foot in back trial

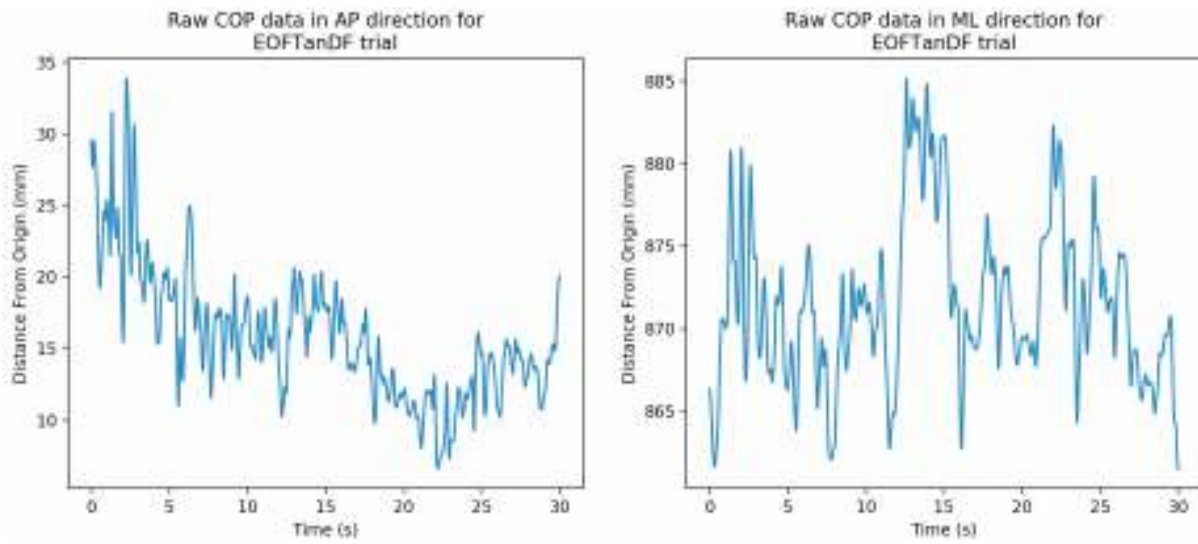


Figure A.3. COP data for eyes open, feet tandem, dominant foot in front trial

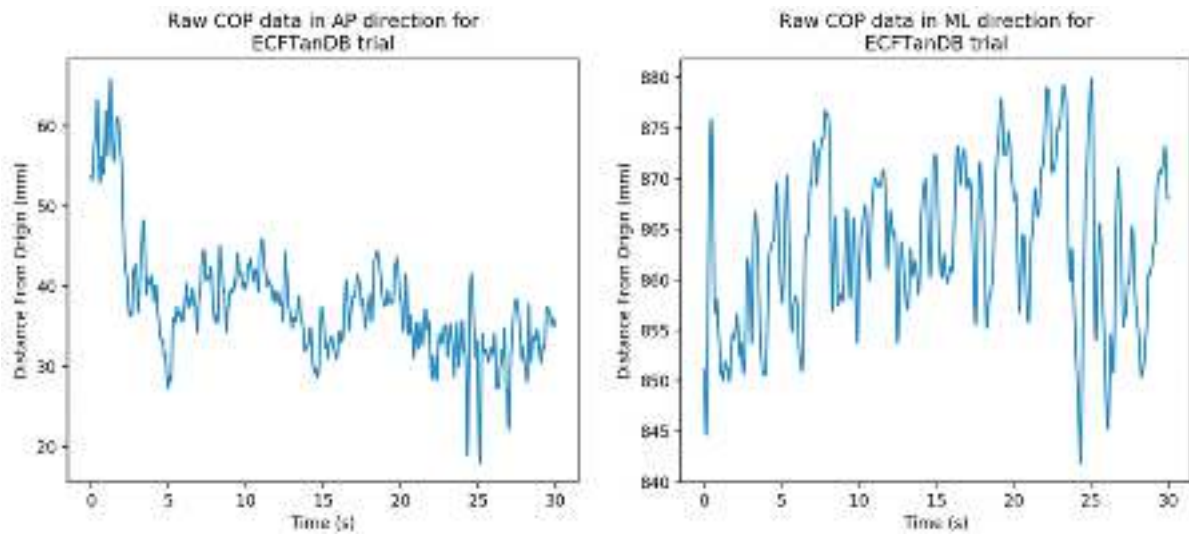


Figure A.4. COP data for eyes closed, feet tandem, dominant foot in back trial

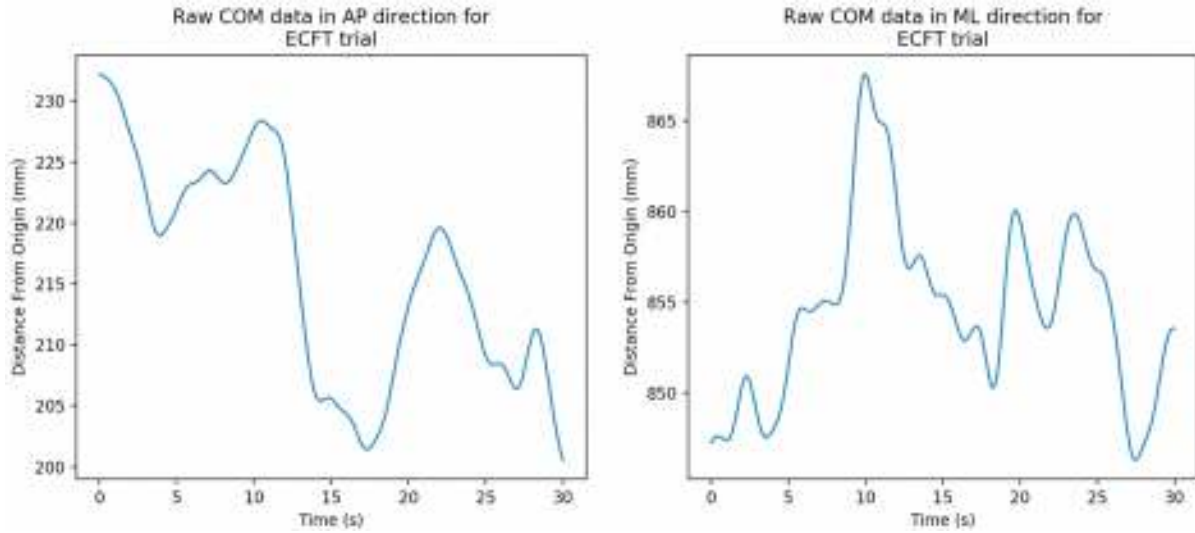


Figure A.5. COM data for eyes closed, feet together trial

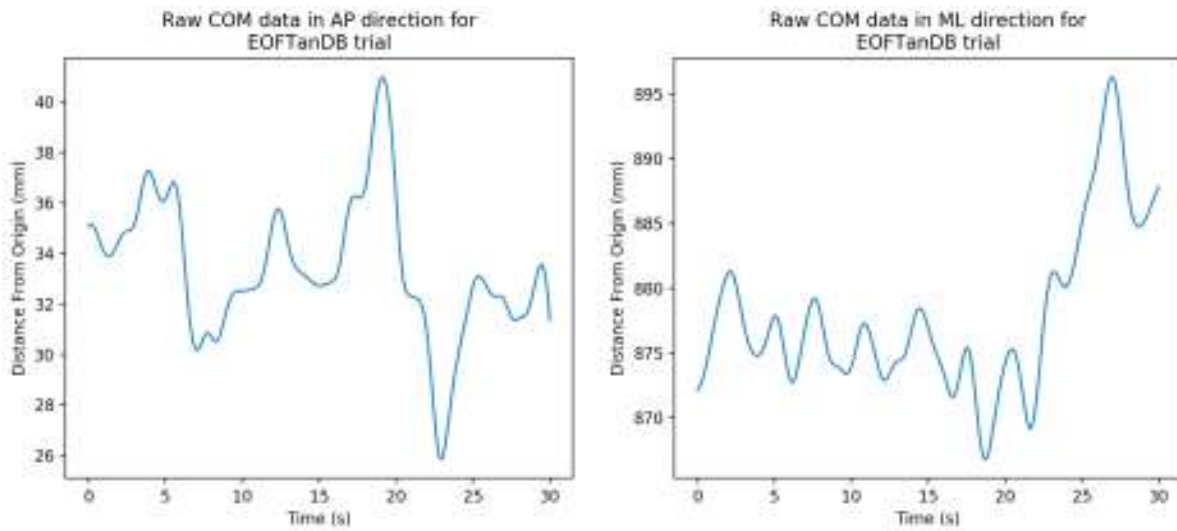


Figure A.6. COM data for eyes open, feet tandem, dominant foot in back trial

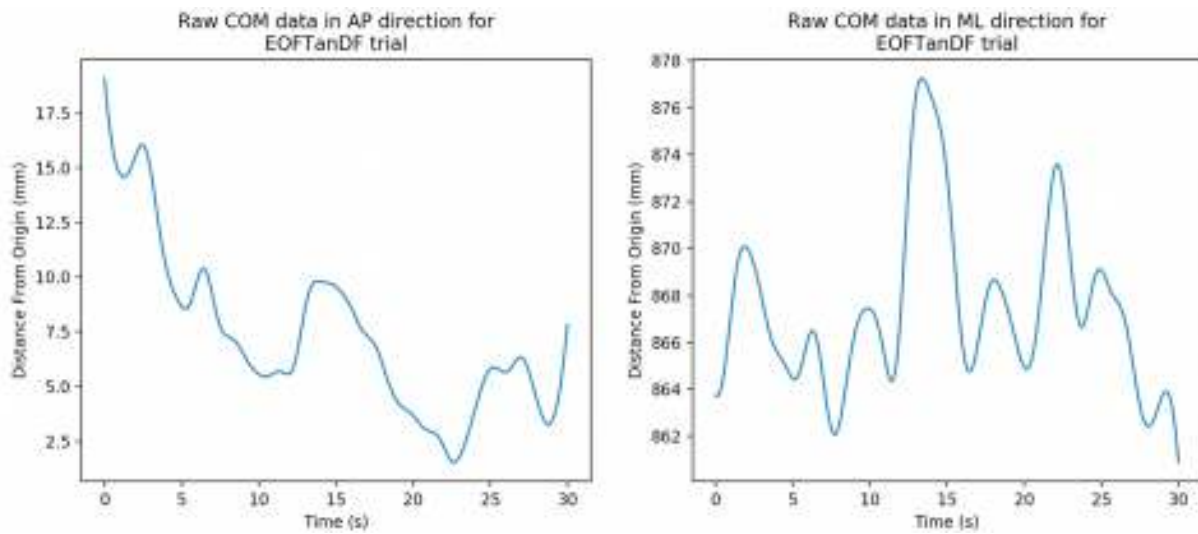


Figure A.7. COM data for eyes open, feet tandem, dominant foot in front trial

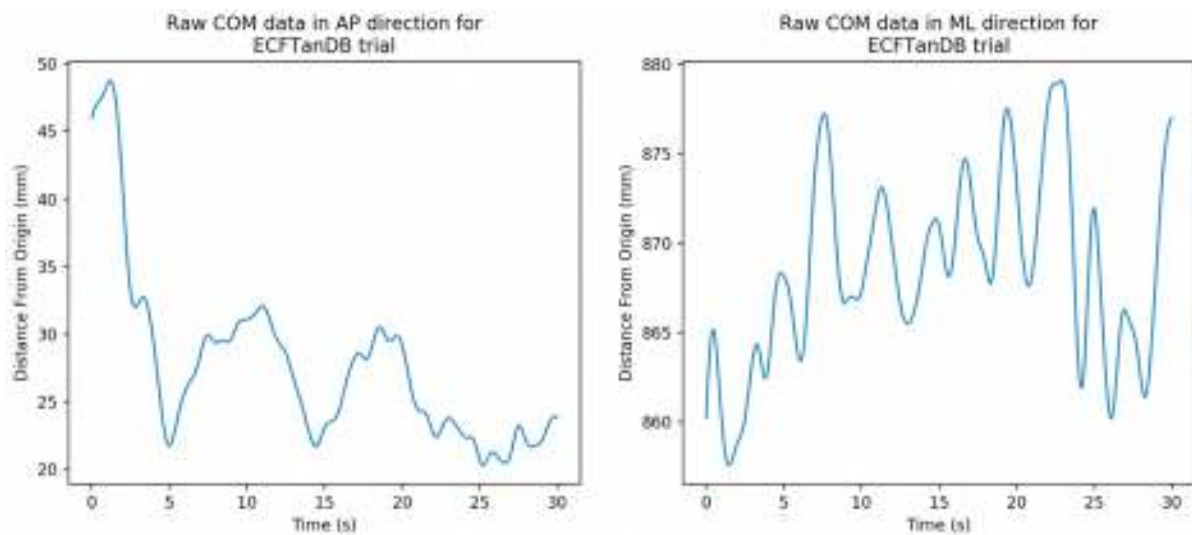


Figure A.8. COM data for eyes closed, feet tandem, dominant foot in back trial

Appendix B. Code

B.1. Correlation Calculations

```
#####  
  
# correlation.py  
#  
# Written by: Natalie Tipton  
# Advisor: Dr. Samhita Rhodes  
#  
# Created on: July 5, 2020  
#  
# Description: Signal Processing of COM  
# and COP to obtain auto and cross  
# correlation for comparison.  
#  
# Last updated: July 29, 2020  
  
#####  
  
# import packages  
import matplotlib.pyplot as plt  
import numpy as np  
import pandas as pd  
import analysis_lib as an  
from scipy.stats import pearsonr  
  
# constants  
fs_com = 120  
fs_cop = 1200  
t_com = np.arange(0, 30, 1 / fs_com)  
t_cop = np.arange(0, 30, 1 / fs_cop)  
  
#####  
  
if __name__ == "__main__":  
  
    # read in COP data  
    x_cop = pd.read_csv("x_cop.csv", index_col=False)  
    y_cop = pd.read_csv("y_cop.csv", index_col=False)  
  
    # read in COM data  
    x_com = pd.read_csv("x_com.csv", index_col=False)  
    y_com = pd.read_csv("y_com.csv", index_col=False)
```

```

# create dictionaries and lists for x-axis data
corr_dict = {}
eoft = []
ecft = []
eoftandb = []
eoftandf = []
ecftandb = []
ecftandf = []

# cycle through each column in x file
for col in x_cop.columns:
    # determine the subject and trial number for column

    # determine subject and trial number of current data
    number = int(col[10:12])
    subject = int(col[2:4])

    # turn column of df into a list
    cop_sig = x_cop[col].to_list()
    com_sig = x_com[col].to_list()

    # create time vector for correlation signal
    n_com = len(com_sig)
    t_corr = np.arange(-n_com / fs_com, n_com / fs_com - 1 / fs_com, 1 / fs_com)

    # resample COP data to match fs of COM
    cop_sig_resample = []
    for i in range(0, n_com):
        cop_sig_resample.append(cop_sig[i * 10])

    # calculate pearson's correlation coefficient between COP and COM
    corr, _ = pearsonr(cop_sig_resample, com_sig)

    # calculate autocorrelation of COP
    auto_corr = np.correlate(cop_sig_resample, cop_sig_resample, mode="full")

    # calculate cross correlation between COP and COM
    cross_corr = np.correlate(cop_sig_resample, com_sig, mode="full")

    # split up pearson's coefficients by condition
    if number < 7:
        eoft.append(corr)
    elif 6 < number < 12:
        ecft.append(corr)
    elif 11 < number < 17:
        eoftandb.append(corr)
    elif 16 < number < 22:
        ecftandb.append(corr)

```

```

elif 21 < number < 27:
    eoftandf.append(corr)
elif 26 < number < 32:
    ecftandf.append(corr)

# set values to keys of each condition in dictionary for pearsons
corr_dict["E0FT"] = eoft
corr_dict["ECFT"] = ecft
corr_dict["E0FTanDB"] = eoftandb
corr_dict["ECFTanDB"] = ecftandb
corr_dict["E0FTanDF"] = eoftandf
corr_dict["ECFTanDF"] = ecftandf

# save pearson's coefficients in dataframe format to a .csv file
corr_df = pd.DataFrame(corr_dict, columns=corr_dict.keys())
corr_df.to_csv("x_correlations.csv")

# repeat above for the y-axis data

```

B.2. Entropy Calculations

```

#####

# entropy.py
#
# Written by: Natalie Tipton
# Advisor: Dr. Samhita Rhodes
#
# Created on: May 6, 2020
#
# Description: Compute approximate entropy
# for all files in x and y and save them
# in one .csv file for all x and another
# for all y
#
# Last updated: July 29, 2020

#####

import matplotlib.pyplot as plt
import numpy as np
import pandas as pd
import skimage
from tqdm import tqdm
from joblib import Parallel, delayed
import multiprocessing
import analysis_lib as an

```

```

import os

# define root folder for data
ROOT = f"{os.environ.get('HOME')}/Code/center_of_pressure/data"

# constants
fs_cop = 1200
t_cop = np.arange(0, 30, 1 / fs_cop)

#####

if __name__ == "__main__":

    # determine all subdirectories in root directory
    folders = [x[0] for x in os.walk(ROOT)]
    # remove the root directory from folders
    folders.remove(ROOT)
    # find all file names in the subdirectories
    files = [
        (os.path.join(ROOT, folder), os.listdir(os.path.join(ROOT, folder)))
         for folder in folders
    ]

    # create a dictionary showing what filenames are within each folder
    dirs = {}
    for folder_name, file_list in files:
        # remove irrelevant file names
        if ".DS_Store" in file_list:
            file_list.remove(".DS_Store")
        dirs[folder_name] = file_list

    # create lists to hold ApEn results for every file
    ent_x_dict = {}
    ent_y_dict = {}

    # loop through all files in all subdirectories
    for directory in dirs:
        print(directory)
        # loop through each file in the directory
        for file in dirs[directory]:
            # Determine which trial number it is
            number = int(file[10:12])

            # read data
            df = pd.read_csv(os.path.join(directory, file), index_col=False)

            # convert data from dataframe into a numpy list and obtain x and y signals
            df = df.to_numpy()

```

```

values = np.delete(df, 0, 1)
x_cop, y_cop = values.T

# calculate moving ApEn for x and y COP signals
ap_ent_x = an.approx_ent(x_cop, 1800, 900, 100, "X CoP")
ap_ent_y = an.approx_ent(y_cop, 1800, 900, 100, "Y CoP")

# save ApEn results into a dictionary under the key of the file name
ent_x_dict["{file}_x_ap_ent"] = ap_ent_x
ent_y_dict["{file}_y_ap_ent"] = ap_ent_y

# turn completed dictionaries into pandas dataframe
ent_x_df = pd.DataFrame(ent_x_dict, columns=ent_x_dict.keys())
ent_y_df = pd.DataFrame(ent_y_dict, columns=ent_y_dict.keys())

# save both dataframes in .csv files
ent_x_df.to_csv("x.csv")
ent_y_df.to_csv("y.csv")

#####

# entropy_analysis.py
#
# Written by: Natalie Tipton
# Advisor: Dr. Samhita Rhodes
#
# Created on: July 3, 2020
#
# Description: Perform analysis on files
# containing Approximate entropy results
# for all files in x and y directions
#
# Last updated: July 29, 2020

#####

# import packages
import matplotlib.pyplot as plt
import numpy as np
import pandas as pd
import analysis_lib as an
import os
import statistics

# constants
fs_cop = 1200
t_cop = np.arange(0, 30, 1 / fs_cop)

```

```

# create dictionaries to hold the trial entropy
# for each subject in both directions
sb01_x = {}
sb02_x = {}
sb04_x = {}
sb05_x = {}
sb06_x = {}
sb08_x = {}

sb01_y = {}
sb02_y = {}
sb04_y = {}
sb05_y = {}
sb06_y = {}
sb08_y = {}

#####

if __name__ == "__main__":

    # read files with x and y ApEn data
    x_ent = pd.read_csv("x.csv", index_col=False)
    y_ent = pd.read_csv("y.csv", index_col=False)

    # cycle through each column in x file
    for col in x_ent.columns:
        # determine the subject and trial number for column
        number = int(col[10:12])
        subject = int(col[2:4])

        # turn column of df into a list
        sig = x_ent[col].to_list()

        # create dictionary key for trial number and save data to it
        # for each subject
        if subject == 1:
            sb01_x[number] = sig
        elif subject == 2:
            sb02_x[number] = sig
        elif subject == 4:
            sb04_x[number] = sig
        elif subject == 5:
            sb05_x[number] = sig
        elif subject == 6:
            sb06_x[number] = sig
        elif subject == 8:
            sb08_x[number] = sig

```

```

# repeat above for y data
for col in y_ent.columns:
    number = int(col[10:12])
    subject = int(col[2:4])

    sig = y_ent[col].to_list()

    if subject == 1:
        sb01_y[number] = sig
    elif subject == 2:
        sb02_y[number] = sig
    elif subject == 4:
        sb04_y[number] = sig
    elif subject == 5:
        sb05_y[number] = sig
    elif subject == 6:
        sb06_y[number] = sig
    elif subject == 8:
        sb08_y[number] = sig

##### Subject 1 #####

# create lists to save different stability conditions to
x_eoft_ent = []
x_ecft_ent = []
x_eoftandb_ent = []
x_ecftandb_ent = []
x_eoftandf_ent = []
x_ecftandf_ent = []

y_eoft_ent = []
y_ecft_ent = []
y_eoftandb_ent = []
y_ecftandb_ent = []
y_eoftandf_ent = []
y_ecftandf_ent = []

x_trial_ent = []
y_trial_ent = []
trial_cond = []

# loop through all trials for subject 1 in x
for trial in sb01_x.keys():
    # save ApEn to proper stability condition list
    if trial < 7:
        trial_cond.append("EOFT")
        x_eoft_ent.append(np.mean(sb01_x[trial]))

```

```

        y_eoft_ent.append(np.mean(sb01_y[trial]))
        x_trial_ent.append(np.mean(sb01_x[trial]))
        y_trial_ent.append(np.mean(sb01_y[trial]))
elif 6 < trial < 12:
    trial_cond.append("ECFT")
    x_ecft_ent.append(np.mean(sb01_x[trial]))
    y_ecft_ent.append(np.mean(sb01_y[trial]))
    x_trial_ent.append(np.mean(sb01_x[trial]))
    y_trial_ent.append(np.mean(sb01_y[trial]))
elif 11 < trial < 17:
    trial_cond.append("EOFTanDB")
    x_eoftandb_ent.append(np.mean(sb01_x[trial]))
    y_eoftandb_ent.append(np.mean(sb01_y[trial]))
    x_trial_ent.append(np.mean(sb01_x[trial]))
    y_trial_ent.append(np.mean(sb01_y[trial]))
elif 16 < trial < 22:
    trial_cond.append("ECFTanDB")
    x_ecftandb_ent.append(np.mean(sb01_x[trial]))
    y_ecftandb_ent.append(np.mean(sb01_y[trial]))
    x_trial_ent.append(np.mean(sb01_x[trial]))
    y_trial_ent.append(np.mean(sb01_y[trial]))
elif 21 < trial < 27:
    trial_cond.append("EOFTanDF")
    x_eoftandf_ent.append(np.mean(sb01_x[trial]))
    y_eoftandf_ent.append(np.mean(sb01_y[trial]))
    x_trial_ent.append(np.mean(sb01_x[trial]))
    y_trial_ent.append(np.mean(sb01_y[trial]))
elif 26 < trial < 32:
    trial_cond.append("ECFTanDF")
    x_ecftandf_ent.append(np.mean(sb01_x[trial]))
    y_ecftandf_ent.append(np.mean(sb01_y[trial]))
    x_trial_ent.append(np.mean(sb01_x[trial]))
    y_trial_ent.append(np.mean(sb01_y[trial]))

# save x and y entropies by trial and condition to a .csv file
zipped = list(zip(x_trial_ent, y_trial_ent, trial_cond))
df_for_stats = pd.DataFrame(zipped, columns=["xEntropy", "yEntropy", "condition"])
df_for_stats.to_csv(f"sb1_entropy_by_condition.csv")

# repeat above for remaining subjects

```

B.3. Velocity Calculations

```
#####  
  
# velocity.py  
#  
# Written by: Natalie Tipton  
# Advisor: Dr. Samhita Rhodes  
#  
# Created on: June 10, 2020  
#  
# Description: Processing of the velocity  
# of COP signals.  
#  
# Last updated: July 29, 2020  
  
#####  
  
# import packages  
import matplotlib.pyplot as plt  
import numpy as np  
import pandas as pd  
import analysis_lib as an  
import os  
import statistics  
  
# define root folder for data  
ROOT = f"{os.environ.get('HOME')}/Code/center_of_pressure/data"  
  
# constants  
fs_cop = 1200  
t_cop = np.arange(0, 30, 1 / fs_cop)  
  
#####  
  
if __name__ == "__main__":  
  
    # determine all subdirectories in root directory  
    folders = [x[0] for x in os.walk(ROOT)]  
    # remove the root directory from folders  
    folders.remove(ROOT)  
    # find all file names in the subdirectories  
    files = [  
        (os.path.join(ROOT, folder), os.listdir(os.path.join(ROOT, folder)))  
        for folder in folders  
    ]
```

```

# create a dictionary showing what filenames are within each folder
dirs = {}
for folder_name, file_list in files:
    # remove irrelevant file names
    if ".DS_Store" in file_list:
        file_list.remove(".DS_Store")
    dirs[folder_name] = file_list

# loop through all files in all subdirectories
for directory in dirs:
    print(directory)

    # create lists to store vel and psd for x and y data
    x_trial_vel = []
    y_trial_vel = []
    x_trial_pow = []
    y_trial_pow = []
    trial_cond = []

    # create lists for vel and PSD of all trial groups
    vel_x_avgs_eotog = []
    pow_x_tot_eotog = []
    vel_y_avgs_eotog = []
    pow_y_tot_eotog = []

    vel_x_avgs_ectog = []
    pow_x_tot_ectog = []
    vel_y_avgs_ectog = []
    pow_y_tot_ectog = []

    vel_x_avgs_eodftan = []
    pow_x_tot_eodftan = []
    vel_y_avgs_eodftan = []
    pow_y_tot_eodftan = []

    vel_x_avgs_ecdftan = []
    pow_x_tot_ecdftan = []
    vel_y_avgs_ecdftan = []
    pow_y_tot_ecdftan = []

    vel_x_avgs_eodbtan = []
    pow_x_tot_eodbtan = []
    vel_y_avgs_eodbtan = []
    pow_y_tot_eodbtan = []

    vel_x_avgs_ecdbtan = []
    pow_x_tot_ecdbtan = []
    vel_y_avgs_ecdbtan = []

```

```

pow_y_tot_ecdbtan = []

# loop through each file in the directory
for file in dirs[directory]:
    # Determine which trial number and subject the file is
    number = int(file[10:12])
    subject = int(file[2:4])

    # if an EOFT trial
    if number < 7:
        trial_cond.append("EOFT")
        # read data
        df = pd.read_csv(os.path.join(directory, file), index_col=False)

        # convert data from dataframe into a numpy list
        df = df.to_numpy()
        values = np.delete(df, 0, 1)
        x_cop, y_cop = values.T

        # get the derivative of the x direction COP data
        vel_x_cop = an.deriv(t_cop, x_cop)

        # take the average of the first 10 data points from x velocity
        # (too time expensive to average all points, and this is accurate)
        vel_x_avgs_eotog.append(np.mean(sorted(vel_x_cop, reverse=True)[:10]))
        x_trial_vel.append(np.mean(sorted(vel_x_cop, reverse=True)[:10]))

        # calculate autocorrelation and then PSD of velocity of x COP
        auto_vel_x_cop = np.correlate(vel_x_cop, vel_x_cop, mode="full")
        Sxx_vel_cop = np.fft.fft(auto_vel_x_cop)

        # sum up all of the x cop frequency content
        pow_x_tot_eotog.append(sum(abs(Sxx_vel_cop)))
        x_trial_pow.append(sum(abs(Sxx_vel_cop)))

        # get the derivative of the y direction COP data
        vel_y_cop = an.deriv(t_cop, y_cop)

        # take the average of the first 10 data points from x velocity
        vel_y_avgs_eotog.append(np.mean(sorted(vel_y_cop, reverse=True)[:10]))
        y_trial_vel.append(np.mean(sorted(vel_y_cop, reverse=True)[:10]))

        # calculate autocorrelation and the PSD of velocity of y COP
        auto_vel_y_cop = np.correlate(vel_y_cop, vel_y_cop, mode="full")
        Syy_vel_cop = np.fft.fft(auto_vel_y_cop)

        # sum up all of the y cop frequency content
        pow_y_tot_eotog.append(sum(abs(Syy_vel_cop)))

```

```

y_trial_pow.append(sum(abs(Syy_vel_cop)))

# if an ECFT trial: complete same steps as above
elif 6 < number < 12:
    trial_cond.append("ECFT")
    df = pd.read_csv(os.path.join(directory, file), index_col=False)

    df = df.to_numpy()
    values = np.delete(df, 0, 1)
    x_cop, y_cop = values.T

    vel_x_cop = an.deriv(t_cop, x_cop)
    vel_x_avgs_ectog.append(np.mean(sorted(vel_x_cop, reverse=True)[:10]))
    x_trial_vel.append(np.mean(sorted(vel_x_cop, reverse=True)[:10]))

    auto_vel_x_cop = np.correlate(vel_x_cop, vel_x_cop, mode="full")
    Sxx_vel_cop = np.fft.fft(auto_vel_x_cop)
    pow_x_tot_ectog.append(sum(abs(Sxx_vel_cop)))
    x_trial_pow.append(sum(abs(Sxx_vel_cop)))

    vel_y_cop = an.deriv(t_cop, y_cop)
    vel_y_avgs_ectog.append(np.mean(sorted(vel_y_cop, reverse=True)[:10]))
    y_trial_vel.append(np.mean(sorted(vel_y_cop, reverse=True)[:10]))

    auto_vel_y_cop = np.correlate(vel_y_cop, vel_y_cop, mode="full")
    Syy_vel_cop = np.fft.fft(auto_vel_y_cop)
    pow_y_tot_ectog.append(sum(abs(Syy_vel_cop)))
    y_trial_pow.append(sum(abs(Syy_vel_cop)))

# if an EOFTanDB trial
elif 11 < number < 17:
    trial_cond.append("EOFTanDB")
    df = pd.read_csv(os.path.join(directory, file), index_col=False)

    df = df.to_numpy()
    values = np.delete(df, 0, 1)
    x_cop, y_cop = values.T

    vel_x_cop = an.deriv(t_cop, x_cop)
    vel_x_avgs_eodbtan.append(
        np.mean(sorted(vel_x_cop, reverse=True)[:10])
    )
    x_trial_vel.append(np.mean(sorted(vel_x_cop, reverse=True)[:10]))

    auto_vel_x_cop = np.correlate(vel_x_cop, vel_x_cop, mode="full")
    Sxx_vel_cop = np.fft.fft(auto_vel_x_cop)
    pow_x_tot_eodbtan.append(sum(abs(Sxx_vel_cop)))
    x_trial_pow.append(sum(abs(Sxx_vel_cop)))

```

```

vel_y_cop = an.deriv(t_cop, y_cop)
vel_y_avgs_eodbtan.append(
    np.mean(sorted(vel_y_cop, reverse=True)[:10])
)
y_trial_vel.append(np.mean(sorted(vel_y_cop, reverse=True)[:10]))

auto_vel_y_cop = np.correlate(vel_y_cop, vel_y_cop, mode="full")
Syy_vel_cop = np.fft.fft(auto_vel_y_cop)
pow_y_tot_eodbtan.append(sum(abs(Syy_vel_cop)))
y_trial_pow.append(sum(abs(Syy_vel_cop)))

# if an ECFTanDB trial
elif 16 < number < 22:
    trial_cond.append("ECFTanDB")
    df = pd.read_csv(os.path.join(directory, file), index_col=False)

    df = df.to_numpy()
    values = np.delete(df, 0, 1)
    x_cop, y_cop = values.T

    vel_x_cop = an.deriv(t_cop, x_cop)
    vel_x_avgs_ecdbtan.append(
        np.mean(sorted(vel_x_cop, reverse=True)[:10])
    )
    x_trial_vel.append(np.mean(sorted(vel_x_cop, reverse=True)[:10]))

    auto_vel_x_cop = np.correlate(vel_x_cop, vel_x_cop, mode="full")
    Sxx_vel_cop = np.fft.fft(auto_vel_x_cop)
    pow_x_tot_ecdbtan.append(sum(abs(Sxx_vel_cop)))
    x_trial_pow.append(sum(abs(Sxx_vel_cop)))

    vel_y_cop = an.deriv(t_cop, y_cop)
    vel_y_avgs_ecdbtan.append(
        np.mean(sorted(vel_y_cop, reverse=True)[:10])
    )
    y_trial_vel.append(np.mean(sorted(vel_y_cop, reverse=True)[:10]))

    auto_vel_y_cop = np.correlate(vel_y_cop, vel_y_cop, mode="full")
    Syy_vel_cop = np.fft.fft(auto_vel_y_cop)
    pow_y_tot_ecdbtan.append(sum(abs(Syy_vel_cop)))
    y_trial_pow.append(sum(abs(Syy_vel_cop)))

# if an EOFTanDF trial
elif 21 < number < 27:
    trial_cond.append("EOFTanDF")
    df = pd.read_csv(os.path.join(directory, file), index_col=False)

```

```

df = df.to_numpy()
values = np.delete(df, 0, 1)
x_cop, y_cop = values.T

vel_x_cop = an.deriv(t_cop, x_cop)
vel_x_avgs_eodftan.append(
    np.mean(sorted(vel_x_cop, reverse=True)[:10])
)
x_trial_vel.append(np.mean(sorted(vel_x_cop, reverse=True)[:10]))

auto_vel_x_cop = np.correlate(vel_x_cop, vel_x_cop, mode="full")
Sxx_vel_cop = np.fft.fft(auto_vel_x_cop)
pow_x_tot_eodftan.append(sum(abs(Sxx_vel_cop)))
x_trial_pow.append(sum(abs(Sxx_vel_cop)))

vel_y_cop = an.deriv(t_cop, y_cop)
vel_y_avgs_eodftan.append(
    np.mean(sorted(vel_y_cop, reverse=True)[:10])
)
y_trial_vel.append(np.mean(sorted(vel_y_cop, reverse=True)[:10]))

auto_vel_y_cop = np.correlate(vel_y_cop, vel_y_cop, mode="full")
Syy_vel_cop = np.fft.fft(auto_vel_y_cop)
pow_y_tot_eodftan.append(sum(abs(Syy_vel_cop)))
y_trial_pow.append(sum(abs(Syy_vel_cop)))

# if an ECFTanDF trial
elif 26 < number < 32:
    trial_cond.append("ECFTanDF")
    df = pd.read_csv(os.path.join(directory, file), index_col=False)

    df = df.to_numpy()
    values = np.delete(df, 0, 1)
    x_cop, y_cop = values.T

    vel_x_cop = an.deriv(t_cop, x_cop)
    vel_x_avgs_ecdftan.append(
        np.mean(sorted(vel_x_cop, reverse=True)[:10])
    )
    x_trial_vel.append(np.mean(sorted(vel_x_cop, reverse=True)[:10]))

    auto_vel_x_cop = np.correlate(vel_x_cop, vel_x_cop, mode="full")
    Sxx_vel_cop = np.fft.fft(auto_vel_x_cop)
    pow_x_tot_ecdftan.append(sum(abs(Sxx_vel_cop)))
    x_trial_pow.append(sum(abs(Sxx_vel_cop)))

    vel_y_cop = an.deriv(t_cop, y_cop)
    vel_y_avgs_ecdftan.append(

```

```

        np.mean(sorted(vel_y_cop, reverse=True)[:10])
    )
    y_trial_vel.append(np.mean(sorted(vel_y_cop, reverse=True)[:10]))

    auto_vel_y_cop = np.correlate(vel_y_cop, vel_y_cop, mode="full")
    Syy_vel_cop = np.fft.fft(auto_vel_y_cop)
    pow_y_tot_ecdftan.append(sum(abs(Syy_vel_cop)))
    y_trial_pow.append(sum(abs(Syy_vel_cop)))

# save velocity data from all conditions in both directions to a .csv
zipped = list(
    zip(x_trial_vel, y_trial_vel, x_trial_pow, y_trial_pow, trial_cond)
)
df_for_stats = pd.DataFrame(
    zipped, columns=["xVelocity", "yVelocity", "xPower", "yPower", "condition"]
)
df_for_stats.to_csv(f"sb{directory[-1]}_velocity_by_condition.csv")

```

B.4. Regression Calculations

```

#####

# regr.py
#
# Written by: Natalie Tipton
# Advisor: Dr. Samhita Rhodes
#
# Created on: May 6, 2020
#
# Description: Performs least squares polynomial
# regression on data to obtain a baseline model
#
# Last updated: July 29, 2020

#####

# import packages
import operator
import numpy as np
import pandas as pd
import matplotlib.pyplot as plt
import matplotlib
import os
import analysis_lib as an
from sklearn.linear_model import LinearRegression

```

```

from sklearn.metrics import mean_squared_error, r2_score
from sklearn.preprocessing import PolynomialFeatures
from scipy.stats import norm

# define root folder for data
ROOT = f"{os.environ.get('HOME')}/Code/center_of_pressure/data"

# constants
fs_cop = 1200
t_cop = np.arange(0, 30, 1 / fs_cop)

# create lists for all data to go into
all_x_data = []
all_y_data = []

#####

if __name__ == "__main__":
    # determine all subdirectories in root directory
    folders = [x[0] for x in os.walk(ROOT)]
    # remove the root directory from folders
    folders.remove(ROOT)
    # find all file names in the subdirectories
    files = [
        (os.path.join(ROOT, folder), os.listdir(os.path.join(ROOT, folder)))
        for folder in folders
    ]

    # create a dictionary showing what filenames are within each folder
    dirs = {}
    for folder_name, file_list in files:
        # remove irrelevant file names
        if ".DS_Store" in file_list:
            file_list.remove(".DS_Store")
        dirs[folder_name] = file_list

    # loop through all files in all subdirectories
    for directory in dirs:

        for file in dirs[directory]:
            # determine trial number
            number = int(file[10:12])

            # change if statement to create groupings of different conditions
            # number < 7 = EOFT, 6 < number < 12 = ECFT, 11 < number < 17 = EOFTanDB
            # 16 < number < 22 = ECFTanDB, 21 < number < 27 = EOFTanDF,

```

```

# 26 < number < 32 = ECFTanDF, number < 32 = all conditions
if number < 32:
    # read COP data
    df = pd.read_csv(os.path.join(directory, file), index_col=False)

    # convert to np array and obtain x and y axis data
    df = df.to_numpy()
    values = np.delete(df, 0, 1)
    Xaxis, Yaxis = values.T

    # turn data into delta values, showing deviation from start
    Xaxis = np.subtract(Xaxis, Xaxis[0])
    Yaxis = np.subtract(Yaxis, Yaxis[0])

    # save data from all files in condition range to a list
    all_x_data.append(Xaxis)
    all_y_data.append(Yaxis)

# turn list into array
all_x_data = np.array(all_x_data)
all_y_data = np.array(all_y_data)

# find average signal from all data in condition range
avg_x_data = np.mean(all_x_data, axis=0)
avg_y_data = np.mean(all_y_data, axis=0)

avg_x_data = avg_x_data[:, np.newaxis]
avg_y_data = avg_y_data[:, np.newaxis]
t_cop = t_cop[:, np.newaxis]

# calculate regression models for AP and ML directions and plot
plt.figure()
poly(t_cop, avg_x_data, 121, "AP")
poly(t_cop, avg_y_data, 122, "ML")
plt.show()

```

B.5. Function Library

```
#####  
  
# analysis_lib.py  
#  
# Written by: Natalie Tipton  
# Advisor: Dr. Samhita Rhodes  
#  
# Created on: May 6, 2020  
#  
# Description: Library of functions for use in  
# code relating to thesis research  
#  
# Last updated: July 29, 2020  
  
#####  
  
import matplotlib.pyplot as plt  
from mpl_toolkits.mplot3d import Axes3D  
import numpy as np  
import pandas as pd  
from sklearn import preprocessing  
import skimage  
from tqdm import tqdm  
from joblib import Parallel, delayed  
import multiprocessing  
from scipy import signal  
from sklearn.linear_model import LinearRegression  
from sklearn.metrics import mean_squared_error, r2_score  
from sklearn.preprocessing import PolynomialFeatures  
from scipy.stats import norm  
  
# reads CoP data in from .csv files for data with feet together, one force plate  
# returns: cx = CoP x position (AP), cy = CoP y position (ML)  
# user specifies:  
# header = which row the data starts on (starting at 0, not 1 like the sheet)  
# usecols = names of the column headers that are to be included  
# nrows = number of data points to be read in  
# rows_skip = the number of any rows to not be included (starting at 0)  
def read_data_onefp(filepath, row_start, cols, num_data, rows_skip):  
    data = pd.read_csv(  
        filepath,  
        header=row_start,  
        usecols=cols,  
        nrows=num_data,  
        dtype={"Cx": np.float64, "Cy": np.float64},
```

```

        skiprows=rows_skip,
    )

    # convert data frame into lists
    cx = data["Cx"].values.tolist()
    cy = data["Cy"].values.tolist()

    return cx, cy, data["Cx"]

# reads CoP data in from .csv files for feet tandem, two force plates
# combines CoP positions from both force plates into 1 resultant CoP
# returns: cx_combined = resultant CoP x position (AP),
#          cy_combined = resultant CoP y position (ML)
# user specifies:
#   header = which row the data starts on (starting at 0, not 1 like the sheet)
#   usecols = names of the column headers that are to be included
#   nrows = number of data points to be read in
#   rows_skip = the number of any rows to not be included (starting at 0)
def read_data_twofp(filepath, row_start, cols, num_data, rows_skip):
    data = pd.read_csv(
        filepath,
        header=row_start,
        usecols=["Fz", "Cx", "Cy", "Fz.1", "Cx.1", "Cy.1"],
        nrows=36000,
        dtype={
            "Fz": np.float64,
            "Cx": np.float64,
            "Cy": np.float64,
            "Fz.1": np.float64,
            "Cx.1": np.float64,
            "Cy.1": np.float64,
        },
        skiprows=[4],
    )

    # convert data frame into lists
    fz = data["Fz"].values.tolist()
    cx = data["Cx"].values.tolist()
    cy = data["Cy"].values.tolist()
    fz_1 = data["Fz.1"].values.tolist()
    cx_1 = data["Cx.1"].values.tolist()
    cy_1 = data["Cy.1"].values.tolist()

    cx_combined = []
    cy_combined = []

    # combine CoP from two force plates into one resultant CoP

```

```

# combined(x,y)=COP1(x,y)+(F1(z)/F1(z)+F2(z))+COP2(x,y)+(F2(z)/F1(z)+F2(z))
for point in range(len(cx)):
    cx_combined.append(
        cx[point] * fz[point] / (fz[point] + fz_1[point])
        + cx_1[point] * fz_1[point] / (fz[point] + fz_1[point])
    )

    cy_combined.append(
        cy[point] * fz[point] / (fz[point] + fz_1[point])
        + cy_1[point] * fz_1[point] / (fz[point] + fz_1[point])
    )

return cx_combined, cy_combined

# reads CoM data in from .csv files
# returns: x = CoM x position (AP), y = CoM y position (ML), z = CoM z position
# user specifies:
# header = which row the data starts on (starting at 0, not 1 like the sheet)
# usecols = names of the column headers that are to be included
# nrows = number of data points to be read in
# rows_skip = the number of any rows to not be included (starting at 0)
def read_data_com(filepath, row_start, cols, num_data, rows_skip):
    data = pd.read_csv(
        filepath,
        header=row_start,
        usecols=cols,
        nrows=num_data,
        dtype={"Cx": np.float64, "Cy": np.float64},
        skiprows=rows_skip,
    )

    # convert data frame into lists
    x = data["X"].values.tolist()
    y = data["Y"].values.tolist()
    z = data["Z"].values.tolist()

    return x, y, z

# standardizes the data given using the equation:
# standard[n] = (data[n] - mean[data]) / standard deviation[data]
def standardize(data):
    avg = np.mean(data)
    sd = np.std(data)

    standard = []

```

```

    for i in range(0, len(data)):
        standard.append((data[i] - avg) / sd)

    return standard

# creates a plot using matplotlib.pyplot
# user specifies:
# x = data to be plotted on x axis
# y = data to be plotted on y axis
# xlabel = string for labeling x axis
# ylabel = string for labeling y axis
# title = string to titling plot
# xlim = min and max limits for the x axis (use None for no lim)
# ylim = min and max limits for the y axis (use None for no lim)
def plot(x, y, xlabel, ylabel, title, xlim, ylim):
    plt.figure()
    plt.plot(x, y)
    plt.title(title)
    plt.xlabel(xlabel)
    plt.ylabel(ylabel)
    plt.xlim(xlim)
    plt.ylim(ylim)
    plt.show()

# calculates the point by point derivative between two lists
# Inputs:
# x = independent variable
# y = dependent variable
def deriv(x, y):
    der = []
    for i in range(0, len(y) - 1):
        der.append((y[i + 1] - y[i]) / (x[i + 1] - x[i]))

    return der

# adapted from https://en.wikipedia.org/wiki/Approximate\_entropy
# returns: the approximate entropy of a data set
# User inputs:
# U = data set
# m = length of compared runs
# r = filter value
def ApEn(U, m, r) -> float:
    def _maxdist(x_i, x_j):
        return max([abs(ua - va) for ua, va in zip(x_i, x_j)])

```

```

def _phi(m):
    x = [[U[j] for j in range(i, i + m - 1 + 1)] for i in range(N - m + 1)]
    C = [
        len([1 for x_j in x if _maxdist(x_i, x_j) <= r]) / (N - m + 1.0)
        for x_i in x
    ]

    return (N - m + 1.0) ** (-1) * sum(np.log(C))

N = len(U)

return abs(_phi(m + 1) - _phi(m))

# collects approximate entroy into a list from each window
# Inputs:
# ent_list = entroy value
# x = list to append values to
def collect_approx_entropy(ent_list, x):
    ent_list.append(x)

# prepares data for moving approximate entropy calculation
# Inputs:
# x = data
# win_size = size of windows for moving calculation
# overlap = amount of overlap in windows
# mult = gain increase for data to exacerbate small differences
# name = data descriptor for plot labeing
def approx_ent(x, win_size, overlap, mult, name) -> list:
    # increase magnitude of signal for more sensitivity in entropy
    x_multiplied = np.multiply(x, mult)

    # create overlapping windows
    x_array = np.asarray(x_multiplied)
    x_overlap = skimage.util.view_as_windows(x_array, win_size, step=overlap)
    rows = x_overlap.shape[0]

    approx_entropy = []

    # calculate moving approximate entropy in multiple threads to speed up process
    Parallel(n_jobs=multiprocessing.cpu_count(), require="sharedmem")(
        delayed(collect_approx_entropy)(approx_entropy, (ApEn(x_overlap[row], 2, 10)))
        for row in tqdm(range(0, rows))
    )

    return approx_entropy

```

```

# function to obtain filter coefficients for butterworth, 4th order, 6 hz lowpass
# Inputs:
#   cutoff = cutoff frequency
#   fs = sampling frequency of data to be filtered
#   order = order of filter
# Outputs:
#   a,b = filter coefficients
def butter_lowpass(cutoff, fs, order=4):
    normal_cutoff = float(cutoff) / (fs / 2)
    b, a = signal.butter(order, normal_cutoff, btype="lowpass", analog=False)
    return b, a

# filters data using filter coefficients from butter_lowpass
# Inputs:
#   data = data to be filtered
#   cutoff_freq = lowpass cutoff frequency
#   fs = sampling frequency of data passed
#   order = order of filter
# Output:
#   y = filtered data
def butter_lowpass_filter(data, cutoff_freq, fs, order=4):
    b, a = butter_lowpass(cutoff_freq, fs, order=order)
    y = signal.filtfilt(b, a, data)
    return y

# https://github.com/NathanMaton/prediction_intervals/blob/master/sklearn_prediction_
# interval_extension.ipynb
# returns a prediction interval for a linear regression prediction
# Inputs:
#   prediction = single prediction
#   y_test = test data that is being used for the regression
#   test_predictions = entire list of regression predictions
#   pi = confidence intervale
# Outputs:
#   lower = a single value of the lower bound
#   upper = a single value of the upper bound
def get_prediction_interval(prediction, y_test, test_predictions, pi=0.95):
    # get standard deviation of y_test
    sum_errs = np.sum((y_test - test_predictions) ** 2)
    stdev = np.sqrt(1 / (len(y_test) - 2) * sum_errs)

    # get interval from standard deviation
    one_minus_pi = 1 - pi
    ppf_lookup = 1 - (one_minus_pi / 2)
    z_score = norm.ppf(ppf_lookup)
    interval = z_score * stdev

```

```

# generate prediction interval lower and upper bound
lower, upper = prediction - interval, prediction + interval

return lower, upper

# calculates the regression and plots the curve with original
# signal and 95% prediction intervals
# Inputs:
# X = x-axis data for regression
# Y = y-axis data for regression
# subplt = which subplot to plot for plotting both directions
# dir = direction (AP/ML) of current data
def poly(X, Y, subplt, dir):
    # determine polynomial features
    polynomial_features = PolynomialFeatures(degree=9)
    X_polynomial = polynomial_features.fit_transform(X)

    # create regression model and fit to the polynomial features
    model = LinearRegression()
    model.fit(X_polynomial, Y)

    # create a regression curve based on model
    y_polynomial_predictions = model.predict(X_polynomial)

    # calculate r squared value
    r2 = r2_score(Y, y_polynomial_predictions)

    # create upper and lower intervals
    X_upper = []
    X_lower = []

    # calculate upper and lower intervals
    for prediction in y_polynomial_predictions:
        lower, upper = get_prediction_interval(prediction, Y, y_polynomial_predictions)
        X_upper.append(upper)
        X_lower.append(lower)

    # create a label to show the r squared value on plot
    label = r"$R^2$ = " + str(round(r2, 3))

    # plot the original signal, regression curve, and prediction intervals
    plt.subplot(subplt)
    plt.plot(X, Y)
    sort_axis = operator.itemgetter(0)
    sorted_zip = sorted(zip(X, y_polynomial_predictions), key=sort_axis)
    x, y_polynomial_predictions = zip(*sorted_zip)

```

```
plt.plot(x, y_polynomial_predictions, color="m")
plt.plot(x, X_upper, color="r")
plt.plot(x, X_lower, color="r")
plt.xlabel("Time (s)")
plt.ylabel("COP Approximation (mm from starting location)")
plt.title(f"Regression model for all trials in the {dir} direction\n{label}")
plt.legend(["Average Signal", "Model", "95% prediction interval"])
plt.ylim([-10, 6])
```

References

- [1] A. S. Pollock, B. R. Durward, P. J. Rowe, and J. P. Paul, “What is balance?,” *Clin. Rehabil.*, Jul. 2016, doi: 10.1191/0269215500cr342oa.
- [2] D. Winter, “Human balance and posture control during standing and walking,” *Gait Posture*, vol. 3, no. 4, pp. 193–214, Dec. 1995, doi: 10.1016/0966-6362(96)82849-9.
- [3] J. Massion, “Postural control system,” *Curr. Opin. Neurobiol.*, vol. 4, no. 6, pp. 877–887, Dec. 1994, doi: 10.1016/0959-4388(94)90137-6.
- [4] M. Fujimoto, W.-N. Bair, and M. W. Rogers, “Center of pressure control for balance maintenance during lateral waist-pull perturbations in older adults,” *J. Biomech.*, vol. 48, no. 6, pp. 963–968, Apr. 2015, doi: 10.1016/j.jbiomech.2015.02.012.
- [5] J. V. Jacobs and F. B. Horak, “Cortical control of postural responses,” *J. Neural Transm.*, vol. 114, no. 10, p. 1339, Mar. 2007, doi: 10.1007/s00702-007-0657-0.
- [6] C. Rochefort, C. Walters-Stewart, M. Aglipay, N. Barrowman, R. Zemek, and H. Sveistrup, “Balance Markers in Adolescents at 1 Month Postconcussion,” *Orthop. J. Sports Med.*, vol. 5, no. 3, p. 2325967117695507, Mar. 2017, doi: 10.1177/2325967117695507.
- [7] S. A. Chvatal, G. Torres-Oviedo, S. A. Safavynia, and L. H. Ting, “Common muscle synergies for control of center of mass and force in nonstepping and stepping postural behaviors,” *J. Neurophysiol.*, vol. 106, no. 2, pp. 999–1015, Aug. 2011, doi: 10.1152/jn.00549.2010.
- [8] N. Oba, S. Sasagawa, A. Yamamoto, and K. Nakazawa, “Difference in Postural Control during Quiet Standing between Young Children and Adults: Assessment with Center of Mass Acceleration,” *PLoS ONE*, vol. 10, no. 10, Oct. 2015, doi: 10.1371/journal.pone.0140235.
- [9] R. D. Catena, P. van Donkelaar, and L.-S. Chou, “Different gait tasks distinguish immediate vs. long-term effects of concussion on balance control,” *J. NeuroEngineering Rehabil.*, vol. 6, p. 25, Jul. 2009, doi: 10.1186/1743-0003-6-25.
- [10] K. Merchant-Borna, C. M. C. Jones, M. Janigro, E. B. Wasserman, R. A. Clark, and J. J. Bazarian, “Evaluation of Nintendo Wii Balance Board as a Tool for Measuring Postural Stability After Sport-Related Concussion,” *J. Athl. Train.*, vol. 52, no. 3, pp. 245–255, Mar. 2017, doi: 10.4085/1062-6050-52.1.13.
- [11] E. Yu *et al.*, “Evaluation of Postural Control in Quiet Standing Using Center of Mass Acceleration: Comparison Among the Young, the Elderly, and People With Stroke,” *Arch. Phys. Med. Rehabil.*, vol. 89, no. 6, pp. 1133–1139, Jun. 2008, doi: 10.1016/j.apmr.2007.10.047.

- [12] A. Mansfield and E. L. Inness, “Force Plate Assessment of Quiet Standing Balance Control: Perspectives on Clinical Application within Stroke Rehabilitation,” *Rehabil. Process Outcome*, vol. 4, p. RPO.S20363, Jan. 2015, doi: 10.4137/RPO.S20363.
- [13] C. S. Versteeg, L. H. Ting, and J. L. Allen, “Hip and ankle responses for reactive balance emerge from varying priorities to reduce effort and kinematic excursion: a simulation study,” *J. Biomech.*, vol. 49, no. 14, pp. 3230–3237, Oct. 2016, doi: 10.1016/j.jbiomech.2016.08.007.
- [14] V. Komisar, K. Nirmalanathan, and A. C. Novak, “Influence of handrail height and fall direction on center of mass control and the physical demands of reach-to-grasp balance recovery reactions,” *Gait Posture*, vol. 60, pp. 209–216, Feb. 2018, doi: 10.1016/j.gaitpost.2017.12.009.
- [15] D. Lafonda, M. Duarteb, and F. Princea, *Journal of Biomechanics 37 (2004) 1421–1426 Comparison of three methods to estimate the center of mass during balance assessment*. 2003.
- [16] D. A. Winter, A. E. Patla, M. Ishac, and W. H. Gage, “Motor mechanisms of balance during quiet standing,” *J. Electromyogr. Kinesiol.*, vol. 13, no. 1, pp. 49–56, Feb. 2003, doi: 10.1016/S1050-6411(02)00085-8.
- [17] B.-J. Hsue, F. Miller, and F.-C. Su, “The dynamic balance of the children with cerebral palsy and typical developing during gait. Part I: Spatial relationship between COM and COP trajectories,” *Gait Posture*, vol. 29, no. 3, pp. 465–470, Apr. 2009, doi: 10.1016/j.gaitpost.2008.11.007.
- [18] N. Sarabon, R. Jernej, S. Loeffler, and H. Kern, “Sensitivity of Body Sway Parameters During Quiet Standing to Manipulation of Support Surface Size,” *J. Sports Sci. Med.*, vol. 9, no. 3, pp. 431–438, Sep. 2010.
- [19] T. E. Prieto, J. B. Myklebust, R. G. Hoffmann, E. G. Lovett, and B. M. Myklebust, “Measures of postural steadiness: differences between healthy young and elderly adults,” *IEEE Trans. Biomed. Eng.*, vol. 43, no. 9, pp. 956–966, Sep. 1996, doi: 10.1109/10.532130.
- [20] P. Corbeil, J.-S. Blouin, F. Bégin, V. Nougier, and N. Teasdale, “Perturbation of the postural control system induced by muscular fatigue,” *Gait Posture*, vol. 18, no. 2, pp. 92–100, Oct. 2003, doi: 10.1016/S0966-6362(02)00198-4.
- [21] C. L. Riach and K. C. Hayes, “Maturation Of Postural Sway In Young Children,” *Dev. Med. Child Neurol.*, vol. 29, no. 5, pp. 650–658, 1987, doi: 10.1111/j.1469-8749.1987.tb08507.x.
- [22] C. J. Dakin and D. A. E. Bolton, “Forecast or Fall: Prediction’s Importance to Postural Control,” *Front. Neurol.*, vol. 9, Oct. 2018, doi: 10.3389/fneur.2018.00924.

- [23] B. Colobert, A. Crétual, P. Allard, and P. Delamarche, “Force-plate based computation of ankle and hip strategies from double-inverted pendulum model,” *Clin. Biomech.*, vol. 21, no. 4, pp. 427–434, May 2006, doi: 10.1016/j.clinbiomech.2005.12.003.
- [24] R. J. Peterka, D. Luca, C. Jj, and D. L. Cj, “Postural control model interpretation of stabilogram diffusion analysis,” p. 9.
- [25] F. B. Horak, “Postural orientation and equilibrium: what do we need to know about neural control of balance to prevent falls?,” *Age Ageing*, vol. 35, no. suppl_2, pp. ii7–ii11, Sep. 2006, doi: 10.1093/ageing/afl077.
- [26] E. Lecompte, “Balance improvement of a humanoid robot while walking,” *DIAL*, 2018, [Online]. Available: <http://hdl.handle.net/2078.1/thesis:14825>.
- [27] J. Baracks *et al.*, “Acute Sport-Related Concussion Screening for Collegiate Athletes Using an Instrumented Balance Assessment,” *J. Athl. Train.*, vol. 53, no. 6, pp. 597–605, Jun. 2018, doi: 10.4085/1062-6050-174-17.
- [28] J. M. Matuszak, J. McVige, J. McPherson, B. Willer, and J. Leddy, “A Practical Concussion Physical Examination Toolbox,” *Sports Health*, vol. 8, no. 3, pp. 260–269, Jun. 2016, doi: 10.1177/1941738116641394.
- [29] S. Pincus, “Approximate entropy (ApEn) as a complexity measure,” *Chaos Interdiscip. J. Nonlinear Sci.*, vol. 5, no. 1, pp. 110–117, Mar. 1995, doi: 10.1063/1.166092.
- [30] A. Schneider, G. Hommel, and M. Blettner, “Linear Regression Analysis,” *Dtsch. Ärztebl. Int.*, vol. 107, no. 44, pp. 776–782, Nov. 2010, doi: 10.3238/arztebl.2010.0776.
- [31] D. A. Winter, “Biomechanics and Motor Control of Human Movement, 4th Edition | Wiley,” *Wiley.com*, Oct. 2009. <https://www.wiley.com/en-us/Biomechanics+and+Motor+Control+of+Human+Movement%2C+4th+Edition-p-9780470398180> (accessed Jul. 29, 2020).
- [32] D. McCrumb, “Analysis of Connectivity in EMG Signals to Examine Neural Correlations in Muscular Activation of Lower Leg Muscles for Postural Stability,” Grand Valley State University, 2020.
- [33] M. Kirchner, “Characterising postural sway fluctuations in humans using linear and nonlinear methods,” Goethe University, Frankfurt, Germany.
- [34] M. L. Latash, S. S. Ferreira, S. A. Wiczorek, and M. Duarte, “Movement sway: changes in postural sway during voluntary shifts of the center of pressure,” *Exp. Brain Res.*, vol. 150, no. 3, pp. 314–324, Jun. 2003, doi: 10.1007/s00221-003-1419-3.
- [35] N. B. Singh, W. R. Taylor, M. L. Madigan, and M. A. Nussbaum, “The spectral content of postural sway during quiet stance: Influences of age, vision and somatosensory inputs,” *J.*

- Electromyogr. Kinesiol.*, vol. 22, no. 1, pp. 131–136, Feb. 2012, doi: 10.1016/j.jelekin.2011.10.007.
- [36] H. J. Woltring, “On Optimal Smoothing and Derivative Estimation From Noisy Displacement Data in Biomechanics,” *Hum. Mov. Sci.*, vol. 4, pp. 229–245, 1985.
- [37] “Combined output from multiple force plates - Nexus 2.6 Documentation - Vicon Documentation.”
<https://docs.vicon.com/display/Nexus26/Combined+output+from+multiple+force+plates>
 (accessed Apr. 27, 2020).
- [38] T. Exell, D. Kerwin, G. Irwin, and M. Gittoes, “CALCULATING CENTRE OF PRESSURE FROM MULTIPLE FORCE PLATES FOR KINETIC ANALYSES OF SPRINT RUNNING,” p. 4, 2011.
- [39] Y. Fusheng, H. Bo, and T. Qingyu, “Approximate Entropy and Its Application to Biosignal Analysis,” in *Nonlinear Biomedical Signal Processing*, John Wiley & Sons, Ltd, 2012, pp. 72–91.
- [40] H. Lee and K. P. Granata, “Process stationarity and reliability of trunk postural stability,” *Clin. Biomech.*, vol. 23, no. 6, pp. 735–742, Jul. 2008, doi: 10.1016/j.clinbiomech.2008.01.008.
- [41] L. Rocchi, L. Chiari, A. Cappello, and F. B. Horak, “Identification of distinct characteristics of postural sway in Parkinson’s disease: A feature selection procedure based on principal component analysis,” *Neurosci. Lett.*, vol. 394, no. 2, pp. 140–145, Feb. 2006, doi: 10.1016/j.neulet.2005.10.020.
- [42] P. Schober, C. Boer, and L. A. Schwarte, “Correlation Coefficients: Appropriate Use and Interpretation,” *Anesth. Analg.*, vol. 126, no. 5, pp. 1763–1768, May 2018, doi: 10.1213/ANE.0000000000002864.
- [43] K.-Y. Seng, V.-S. Lee Peter, and P.-M. Lam, “Neck muscle strength across the sagittal and coronal planes: an isometric study,” *Clin. Biomech.*, vol. 17, no. 7, pp. 545–547, Aug. 2002, doi: 10.1016/S0268-0033(02)00067-0.
- [44] S. Kumar, Y. Narayan, and T. Amell, “Cervical strength of young adults in sagittal, coronal, and intermediate planes,” *Clin. Biomech.*, vol. 16, no. 5, pp. 380–388, Jun. 2001, doi: 10.1016/S0268-0033(01)00023-7.
- [45] D. A. Winter, A. E. Patla, F. Prince, M. Ishac, and K. Giello-Perczak, “Stiffness Control of Balance in Quiet Standing,” *J. Neurophysiol.*, vol. 80, no. 3, pp. 1211–1221, Sep. 1998, doi: 10.1152/jn.1998.80.3.1211.

- [46] T. Paillard and F. Noé, “Techniques and Methods for Testing the Postural Function in Healthy and Pathological Subjects,” *BioMed Research International*, Nov. 12, 2015. <https://www.hindawi.com/journals/bmri/2015/891390/> (accessed Jun. 25, 2020).
- [47] Y. Brenière and B. Bril, “Development of postural control of gravity forces in children during the first 5 years of walking,” *Exp. Brain Res.*, vol. 121, no. 3, pp. 255–262, Aug. 1998, doi: 10.1007/s002210050458.
- [48] M. B. Parkinson, “Balance maintenance in normal seated reach,.” 2004. /paper/Balance-maintenance-in-normal-seated-reach.- Parkinson/65d4e557768db6215db4a06cc1ab859f8a1a7aab (accessed Jul. 07, 2020).
- [49] F. B. Horak, “Clinical Measurement of Postural Control in Adults,” *Phys. Ther.*, vol. 67, no. 12, pp. 1881–1885, Dec. 1987, doi: 10.1093/ptj/67.12.1881.
- [50] R. E. A. van Emmerik and E. E. H. van Wegen, “On the Functional Aspects of Variability in Postural Control,” *Exerc. Sport Sci. Rev.*, vol. 30, no. 4, pp. 177–183, Oct. 2002.
- [51] M. A. Hughes, P. W. Duncan, D. K. Rose, J. M. Chandler, and S. A. Studenski, “The relationship of postural sway to sensorimotor function, functional performance, and disability in the elderly,” *Arch. Phys. Med. Rehabil.*, vol. 77, no. 6, pp. 567–572, Jun. 1996, doi: 10.1016/S0003-9993(96)90296-8.
- [52] A. D. Kloos and D. L. Givens, “Exercise for Impaired Balance,” in *Therapeutic Exercise: Foundations and Techniques, 6e* | F.A. Davis PT Collection | McGraw-Hill Medical, .
- [53] S. I. Fox, *Human Physiology*, 15th ed. McGraw-Hill Education, 2019.
- [54] K. B. Bhattacharyya, “The stretch reflex and the contributions of C David Marsden,” *Ann. Indian Acad. Neurol.*, vol. 20, no. 1, pp. 1–4, 2017, doi: 10.4103/0972-2327.199906.
- [55] P. Morasso, A. Cherif, and J. Zenzeri, “Quiet standing: The Single Inverted Pendulum model is not so bad after all,” *PLOS ONE*, vol. 14, no. 3, p. e0213870, Mar. 2019, doi: 10.1371/journal.pone.0213870.
- [56] I. J. Pinter, R. van Swigchem, A. J. K. van Soest, and L. A. Rozendaal, “The Dynamics of Postural Sway Cannot Be Captured Using a One-Segment Inverted Pendulum Model: A PCA on Segment Rotations During Unperturbed Stance,” *J. Neurophysiol.*, vol. 100, no. 6, pp. 3197–3208, Dec. 2008, doi: 10.1152/jn.01312.2007.
- [57] Y. Suzuki, T. Nomura, and P. Morasso, “Stability of a double inverted pendulum model during human quiet stance with continuous delay feedback control,” in *2011 Annual International Conference of the IEEE Engineering in Medicine and Biology Society*, Aug. 2011, pp. 7450–7453, doi: 10.1109/IEMBS.2011.6091747.

- [58] T. C. Valovich McLeod and T. D. Hale, “Vestibular and balance issues following sport-related concussion,” *Brain Inj.*, vol. 29, no. 2, pp. 175–184, Jan. 2015, doi: 10.3109/02699052.2014.965206.
- [59] R. D. Catena, P. van Donkelaar, and L.-S. Chou, “The effects of attention capacity on dynamic balance control following concussion,” *J. NeuroEngineering Rehabil.*, vol. 8, no. 1, p. 8, Feb. 2011, doi: 10.1186/1743-0003-8-8.
- [60] M. Gaetz, D. Goodman, H. Weinberg, “Electrophysiological evidence for the cumulative effects of concussion,” *Brain Inj.*, vol. 14, no. 12, pp. 1077–1088, Jan. 2000, doi: 10.1080/02699050050203577.
- [61] “Help Online - Origin Help - The Polynomial Regression Dialog Box.” <https://www.originlab.com/doc/Origin-Help/PR-Dialog> (accessed Jun. 29, 2020).